UNIVERSITY OF TURKU

HYDROTHERMALLY INDUCED NANOSTRUCTURED TiO_2 COATINGS

With Special Reference to Biologic Events of Peri-implant Tissue Integration

Nagat Areid

TURUN YLIOPISTON JULKAISUJA – ANNALES UNIVERSITATIS TURKUENSIS
SARJA - SER. D OSA - TOM. 1537 | MEDICA - ODONTOLOGICA | TURKU 2021

UNIVERSITY OF TURKU

HYDROTHERMALLY INDUCED NANOSTRUCTURED TiO_2 COATINGS

With Special Reference to Biologic Events of Peri-implant Tissue Integration

Nagat Areid

TURUN YLIOPISTON JULKAISUJA – ANNALES UNIVERSITATIS TURKUENSIS
SARJA – SER. D OSA – TOM. 1537 | MEDICA – ODONTOLOGICA | TURKU 2021

University of Turku

Faculty of Medicine
Institute of Dentistry
Department of Prosthetic Dentistry and Stomatognathic Physiology
Finnish Doctoral Program in Oral Sciences (FINDOS-Turku)

Supervised by

Professor Timo Närhi, DDS, PhD
Department of Prosthetic Dentistry and
Stomatognathic Physiology
Institute of Dentistry
University of Turku
Turku, Finland

Reviewed by

Professor Lari Häkkinen, DDS, PhD
Department of Oral Biological and
Medical Sciences
University of British Columbia
Vancouver, BC, Canada

Docent Taina Tervahartiala, DDS, PhD
Department of Oral and
Maxillofacial Diseases
University of Helsinki
Helsinki, Finland

Opponent

Professor Nicola Zitzmann,
Dr. med. dent., PhD
Department of Reconstructive Dentistry
University of Basel
Basel, Switzerland

The originality of this publication has been checked in accordance with the University of Turku quality assurance system using the Turnitin Originality Check service.

ISBN 978-951-29-8388-9 (PRINT)
ISBN 978-951-29-8389-6 (PDF)
ISSN 0355-9483 (Print)
ISSN 2343-3213 (Online)
Painosalama Oy, Turku, Finland 2021

"In the name of GOD, the Most Gracious, the Most Merciful"

To my parents,
My husband, Faleh,
My kids, Rahaf, Roua, Ahmed, and Mohamed
I love you to the moon and back. Thank you for everything

UNIVERSITY OF TURKU
Faculty of Medicine
Institute of Dentistry
Department of Prosthetic Dentistry and Stomatognathic Physiology
NAGAT AREID: Hydrothermally induced nanostructured TiO_2 coatings-with special reference to biologic events of peri-implant tissue integration
Doctoral Dissertation, 138 pp.
Finnish Doctoral Program in Oral Science (FINDOS-Turku)
March 2021

ABSTRACT

Soft tissue integration between the oral implant and the surrounding tissue is considered crucial for implant success. Various surface modifications have been used to obtain bioactive TiO_2 coatings on the implant surface to improve osseointegration, bioactivity, and antibacterial properties. Among these methods, the hydrothermal (HT) coating technique has recently gained attention to produce anatase crystalline TiO_2 coating for improved bioactivity and enhanced osteoconductivity. However, little is known about HT induced TiO_2 coatings effect on the peri-implant soft tissue attachment.

The objectives of this series of experimental studies were to develop new HT treatment based TiO_2 coatings for titanium implants, which promotes wound healing and enhances soft tissue attachment. Another aim was to investigate the effect of UV light treatment on the bioactivity and antibacterial properties of HT induced TiO_2 coatings.

Hydrothermal induced TiO_2 coatings were prepared by mixing titanium dioxide, purified water and tetramethylammonium hydroxide at 150 ± 10 ºC for 48 hours. The HT coatings were characterized using X-ray photoelectron spectroscopy and scanning electron microscope. The surface wettability was determined using contact angle measurements. Blood clotting ability, plasma protein adsorption, platelet adhesion, and activation, were evaluated. Human gingival fibroblast adhesion and proliferation were studied in a cell culture environment. The effect of UV light on the surface wettability, blood coagulation, and cellular response was investigated on coated and non-coated substrates. A novel tissue culture model using pig mandibular block, including alveolar bone and gingival tissues, was used to evaluate the tissue attachment on coated and non-coated titanium implants. Early biofilm formation on the coated and non-coated titanium substrates was examined *in vivo*. The effect of UV light treatment on the biofilm formation was also studied.

The HT treated titanium surfaces were entirely covered with coating crystals consisting of nearly spherical TiO_2 nanoparticles. Higher carbon contents were observed on non-UV treated surfaces compared to UV treated surfaces, and carbon content was noticed to reduce with increasing UV exposure time. TiO_2 coated substrates accelerated blood clotting and improved platelet responses compared with non-coated substrates. Coated substrates showed higher surface free energy and better wettability than non-coated ones. UV treatment enhanced the wettability and improved blood clotting of all examined surfaces. Although no differences in protein adsorption was observed. Fibroblast cell adhesion strength was significantly higher on coated substrates. Histological analysis of pig tissue explants showed epithelial, connective, and bone tissue attachment to both coated and non-coated implant surfaces. The peri-implant epithelium appeared to be in close contact with the coated surfaces. Immunohistochemical staining showed CK14 positivity in the basal cell layer of stratified gingival epithelium. TiO_2 coating does not enhance salivary microbial adhesion and initial biofilm formation *in vivo*. The UV treatment provided titanium surfaces with antibacterial properties and showed a trend towards less biofilm formation than non-UV treated surfaces.

It can be concluded that HT derived TiO_2 coatings enhance biological events related to wound healing and soft tissue integration on the titanium alloy surface. The UV light treatment improved wettability, thrombogenicity and provided the titanium surfaces with antibacterial properties.

KEYWORDS: adhesion, antibacterial, biofilm, blood, fibroblast, hydrothermal, implant, peri-implant soft tissue, titanium, TiO_2, UV light, wettability.

TURUN YLIOPISTO
Lääketieteellinen tiedekunta
Hammaslääketieteen laitos
Hammasprotetiikka ja purentafysiologia
NAGAT AREID: Hydrotermaalisesti indusoidut nanorakenteiset TiO_2 pinnoitteet– tutkimuksia peri-implanttikudosten kiinnittymiseen liittyvistä biologisista tapahtumista. Väitöskirja, 138 s.
Kansallinen suun terveystieteiden tohtoriohjelma (FINDOS-Turku)
Maaliskuu 2021

TIIVISTELMÄ

Pehmytkudosten kiinnittyminen hammasimplantin pinnalle on tärkeää implanttihoidon onnistumiselle. Erilaisten pintakäsittelyiden avulla implantteihin on pyritty tuottamaan bioaktiivisia TiO_2 pinnoitteita parantamaan osseointegraatiota, bioaktiivisuutta ja antimikrobisia ominaisuuksia. Näistä erityisesti hydrotermaalinen (HT) pinnoitusmenetelmä on herättänyt mielenkiintoa kiteisen anataasimuotoisen TiO_2 pinnoitteen teossa paremman bioaktiivisuuden ja osteokonduktiivisuuden saavuttamiseksi. Menetelmän vaikutuksia implanttia ympäröivien pehmytkudosten kiinnittymiseen ei tunneta.

Tämän väitöskirjan tutkimusten tavoitteina oli kehittää titaani implantteihin uusi HT menetelmällä valmistettu TiO_2 pinnoite, joka edesauttaa haavan paranemista ja parantaa ienkudosten kiinnittymistä. Toisena tavoitteena oli tutkia UV-valo käsittelyn vaikutusta HT menetelmällä tuotettujen TiO_2 pinnoitteiden bioaktiivisuuteen ja antimikrobisiin ominaisuuksiin.

Hydrotermaaliset TiO_2 pinnoitteet valmistettiin sekoittamalla titaanidioksidia, puhdistettua vettä ja tetrametyyliammonium hydroksidia 150 ± 10 ºC 48 tunnin ajan. HT pinnoitteet karakterisoitiin RTG-fotoelektronispektroskopiaa ja pyyhkäisyelektronimikroskopiaa käyttämällä. Pintojen kostumisominaisuuksia tutkittiin kontaktikulmamittausta käyttäen. Veren reaktioita selvitettiin mittaamalla hyytymistä ja plasmaproteiinien kiinnittymistä sekä tutkimalla verihiutaleiden tarttumista ja morfologiaa. Ihmisen ikenen fibroblastisolujen vaste – kiinnittyminen ja jakautuminen - tutkittiin soluviljelyolosuhteissa. UV-valon vaikutus pinojen kostumiseen, veren hyytymiseen ja solujen käyttäytymiseen tutkittiin pinnoitetuilla ja pinnoittamattomilla näytteillä. Uutta kudosviljelymallia käytettiin tutkittaessa sian alaleuan blokkeihin asetettujen pinnoitettujen ja pinnoittamattomien titaani-implanttien kiinnittymistä luuhun ja implanttia ympäröivään ienkudokseen. Varhaisen biofilmin muodostumista pinnoitettuihin ja pinnoittamattomiin titaaninäytteisiin tutkittiin *in vivo* olosuhteissa. Lisäksi selvitettiin UV-valo käsittelyn vaikutusta biofilmin muodostumiseen.

HT menetelmällä käsitellyt pinnat olivat kokonaan kiteisten lähes pyöreiden TiO_2 nanopartikkeleiden peittämät. UV-valolla käsittelemättömillä pinnoilla todettiin suurempi hiilikontaminaatio UV-käsiteltyihin pintoihin verrattuna ja hiilipitoisuuden havaittiin pienenevän UV-käsittelyajan pidentyessä TiO_2 pinnoite nopeutti veren hyytymistä ja paransi verihiutaleiden reaktioita pinnoittamattomiin näytteisiin verrattuna. Pinnoitettujen titaaninäytteiden vapaa pintaenergia sekä pintojen kostuminen olivat selvästi pinnoittamattomia paremmat. UV käsittely paransi pintojen kostumista ja nopeutti veren hyytymistä kaikilla pinnoilla. Proteiinin adsorboitumisessa ei kuitenkaan havaittu eroja. Fibroblastit kiinnittyivät selvästi voimakkaammin pinnoitetuille näytteille. Sian kudosnäytteillä tehty tutkimus osoitti epiteeli-, side- ja luukudoksen kiinnittyvän hyvin sekä pinnoitettuihin että pinnoittamattomiin implantteihin. Peri-implantti epiteeli oli läheisessä kontaktissa pinnoitettuihin pintoihin. Immunohistokemiallinen värjäys osoitti CK14 positiivisuutta stratifioidun ienepiteelin basaalisolukerroksessa. TiO_2 pinnoite ei lisää syljen mikrobien kiinnittymistä tai varhaisen biofilmin muodostumista *in vivo.* UV-valo käsittely muutti pintoja antimikrobisiksi ja vähemmän biofilmin muodostusta suosivaksi käsittelemättömiin pintoihin verrattuna.

Tulokset osoittivat, että HT menetelmällä valmistetut TiO_2 pinnoitteet tehostavat haavan paranemisen biologisia tapahtumia ja pehmytkudosten kiinnittymistä titaanin pinnalle. UV-valo käsittely lisää pintojen kostumista, trombogeenisyyttä ja muuttaa pintojen ominaisuuksia antimikrobisiksi.

AVAINSANAT: antimikrobinen, biofilmi, fibroblasti, hydrotermaalinen, implantti, kiinnittyminen, Kostuminen, peri-implanttikudos, titaani, TiO_2, UV valo, veri.

Table of Contents

Abbreviations

ANOVA	Analysis of variance
°C	Degrees of Celsius
CFU	Colony-Forming Unit
CK	Cytokeratin
CpTi	Commercially pure titanium
HMDS	Hexamethyldisilazane
HA	Hydroxyapatite
HRP	horseradish peroxidase
HT	Hydrothermal
JE	Junctional epithelium
n	Number of substrates per group
NC	Non-coated
nm	nanometer
MA	MetAliveTM
$O2^-$	Superoxide radical
•OH	Hydroxyl radical
PBS	Phosphate-buffered saline
PIE	Peri-implant epithelium
PMMA	Polymethyl methacrylate
ROS	Reactive oxygen species
SD	Standard deviation
SEM	Scanning electron microscopy
SFE	Surface free energy
SPSS	Statistical Package for Social Science
TBS	Trisbuffered saline
$TiO2$	Titanium dioxide
TPS	Titanium plasma spraying
TMAH	Tetramethylammonium hydroxide $(N(CH3)4+OH)^-$
TSB	Tryptic soy broth
UV	Ultraviolet light
W	Watt
XPS	X-ray photoelectron spectroscopy

List of Original Publications

This thesis is based on the following original publications, which are referred to in the text by their Roman numerals (I–IV):

I **Areid N**, Kangasniemi I, Söderling E, Närhi T.O. Ultraviolet photofunctionalization of nanostructured titanium surfaces enhances thrombogenicity and platelet response. Journal of Materials Science: Materials in Medicine. 2018; 29:1–12.

II **Areid N**, Peltola A, Kangasniemi I, Ballo A, Närhi T. Effect of ultraviolet light treatment on surface hydrophilicity and human gingival fibroblast response on nanostructured titanium surfaces. Clinical and Experimental Dental Research. 2018; 4:78–85.

III **Areid N**, Willberg J, Kangasniemi I, Närhi T. Organotypic *in vitro* block culture model to investigate tissue-implant interface. An experimental study on pig mandible. *Manuscript in the reviewing stage.*

IV **Areid N,** Söderling E, Tanner J, Kangasniemi I, Närhi T. Early biofilm formation on UV light activated nanoporous TiO_2 surfaces *in vivo*. International Journal of Biomaterials. 2018;1–8.

1 Introduction

Restoring missing teeth with dental implants is an excellent treatment modality with highly predictable clinical outcomes. However, implant-associated infection is a common complication of dental implant treatment. Therefore, a protective soft tissue bond between the implant abutments and the surrounding soft tissue is considered very important for protecting the tissue-implant interface from bacterial invasion. Moreover, this may lead to unwanted clinical complications and eventually result in implant loss (Esposito et al., 1998; Mombelli & Lang, 1998).

The surface modification of the transmucosal area has been shown to promote firm attachment between the implant abutment and the surrounding soft tissue (Schupbach & Glauser, 2007; Welander et al., 2008), impede bacterial biofilm adhesion (Frojd et al., 2011), and maintain the crestal bone (Botos et al., 2011).

Titanium and titanium-based alloy such as Ti-6Al-4V are commonly used biomaterials in dental and orthopedic applications due to their excellent biocompatibility and high corrosion resistance. These properties arise from titanium dioxide (TiO_2) thin film that forms on titanium surface when exposed to air or water. However, this native nanocrystalline film is mechanically weak and does not enhance the wound healing process (Liu et al., 2004). Therefore, various advanced modification techniques have been developed to obtain a stable and uniform TiO_2 surface and enhance the properties required, e.g., bioactivity and bactericidal properties. These techniques include anodic oxidation (Jimbo et al., 2008), a sol-gel coating method (Peltola et al., 1998), chemical and hydrothermal methods (Kim et al., 1996). These techniques can also be applied to provide the surfaces with photocatalytic properties.

Among the above methods, the hydrothermal treatment appears to be a simple and effective surface modification technique that has been currently used to produce TiO_2 coating with bioactive surface composition. Previous animal studies have shown that hydrothermal treatment has the potential to improve bioactivity and enhance osteoconductivity of a titanium implant (Zuldesmi et al., 2015). Also, hydrothermal treatment with $CaCl_2$ promotes epithelial cell adhesion and improves soft tissue cells' integration with the titanium implant (Oshiro et al., 2015).

Photocatalytic TiO_2 coatings are multifunctionally useful in biomedical applications due to their superhydrophilic and bactericidal properties induced by Ultraviolet (UV) light (Rupp et al., 2010). UV light treatment of titanium surfaces has drawn significant attention recently as a surface modification method to enhance the biological capacity and physicochemical properties of titanium surfaces (Aita et al., 2009a; Iwasa et al., 2010). Different methods have been developed to obtain photocatalytic active TiO_2 coatings (Rupp et al., 2010; Unosson et al., 2012). The hydrothermal treatment has the advantage of being a feasible and straightforward chemical coating method to produce anatase crystalline TiO_2 coatings for enhanced osteoconductivity (Nakagawa et al., 2005; Zuldesmi et al., 2015), whereas little is known regarding its effect on peri-implant soft tissues.

This project aims to develop a nanostructure TiO_2 implant coating based on hydrothermal treatment of titanium surfaces. The aim is also to investigate its tissue and cellular responses in a soft tissue environment. Another purpose is to explore the effect of UV light on the biological and bactericidal properties of hydrothermal TiO_2 surfaces.

2 Review of the Literature

2.1 Soft tissue structure around natural teeth and implant surfaces

2.1.1 Gingival and peri-implant epithelial attachment

Although the soft tissue around dental implants has many features in common with the soft tissue attached to the natural teeth, represented by the presence of oral epithelium and continuous with a junctional epithelium, there are several fundamental dissimilarities between them (Berglundh et al., 1991; Listgarten et al., 1991). The soft tissue around natural teeth is termed gingiva. The gingival epithelium extends from the gingival crest to the junctional epithelium, and it is composed of three types of epithelium: oral epithelium, oral sulcular epithelium, and junctional epithelium (JE) (Figure 1). The junctional epithelium has two basal laminas: the internal basal lamina that attaches the junctional epithelium cells to the tooth surface and the external basal lamina through which the junctional epithelium attaches to the gingival connective tissue (Cate & Nanci, 2017; Schroeder & Listgarten, 1977). The epithelial attachment to both basal laminas is reinforced by hemidesmosomes along the entire length of the junctional epithelium (Listgarten, 1975; Stern, 1981., Larjava et al., 2011). This adherence to the tooth surface indicates that the junctional epithelium plays several protective roles and has a unique defense structure against microbial colonization of the underlying tissues (Bosshardt & Lang, 2005).

In dental implants, the soft tissue collar that surrounds the implant's transmucosal part is termed "peri-implant mucosa". It develops following implant placement and comprises epithelium components, which form an external barrier between the oral environment and the underlying connective tissues. The peri-implant mucosa composed of three types of epithelium: keratinized oral epithelium, peri-implant sulcular epithelium, and peri-implant epithelium (PIE), as well as the underlying connective tissue. These components, specifically the epithelial components, are in many ways analogous to those that surround natural teeth (Abrahamsson et al., 1996; Berglundh et al., 1991; Chai et al., 2010; Ivanovski & Lee, 2018). However, some differences are still evident.

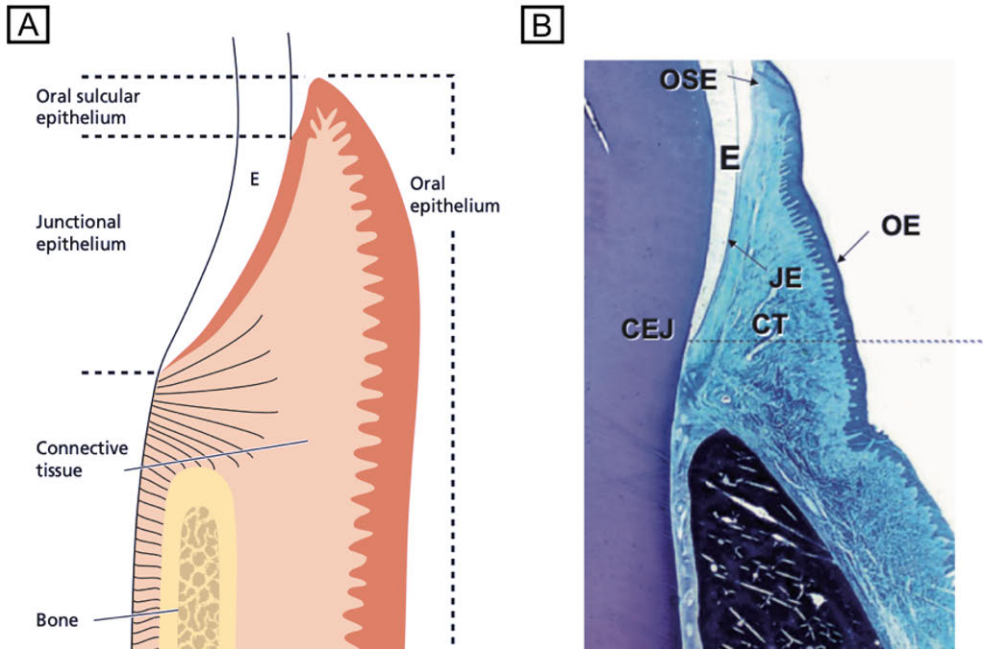

Figure 1. Gingival epithelial tissue. (**A**) a schematic drawing of a histologic section (**B**). The epithelium covering the free gingiva is differentiated as follows: OE, oral epithelium; OSE, oral sulcular epithelium; and JE, junctional epithelium. E, enamel; CT, connective tissue; CEJ, cemento-enamel junction. (Source: Lindhe J. (2008) Clinical periodontology and implant dentistry).

The soft tissue seal that develops around teeth and the dental implant is known as the biologic width. It comprises both epithelial (junctional epithelium) and connective tissue components and extending from the bottom of the oral sulcular epithelium to the top of the alveolar bone (Ingber et al., 1977). The biologic width around natural teeth is approximately 2.04 mm, composed of 0.97 mm junctional epithelium (JE) and 1.07 mm connective tissue attachment (Gargiulo et al., 1961). In contrast, the biological width around dental implants has slightly larger values ranging around 3 to ~ 4 mm with an average value of 2 mm of epithelial attachment and 1 to1.5 mm of connective tissue attachment (Abrahamsson et al., 1996; Berglundh et al., 1991; Berglundh &Lindhe, 1996; Buser et al., 1992; Cochran et al., 1997).

This attachment structure serves as a mechanical barrier against the bacterial invasion and thus resists pocket formation, gingival recessions, and alveolar bone loss (Berglundh & Lindhe, 1996; Cochran et al., 1997). The JE cells attach to natural teeth via internal basal lamina and hemidesmosomes throughout the JE-tooth interface. In comparison, the peri-implant epithelium displays slower cell proliferation with no evidence of true adhesion to abutment surfaces (Rompen et

al., 2006; Larjava et al., 2011). Previous studies reported that internal basal lamina and hemidesmosomes were confined only at the apical region of the PIE–titanium interface (Atsuta et al., 2005; Ikeda et al., 2002). This difference in epithelial attachment indicates that the peri-implant epithelial tissue has a lower functional sealing capacity than junctional epithelium around natural teeth (Atsuta et al., 2005; Buser et al., 1992; Ikeda et al., 2002). The weak PIE attachment may facilitate the formation of inflammatory lesions and bone loss around the implants, which may lead to unwanted clinical complications (Roos-Jansaker et al., 2006a, b).

2.1.2 Gingival and peri-implant connective tissue

The connective tissue attachment (lamina propria) extends from the apical end of the junctional epithelium to the alveolar bone crest. It has a cellular and an extracellular compartment composed of collagen fibers, fibroblasts, and blood vessels embedded in an amorphous ground substance (Bartold et al., 2000). In natural teeth, the collagen fibers are inserted into the tooth cementum in different orientations and form dense collagen fiber bundles called the gingival fibers. These fibers are named and described according to their origin, orientation, and termination (Schroeder & Listgarten, 1997). The most dominant fibers are the dento-gingival fibers that extend from the cementum to the lamina propria of the free and attached gingiva (Cate & Nanci, 2017). These fibers are predominantly inserted perpendicular/oblique to the root (cementum) surface and serve as a physical barrier against epithelial down growth and bacterial invasion.

The fibers orientation in the connective tissue around dental implants is fundamentally different from those around natural teeth. These fibers extend from the bone and run relatively parallel to the implant surface with no evidence of insertion into the implant surface owing to the lack of cementum and periodontal ligament around the implant (Abrahamsson et al., 1998; Berglundh et al., 1991; Buser et al., 1992; Listgarten et al., 1991; Listgarten, 1975) (Figure 2). Another difference concerning the peri-implant and gingival connective tissues is the degree of vascularization. The peri-implant connective tissue is very collagenous and exhibits a reduced amount of vascular supply compared to the highly vascularized connective tissue around natural teeth. The parallel orientation of the collagen fibers to the implant surface combined with few fibroblasts and vascular structures in the peri-implant connective tissue weakens the defense mechanism around the implants and make them more susceptible to bacterial invasion when compared with natural dentition (Abrahamsson et al., 1998; Ivanovski & Lee, 2018; Schupbach & Glauser 2007).

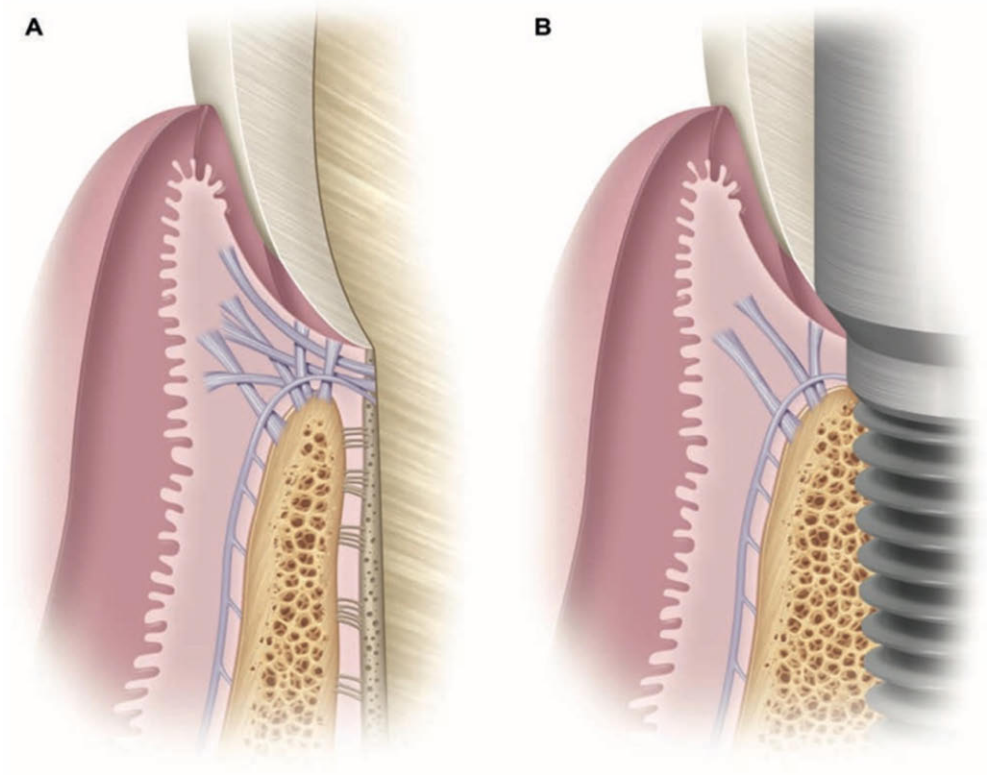

Figure 2. Comparison of tissues around natural tooth versus dental implant. (Source: Hupp JR, 2017). Introduction to implant dentistry. **A**. The natural tooth has periodontal ligaments between the tooth root and surrounding bone. The connective tissue fibers insert into the cementum. The gingival epithelium is composed of oral epithelium, oral sulcular epithelium, and junctional epithelium. **B**. The dental implant has no periodontal ligaments. The connective tissue fibers run parallel to the implant surface and have no insertion into it. The peri-implant mucosa is composed of keratinized oral epithelium, peri-implant sulcular epithelium, and peri-implant epithelium.

2.2 Wound healing at soft tissue/implant interface

The wound healing process around dental implants follows the same general principles and stages of periodontal tissue wound healing. It begins with coagulation of blood and hemostasis phase, followed by recruitment of inflammatory cells (an inflammatory phase), and finally granulation tissue formation and remodeling phase (Häkkinen et al., 2015). However, it has been found that at the early wound healing stage, the peri-implant tissues are characterized by a higher pro-inflammatory state compared to periodontal tissues (Emecen-Huja et al., 2013). This inflammation is considered necessary for wound healing and tissue regeneration (Tomasi et al., 2016).

Peri-implant wound healing initiates immediately after the closure of the mucoperiosteal flap around the neck portion of implant placement (one-stage procedure) or after abutment connections to an already installed implant (two-stage procedure). During implantation, the first tissue that comes into contact with the implant surface is blood (Park & Davies., 2000). The contact of blood to the implant surface begins with the adsorption of plasma or serum proteins, followed by a blood clot (Park & Davies., 2000; Hong et al., 1999). This clot (blood coagulum), which includes blood cells and activated and aggregated platelets, serves as a natural scaffold intermediating the surrounding living tissues and the implant material. (Park et al., 2001; Thor et al., 2007). Platelet adhesion and activation are important events in blood-material interaction. They release cytokines and growth factors that modulate other events such as cell migration, proliferation, and differentiation and play a crucial role in the peri-implant healing process (Park et al., 2001; Thor et al., 2007). The blood clot is then infiltrated by inflammatory cells (neutrophils and monocytes) that clear the wound site from invading bacteria and later on replaced by the granulation tissues (Sculean et al., 2014).

The build-up of soft tissue barriers around dental implants results from a wound healing process that takes several weeks. Berglundh et al. 2007 evaluated the process of wound healing around non-submerged commercially pure titanium implants in dogs. They observed that, immediately after implant placement, the blood clot occupied the implant-mucosa interface. The blood clot is then infiltrated and degraded by neutrophil granulocytes. At four days of healing, the initial soft tissue seal is formed by the clustering of leukocytes in a dense fibrin network. A few days later, the fibroblasts and the collagen occupy the apical part of the mucosal interface (Berglundh et al. 2007). Within a few days of the healing process, the epithelial cells begin to migrate from the surrounding wound margins towards the abutment surface. One to two weeks later, proliferation of the epithelial cells initiated, which eventually leads to the formation of the junctional epithelium. Two weeks after surgery, a newly formed connective tissue characterized by a high density of fibroblasts and blood vessels comes into contact with the abutment surfaces. After about three weeks, the number of fibroblasts decreased, the amount of collagen and matrix components increased, and eventually, the collagen fibers are organized in bundles after 4–6 weeks. The formation of the biological width and the maturation of barrier epithelium is completed after 6–8 weeks of healing. The peri-implant soft tissue's whole maturation and remodeling took place between 6 and 12 weeks of healing (Berglundh et al. 2007). The establishment of the above soft tissue attachments are essential for maintaining peri-implant tissue health.

2.3 Peri-implant infective diseases

Peri-implant diseases are inflammatory conditions affecting the tissues that are surrounding implants and their restorative components (Zitzmann & Berglundh, 2008). These inflammatory diseases are categorized into peri-implant mucositis and peri-implantitis, and they are associated with the accumulation of bacterial biofilms on the implant surface. Based on the Consensus Report of the 11th European Workshop on Periodontology (EWOP), the prevalence of peri-implantitis and peri-implant mucositis was reported to be around 22% and 43%, respectively (Derks & Tomasi, 2015). In another recent systemic review, the prevalence rate of peri-implantitis was about 9.2% at the implant level and 19.8% at the patient level. Whereas peri-implant mucositis was reported to be about 29% and 46,8% at implant and patient-level, respectively (Lee et al., 2017). The prevalence of peri-implant infective diseases has been reported in a wide range of values due to inconsistent criteria used to diagnose peri-implant diseases, varying study designs, and sample sizes (Lee et al., 2017; Zitzmann & Berglundh, 2008). These conditions can develop in the early period as a result of impaired wound healing (early infection) or later on after the implant integration process (late infection) (Jakobi et al., 2015).

2.3.1 Peri-implant mucositis vs. peri-implantitis

Peri-implant mucositis is an inflammatory disease in which the presence of inflammation is confined to the mucosa surrounding a dental implant without any loss of the bone supporting the implant (Albrektsson & Isidor, 1994; Berglundh et al., 2018; Lindhe & Meyle, 2008; Zitzmann & Berglundh, 2008). It is similar to gingivitis around natural teeth, and it may or may not progress to peri-implantitis (Pontoriero et al., 1994; Salvi et al., 2012). The initiation of peri-implant mucositis is associated with plaque accumulation and the formation of bacterial biofilms on the implant surfaces in a way similar to that found around natural teeth. Moreover, experimental peri-implant mucositis studies in humans have shown strong evidence of a relationship between the formation of bacterial biofilms on the implant surface and the development of an inflammatory response (Meyer et al., 2017; Pontoriero et al., 1994; Salvi et al., 2012; Zitzmann et al., 2001). This inflammatory response is more pronounced in peri-implant mucosa than an inflammatory response in the gingiva when exposed to the same bacterial challenge (Berglundh et al., 2011). The experimental peri-implant mucositis lesion is characterized by an inflammatory cell infiltrate present within the connective tissue lateral to junctional epithelium rich in plasma cells and lymphocytes (Heitz-Mayfield & Salvi, 2018).

The clinical signs of peri-implant mucositis may include redness, bleeding on probing, swelling, and suppuration (Heitz-Mayfield & Salvi, 2018). The accumulation of plaque, lack of compliance to maintenance care, smoking, and

radiation therapy are identified as risk indicators for developing peri-implant mucositis (Karbach et al., 2009; Rodrigo et al., 2012; Roos-Jansaker et al., 2006a, b). Peri-implant mucositis is a reversible condition if it is effectively treated (Pontoriero et al., 1994; Salvi et al., 2012). However, it is believed to be a precursor for peri-implantitis (Jepsen et al., 2015). Therefore, a regular supportive peri-implant therapy with biofilm removal is a prerequisite for preventing and managing peri-implant mucositis and hindering its progression to peri-implantitis.

Peri-implantitis is a plaque-associated pathological condition occurring in tissues around dental implants. It's characterized by soft tissue inflammation that includes redness, edema, mucosal enlargement, bleeding on probing and/or suppuration, along with increased probing depths. In addition to progressive loss of supporting bone compared to baseline measurements with or without recession of the mucosal margin (Berglundh et al., 2011; Carcuac & Berglundh, 2014; Berglundh et al., 2018; Zitzmann & Berglundh, 2008). Soft tissue inflammation is evaluated clinically by probing and the other signs of inflammation, while radiographs are used to detect bone loss (Schwarz et al., 2018). Similar to the peri-implant mucositis, the development of peri-implantitis is associated with the accumulation of bacterial biofilm on implant surfaces and their restorative components. As mentioned earlier, peri-implant mucositis is anticipated to precede peri-implantitis; however, the exact mechanisms where peri-implant mucositis converts to peri-implantitis have not been identified.

Peri-implantitis and periodontitis have many features in common. These similarities are in terms of clinical features and the etiological factors (Berglundh et al., 2011). However, the severity of inflammatory signs and disease progression rate may differ significantly (Carcuac et al., 2013). Human and animal experimental studies of undisturbed plaque formation on dental implants and teeth have shown more inflammatory cell infiltrate, including plasma cells and lymphocytes, along with neutrophils and macrophages in the peri-implant mucosa (Berglundh et al., 2011; Carcuac & Berglundh, 2014). The inflammatory lesions in peri-implantitis have a larger inflammatory cell infiltrate, approaching the crestal bone around implants with more tissue destruction (Berglundh et al., 2011).

An experimentally created peri-implantitis and periodontitis study suggested that peri-implantitis progresses faster with more rapid and pronounced bone loss (Carcuac et al., 2013). This faster progression could be related to the structural differences between peri-implant and periodontal tissues. Lack of cementum and the periodontal ligaments and the parallel orientation of the collagen fibers with the absence of collagen fiber insertions may have significant effects on disease susceptibility and progression (Berglundh et al., 2011). Additionally, inflammation and severe bone loss around implants may occur due to poor peri-implant epithelium attachment, reduced blood flow, and a deeper sulcus, thereby allowing for more

apical penetration of bacteria and subsequent infection than periodontal tissues (Schupbach & Glauser, 2007; Larjava et al., 2011). There is a strong correlation between the history of chronic periodontitis, poor plaque control skills, lack of regular maintenance, and an increased risk of developing peri-implantitis (Costa et al., 2012; Roccuzzo et al., 2012). Firm peri-implant soft tissue seal is essential for maintaining peri-implant tissue health; therefore, further surface modifications of the implant transmucosal component is necessary to improve the soft tissue attachment and obtain optimal healing process.

2.4 Titanium as a biomaterial

Over the last decades, commercially pure titanium (CpTi) and titanium alloys have been the most important metals used successfully and widely in biomedical and dental applications. They are considered the material of choice in dental implants, primarily due to their excellent biocompatibility in living tissues, good chemical stability, and high corrosion resistance (Kasemo, 1983). Moreover, they have desirable biomaterial properties in the oral environment such as good mechanical strength, successful integration with surrounding bone with a modulus of elasticity similar to that of bone as well as a low toxicity, allowing a favorable biological response (Kasemo, 1983; Niinomi, 2008).

Titanium is a dimorphic metal with two phases, α and β phase. α phase is a hexagonal close-packed crystal structure, and β phase is body-centered cubic crystal structure. During the processing, titanium exists as α phase up to a temperature of 882.5°C and it transforms to β phase above this temperature (Collings, 1984). Titanium alloys are classified into α, β, and α + β phases according to the room temperature microstructure (Polmear, 1981). As already mentioned, the titanium used in dental implants is mainly composed of commercially pure titanium (CpTi) or (Ti-6Al-4V) alloy. The CpTi is a single (alpha) phase crystal at body temperature. It is divided into four grades from 1 to 4 with various degrees of purity according to oxygen, carbon, and iron content (Darvell, 2018). In contrast, Ti-6Al-4V is an α + β phase alloy composed of 6% of aluminum and 4% of vanadium, with the addition of 0.25% of iron and 0.2% of oxygen. The remaining alloy is titanium. Ti-6Al-4V has higher strength, lower elastic modulus, and better corrosion resistance than commercially pure titanium (CpTi) (Liu et al., 2017).

Biocompatibility is the ability of the materials to perform in the presence of an appropriate host for a specific situation (Williams, 2008). Titanium and titanium alloys are generally regarded to have excellent biocompatibility that arises from the presence of a thin passivation film on titanium surfaces. It is well known that this native titanium dioxide (TiO_2) film with few nanometer thicknesses grows on titanium surfaces upon exposure to air or water and results in excellent corrosion

resistance and superior biocompatibility. However, this oxide film layer is usually non-uniform, very thin (3–7 nm), mechanically weak, and does not enhance the wound healing process (Liu et al., 2004). Moreover, titanium is considered a bioinert material because of its good anticorrosive properties (Ellingsen, 1991; Klinger et al., 1997). As a result of its bioinert nature, there seems to be a lack of direct interaction of titanium surfaces with biological molecules such as proteins and cells, and they require ionic bridges to attract necessary proteins (Ellingsen, 1991; Klinger et al., 1997; Steinberg et al., 1995). Therefore, numerous surface modification techniques have been developed to obtain a stable and uniform TiO_2 surface to enhance properties required for osseointegration (Liu et al., 2004), some of which will be further discussed.

Although most dental implant studies have focused on osseointegration, successful treatment depends on hard and soft-tissue integration. The soft tissue seal around the transmucosal implant surface is the main barrier to bacterial invasion into peri-implant tissues (Abrahamsson et al., 1998). The transmucosal area of the implant surface is usually made of a smooth turned titanium surface to reduce bacterial adhesion and biofilm formation. However, there is good evidence that surface modification of the transmucosal area can promote the soft tissue attachment (Hoshi et al., 2010; Werner et al., 2009), hamper the bacterial biofilm adhesion (Frojd et al., 2011), and facilitate firm attachment between the implant abutment and the surrounding soft tissue (Schupbach & Glauser, 2007; Welander et al., 2008).

2.5 Factors influencing peri-implant soft tissue attachment

The establishment of a proper soft tissue seal between the oral environment and the underlying peri-implant tissue is considered essential for the long-term success of implant therapy (Abrahamsson et al., 1998). This soft tissue seal around transmucosal abutment protects the tissue-implant interface from bacterial invasion, which may lead to marginal bone resorption and soft tissue recession. Abutment material and their surface characteristics such as surface chemistry, surface roughness, and surface wettability have been recognized as crucial factors that affect soft tissue health and stability (Abrahamsson et al., 2002; Burgers et al., 2010; Hamdan et al., 2006; Linkevicius & Apse, 2008; Teughels et al., 2006; van Brakel et al., 2011).

2.5.1 Abutment material

For decades, titanium has been the preferred material for dental implant abutment due to its well-documented biocompatibility as well as its mechanical and physical

properties (Adell et al., 1986). Titanium abutment has excellent clinical performance and a distinguished record on soft tissue response and mucosal healing (Lekholm et al., 2006; Zembic et al., 2014). Moreover, data from human and animal studies have shown that all commercially available abutment materials such as titanium, gold, and zirconia have desirable biocompatibility toward the surrounding tissue and allow for healthy mucosal attachment (Abrahamsson & Cardaropoli, 2007; Andersson et al., 2001; Lops et al., 2013; Vigolo et al., 2006; Linkevicius & Apse, 2008). However, currently, there is a trend towards tooth-colored abutment materials to improve esthetic outcomes. Linkevicius and Vaitelis (2015) published a systemic review and meta-analysis on the effect of zirconia and titanium abutment materials on soft peri-implant tissues. They reported that there is no clear preference for the use of zirconia or titanium as abutment materials concerning peri-implant soft tissue response. The meta-analysis demonstrated a better esthetic outcome for zirconia abutments in developing natural soft tissue color compared to titanium abutments.

2.5.2 Surface chemistry

The implanted material's interaction with the tissue or biological fluid is guided mostly by its surface properties and chemical composition. These properties may differ from that of the bulk material due to surface reactivity and preferential presentation of certain elements (Rompen et al., 2006). For example, the favorable properties of titanium and titanium alloys, such as their chemical inertness, corrosion resistance, and even biocompatibility, arise from the presence of a native oxide film that grows spontaneously on the surface upon exposure to air, as mentioned before. These properties are different from the bulk properties of titanium metal. Moreover, this thin oxide layer on the surface protects the bulk material from any further corrosion under normal conditions and provides the titanium and titanium alloys with excellent biological performance (Kasemo, 1983).

2.5.3 Surface wettability

The wettability of implant material is a vital surface property known to affect the biological response to the implant, and it has been recognized as a predictive indicator of cytocompatibility (Kasemo, 1983). Furthermore, good wettability improves protein and platelet adhesion on implant surfaces (Gittens et al., 2014; Kohavi et al., 2013).

The surface free energy (SFE) of a material is an indicator of its wettability. It is the excess energy that the surface has compared to the bulk of the material. It can be determined indirectly by measuring the liquid-solid contact angle (θ_C) in the presence of the different liquids based on Young's equation using different

mathematical approaches (Rupp et al., 2014). The contact angle is defined as the angle between the solid surface and the tangent line of the liquid phase at the solid-liquid-gas interphases. When a liquid is placed on a lower energy surface, the resulting contact angle will be higher as compared with a higher energy surface (Baier et al., 1968) and a high contact angle indicates poor wettability. In contrast, a low contact angle indicates good wettability (Kasemo, 1983) (Figure 3).

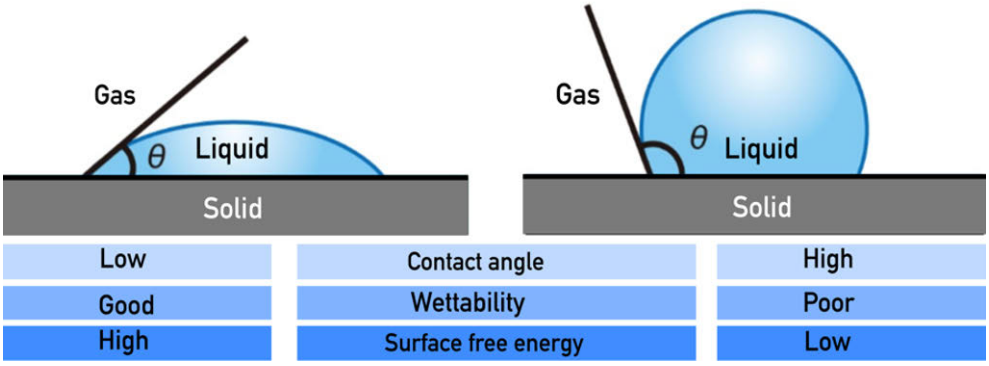

Figure 3. The contact angle (θ_C).

Many studies have shown that hydrophilic surfaces with high SFE promote fibroblast attachment, spreading, and proliferation compared with hydrophobic surfaces (Altankov et al., 1996; Ruardy et al., 1995; Webb et al., 1998). Wilson et al. (2005) reported that protein adsorption is promoted when blood and other biological fluids come in contact with hydrophilic surfaces which enhances cell adhesion. In contrast, hydrophobic surfaces disturb protein structure leading to less accessible cell-binding sites and eventually diminish cell adhesion. Schwarz et al. (2007) demonstrated that soft tissue integration is influenced by hydrophilicity rather than microtopography. Moreover, Schwarz et al. (2013) used a human model to histologically evaluate the peri-implant soft tissue attachment on healing abutments with either hydrophobic or hydrophilic surface properties. They demonstrated that healing abutments with hydrophilic surfaces showed the highest epithelial and connective tissue contact to the abutment surface and thus have the potential to enhance soft tissue adhesion at the transmucosal aspect of titanium implants.

Titanium surfaces exhibit good wettability and high surface energy due to their native oxide layer. However, these surfaces with high energy adsorb hydrocarbon contaminants from the atmosphere resulting in changes in surface chemical composition and low surface energy, thus reducing their bioactivity (Kasemo & Lausmaa, 1988; Morra et al., 2003). Hydrocarbon contaminations on implant surfaces have been shown to reduce the surface energy, interfere with protein

adsorption, and compromise the initial stages of tissue-healing (Baier et al., 1984; Rupp et al., 2018). Cleaning the contaminated implant surfaces increases surface energy and enhances cell adhesion and spreading (Baier et al., 1984; Doundoulakis, 1987). Therefore, different chair-side treatment methods such as plasma treatments and UV irradiation aim to reduce contaminations, increase hydrophilicity, and improve albumin adsorption and osteoblast attachment on the implant or abutment surfaces (Canullo et al., 2016; Choi et al., 2016). However, the degree of hydrophilicity for optimal biological and clinical outcomes remains unclear (Gittens et al., 2014).

2.5.4 Surface roughness

The surface roughness and topography of dental implant materials are important surface characteristics that have a significant role in determining implant success (Rupp et al., 2018). Dental implant topography can be divided into macro, micro, and nanoscale levels ranged from few millimeters to nanometers (Le Guéhennec et al., 2007). While high surface roughness of more than 10 µm has shown to enhance the early osseointegration and long-term mechanical stability, it may increase the risk of peri-implantitis ((Buser et al., 1991; Becker et al., 2000). However, a surface profile with a nanometer range has been shown to enhance protein adsorption, bone cell adhesion, and thus rate of osteointegration (Wennerberg et al., 2014). Moreover, nanostructured titanium surfaces have been shown to enhance human gingival fibroblast adhesion, proliferation, and extracellular matrix deposition, which ultimately affects the rate and quality of new tissue formation (Guida et al., 2013).

There are various types of tissue interfaces with the dental implant surfaces, consisting of subgingival hard tissue interface, soft tissue transgingival interface, and the interface to the oral cavity at the supragingival region. At the hard tissue interface, osteogenic properties are required to optimize osseointegration (Andrukhov et al., 2016). In contrast, at the soft tissue interface, the creation of epithelium and connective tissue seal is essential to prevent bacterial infiltration and inhibit epithelial down growth (Larjava et al., 2011; Quirynen et al., 2002). Therefore, dental implant surface should be improved to accomplish the different demands of the respective interfaces (Rupp et al., 2018).

Different surface modification techniques have been developed to alter titanium implants' surface topography, such as grit-blasting, acid etching, Ti plasma spraying, electrochemical anodic oxidation, and coatings. These techniques result in implant surfaces with different surface topographies (Wennerberg & Albrektsson, 2009). The transmucosal implant surface is usually made of a smooth turned titanium surface to reduce bacterial adhesion and biofilm formation. Many *in vitro* studies have indicated that the initial adhesion of human gingival fibroblasts and epithelial

cells is higher on smooth titanium surfaces than on rough surfaces (Baharloo et al., 2005; Cochran et al., 1994). Furthermore, some studies state that a surface roughness value of 0.2 μm is considered a threshold to form stable soft tissue attachment around titanium abutments (Bollen et al., 1996; Kim et al., 2015). Increased roughness value more than 0.2 μm results in colonization of the surface with bacterial biofilm rather than cells and tissue (Bollen et al., 1996; Kim et al., 2015; Quirynen & Bollen, 1995; Teughels et al., 2006). However, there is good evidence that surface modification of the transmucosal area can facilitate peri-implant soft tissue attachment (Hoshi et al., 2010; Werner et al., 2009), preserve the crestal bone (Botos et al., 2011), and impede the bacterial biofilm adhesion (Frojd et al., 2011). Moreover, Nevins et al. (2010, 2012) demonstrated an intimate connective tissue attachment to laser-micro-grooved abutment surfaces in their histological studies.

Ra and Sa are the most commonly used parameters to describe the surface roughness of dental implants. Ra (profile) is the two-dimensional counterpart of the three-dimensional descriptor Sa (area). They are defined as the arithmetic mean of the absolute departures from a mean plane (Wennerberg & Albrektsson, 2009). However, at present, the measurement and the evaluation techniques for surface roughness of dental implant materials need to be standardized, and different roughness parameters should be used to provide better characterization for implant surfaces (Rupp et al., 2018).

2.6 Titanium surface modification

In the last few decades, different titanium surface modification techniques have been developed to increase bone-implant contact and improve the osseointegration of titanium implants. These modifications can alter surface topography or surface chemistry in order to promote the wound healing process and improve long-term implant success (Rupp et al., 2018). Titanium implants are roughly divided into three different types of surface roughness (S_a): machined or minimally rough (± 0.5 μm), moderately rough (1.0–2.0 μm), which is the most currently marketed implants, and rough (> 2.0 μm) (Albrektsson & Wennerberg, 2004). Several surface modifications were developed and applied to titanium implants by various subtractive and additive methods (Wennerberg & Albrektsson, 2009).

2.6.1 Subtractive processes

In these procedures, the implant is subjected to various physical and chemical agents, which make the surface rough by removing a small amount of material to create pits or pores on the surface. Some examples of subtractive procedures include

electropolishing, mechanical polishing, blasting, etching, and oxidation (Wennerberg & Albrektsson, 2009).

Grit/Sandblasting surfaces

Sandblasting is one approach used for roughening the titanium surface. The method consists of blasting the implants with abrasive ceramic particles such as alumina (Al_2O_3), titanium dioxide (TiO_2), or calcium phosphate particles under high pressure. These ceramic particles should be chemically stable, biocompatible, and should not hinder the osseointegration. Depending on the size of the ceramic particles, different surface roughnesses can be produced on titanium implants. For instance, blasting titanium dental implants using titanium oxide particles with an average size of 25 μm can produce a surface with an average roughness of 1–2 μm, placing it within the category of moderately rough surfaces (Le Guéhennec et al., 2007). Many experimental studies have demonstrated a higher bone-to-implant contact with blasted surfaces than machined surfaces (Müeller et al., 2003; Novaes et al., 2002). Comparative clinical studies showed higher marginal bone levels and survival rates for TiO_2-blasted implants than for machined implants (Astrand et al., 1999; van Steenberghe et al., 2000).

Acid etching surfaces

This technique aims to increase surface roughness and remove contaminants from the implant surface (Rupp et al., 2018). It can be performed by immersing the titanium dental implant into a strongly acidic solution such as hydrochloric, sulfuric, nitric, hydrofluoric, or a combination of different acids. These acids will etch the surfaces by removing a small amount of material and create micro-pits on titanium surfaces with sizes ranging from 0.5 to 2 μm in diameter (Massaro et al., 2002). Acid-etched surfaces have been shown to increase active surface area, improve cell adhesion, and enhance osseointegration (Wong et al., 1995). Treating titanium implants in fluoride solutions is another chemical approach that aims to create a surface roughness and enhance osseointegration of dental implants (Ellingsen, 1995). Fluoride-modified implants demonstrated more significant bone to implant contact and higher removal torque than non-modified control implants (Ellingsen, 1995; Ellingsen et al., 2004).

Sandblasted and acid-etched (SLA) surfaces

A combination of blasting and etching has been a commonly used surface modification technique. The acid treatments are carried out after a blasting step to

remove blasting damaged surface zones and to refine at the same time surface roughness characteristics. SLA treatment can produce surfaces with an average roughness of 1.5–2 μm (Wennerberg & Albrektsson, 2009). This method is one of the earliest methods that have been commercially available for a long time. The sandblasted and etched surface has demonstrated higher removal torque value (Buser et al., 1998) and a greater amount of bone-to-implant contact than the machined surface (Grassi et al., 2006).

Oxidized surfaces

These surfaces are commonly achieved with heat treatment or with the implant placed as an anode in a galvanic cell with a suitable electrolyte. Anodic oxidation is an electrochemical process where the implant is immersed in strong acids at high current density. The implant becomes an anode resulting in micro or nanoporous surfaces of variable diameter and an increase of the overlying titanium oxide layers. This technique alters the surface topography and surface chemistry, which are essential for the biological bone response (Sul et al., 2005). Oxidized implant showed more bone-to-implant contact and higher removal torque value than machined implant surface (Ivanoff et al., 2003; Park et al., 2007; Shibli et al., 2007; Sul et al., 2006).

2.6.2 Additive processes

They are surface treatment methods in which the implant surface is coated with various biomaterials that improve the implant's biological and biomechanical properties. Few examples of additive processes include titanium plasma spraying (TPS), plasma-sprayed hydroxyapatite (HA) coating and calcium phosphate (CaP) coatings, ion deposition, ceramic coating, and fluoride coating (Mendonca et al., 2008; Wennerberg & Albrektsson, 2009). Some common titanium modification techniques are described in this section.

Plasma spray coating

The plasma spraying technique includes spraying of thermally melted materials onto the implant surfaces. In this technique, hydroxyapatite and titanium particles are injected into a plasma torch at high temperatures and projected onto the titanium surface (Coelho et al., 2009). The resulting titanium plasma-sprayed coatings can be deposited with an average roughness of around 7 μm (Wennerberg & Albrektsson, 2009), which increases the surface area of the implant. It has been shown that the bone-implant interface forms faster with a titanium plasma spray surface than with

smooth surface implants (Buser et al., 1991). Plasma-sprayed coatings can be deposited with a thickness ranging from a few micrometers to a few millimeters (Le Guéhennec et al., 2007).

The hydroxyapatite coatings have been shown to improve the initial healing process and enhance bone formation (Block et al., 1987). However, the plasma-sprayed coating has common drawbacks, such as porosity of the coating and residual stress at the substrate-coating interface (Browne & Gregson, 2000). One of the concerns with plasma-sprayed coatings is the coating delamination from the surface of the titanium implant and failure at the implant-coating interface (Ong et al., 2004). Furthermore, clinical studies demonstrated more marginal bone resorption around titanium plasma spray surfaces than minimally to moderately rough surfaces (Åstrand et al., 2000; Becker et al., 2000). Magnetron sputtering method has also been used to obtain hydroxyapatite coating on metal surfaces (Surmenev et al., 2017). This method allows for the deposition of calcium phosphate coatings with uniform thickness and good adhesion to the substrate (Hulshoff et al., 1996; Huang et al., 2017).

2.7 Surface roughness at the nanoscale level

The modification of the implant surface roughness at the nanoscale level (i.e., composed of nanosized materials with a size range between 1–100 nm) is a current interest approach. Nanoscale modification of the titanium implant surface may affect the surface chemistry and topography and change the implant surface interaction with ions, protein, and cells (Mendonca et al., 2008). These interactions can positively influence molecular and cellular activities and promote tissue healing at the titanium–bone interface (Kubo et al., 2009; Tomsia et al., 2013). Different methods have been developed to modify titanium implants with nanoscale features. Some of these approaches involve physical methods (Webster, 2004), chemical treatments (Cooper, 2006), innovative sandblasting/acid etching (Ellingsen et al., 1995, 2004), peroxidation and galvanostatic anodization (Sul et al., 2005; Wang et al., 2002), and crystal deposition of nanoparticles onto the titanium surface (Kim et al., 2004). Several studies have demonstrated that implants with nanostructure surface modification enhance osteoblast adhesion, proliferation, and improve bone tissue integration (Meirelles et al., 2008; Wennerberg et al., 2014). However, the optimal size and distribution of nanometer particles or pores applied to implant surfaces is still unknown.

Nanostructure modifications can be applied on implant surfaces with the use of nanosized HA or TiO_2 particles. Various surface modifications have been used to obtain a bioactive titanium oxide layer on the titanium surface and enhance its properties. These include plasma spraying (Lee et al., 2004), chemical treatments

using acids, alkaline solution or hydrogen peroxide (Kim et al., 1996; Wang et al., 2002), sol-gel coating method (Peltola et al., 1998), anodic oxidation (Yang et al., 2004) and hydrothermal surface treatment (Takebe et al., 2012). Among these, the hydrothermal (HT) treatment appeared as a simple, cost-effective, and more feasible chemical coating method to produce thin, firmly attached layers of anatase crystalline TiO_2 coating of well-defined morphology (Byrappa & Adschiri, 2007; Nakagawa et al., 2005).

2.7.1 Hydrothermal treatment of titanium surface

The hydrothermal processing can be defined as any heterogeneous reaction in the presence of aqueous solvents or mineralizers under high pressure and relatively low-temperature conditions to dissolve and recrystallize materials that are relatively insoluble under ordinary conditions. HT treatment is a chemical method used to produce crystalline titania coatings on various metal substrates (Drnovšek et al., 2009; Ueda et al., 2008). The titania coating has a good bone-bonding ability, and its bioactivity is attributed to the formation of OH^- groups on the coated surface (Kokubo et al., 2003). In contrast to bioactive coatings, such as bioactive glass, which dissolves in body fluid, the HT induced TiO_2 remains as a protective coating on the metallic implants (Albayrak et al., 2008; Kim et al., 2004).

Several attempts have been made to produce an anatase crystalline TiO_2 coating layer on titanium and titanium alloy surfaces using a hydrothermal (HT) treatment (Cheng et al., 2004; Ueda et al., 2008; Wong et al., 2007). Furthermore, a homogenous crystalline coating can be obtained directly at the relatively low reaction temperature, and it can be used on surfaces with complex shapes and topographies (Zuldesmi et al., 2015). Hamad et al. (2002) performed a surface modification of titanium with HT treatment in calcium solutions. They showed that HT treatment enhances the precipitation of apatite on the titanium surface. Also, HT treatment has been found to improve osteoconductivity, enhance wettability and encourage human gingival fibroblast adhesion and proliferation on titanium surfaces (Nakagawa et al., 2005; Shi et al., 2015; Zuldesmi et al., 2015). Furthermore, *in vivo* animal studies using HT titanium implants have demonstrated that HT treatment enhanced the epithelial cell attachment and reduced epithelial down-growth (Ayukawa et al., 2019; Oshiro et al., 2015). However, the studies evaluating HT coatings effect on peri-implant soft tissues are still limited.

2.8 Photocatalysis on TiO_2

Photocatalysis of TiO_2 has been studied extensively during the last few decades. This technology provides self-cleaning, self-sterilizing capabilities and is considered as

an alternative approach to achieve antibacterial properties on biomaterials based on the photo-induced hydrophilicity and decomposition reaction (Fujishima et al., 2008; Foster et al., 2011; Riley et al., 2005; Unosson et al., 2013). Different coating approaches have been developed to achieve photocatalytic bactericidal properties of TiO_2 (Riley et al., 2005; Rupp et al., 2010; Suketa et al., 2005; Unosson et al., 2012). UV photofunctionalization of titanium has gained much attention recently as a surface modification method for titanium surfaces. It has been shown to enhance the biological capacity and physicochemical properties of titanium surfaces without altering the implant surface topographical or morphological features (Aita et al., 2009a; Iwasa et al., 2010).

TiO_2 photocatalytic capacity involves the light-induced catalysis of reducing and oxidizing reactions on its surface. This photocatalytic reaction occurs when a light source with short enough wavelengths interacts with the surface of this semiconductor. TiO_2 has three crystalline forms: anatase, brookite, and rutile. The crystalline anatase TiO_2 is considered a semiconductor with a band gap energy of 3.2 eV, i.e., the gap between the valence band (VB) and conduction band (CB), meaning that its electrons cannot move freely without energy input. When irradiated with UV light of equal or higher energy (i.e., a wavelength shorter than 385 nm), it promotes electrons (e^-) to the CB and leaves a positively charged electron hole (h^+) behind in the valence band VB and as a result, an electron-hole pair with substantial reducing and oxidizing potentials, are generated (Equation 1). The hole in the valence band can oxidize the hydroxide ions or water adsorbed on the surface to produce hydroxyl radicals (•OH) and hydrogen peroxide (H_2O_2). In contrast, the electron in the conduction band can reduce oxygen to generate superoxide radicals (O_2^-) (Equation 2–5).

$$TiO_2 + h\nu \longrightarrow e^-_{CB} + h^+_{VB} \quad (h\nu = \text{high voltage/high energy}) \quad (1)$$

$$H_2O + h^+_{VB} \longrightarrow \bullet OH + H^+ \quad (2)$$

$$OH^- + h^+_{VB} \longrightarrow \bullet OH \quad (3)$$

$$\bullet OH + \bullet OH \longrightarrow H_2O_2 \quad (4)$$

$$O_2 + e^-_{CB} \longrightarrow O_2^- \quad (5)$$

The products •OH, O_2^- and H_2O_2 are free radicals known as reactive oxygen species (ROS) generated in the photocatalytic reaction (Foster et al., 2011). These ROS are strong oxidants that can react with organic material, such as adherent bacteria and mineralizing them into CO_2 and H_2O (Fujishima et al., 2008; Maness et al., 1999) (Figure 4). The bactericidal activity of photocatalytic TiO_2 has been attributed to lipid peroxidation that damages the bacterial cell membrane and or cell wall, leading to cell death (Maness et al., 1999).

UV treatment converts hydrophilic nanostructured Ti alloy surfaces to super hydrophilic and cleans the contaminants of hydrocarbons that accumulate on titanium surfaces (Aita et al., 2009b).

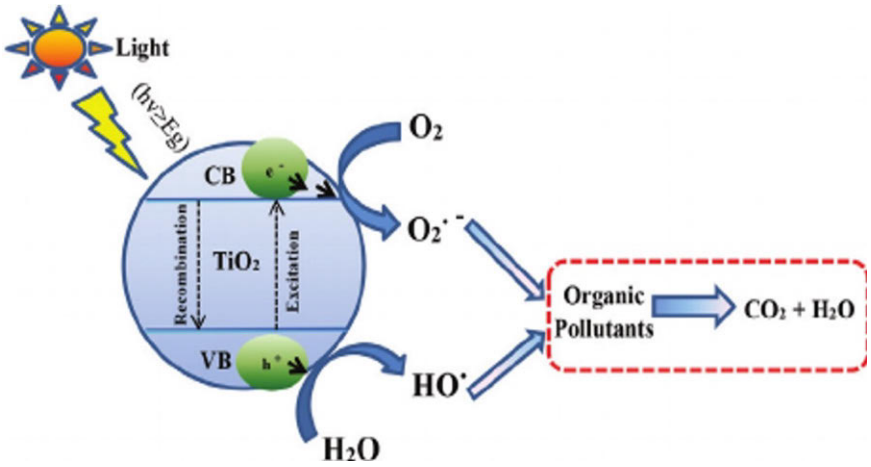

Figure 4. The mechanism of photocatalysis process on anatase TiO_2. (Source: Samsudin et al., 2015).

Photocatalytic TiO_2 films are multifunctionally useful in biomedical applications due to their superhydrophilic and potential bactericidal properties, both induced by UV treatment (Rupp et al., 2010, 2018). Numerous studies have shown that UV-treated titanium implant surfaces increase the rates of attachment, proliferation, and differentiation of osteoblast cells and enhance protein adsorption (Aita et al., 2009a, b; Hori et al., 2010a). Furthermore, UV light treatment on various titanium surfaces has been shown to reduce the bacterial attachment and subsequent biofilm formation of wound pathogens (de Avila et al., 2015; Yamada et al., 2014). Therefore, the possibility of adding an *in situ* self-cleaning and antibacterial feature to biomedical implants and devices where UV light can access, using a simple method, can be an effective measure to reduce implant infection-related complication.

3 Aims

The research presented in this thesis was performed to develop a nanostructured TiO_2 implant coating based on hydrothermal treatment of titanium surfaces, which aimed to be used as oral implant and abutment coatings. The aim was also to investigate its tissue and cellular responses in a soft tissue environment. Furthermore, to explore the effect of UV light treatment on the biological and bactericidal properties of HT induced TiO_2 coatings.

This research was based on the working hypothesis that HT produced TiO_2 coatings will improve wound healing and enhance soft tissue attachment on titanium surfaces. It was also hypothesized that HT produced TiO_2 coatings could be further activated with UV light treatment. The following specific studies were set to test the hypotheses:

1. Evaluate blood clotting ability, platelet activation, and protein adsorption on the HT coated and non-coated titanium surfaces (Study **I**).
2. Explore the effect of UV light treatment on the HT coated and non-coated titanium surface wettability, blood thrombogenicity, and cellular response (Study **I** and **II**).
3. Study the adhesion and the proliferation of human gingival fibroblasts on HT coated and non-coated titanium surfaces *in vitro* (Study **II**).
4. Examine the HT coating effect on the formation of peri-implant tissue attachment *in vitro* (Study **III**).
5. Assessment of early biofilm formation on HT coated and non-coated titanium surfaces *in vivo* and examine the effect of UV light treatment on the biofilm development (Study **IV**).

4 Materials and Methods

4.1 Substrate preparation

Ti-6Al-4V (α + β) titanium alloy substrates with different shapes were fabricated for each experiment (I, II, and IV). The specimens were ground using silicon carbide grinding paper of 1200 grit to a Ra value of 0.15 μm, after which they were cleaned ultrasonically with acetone and ethanol (5 + 5 minutes) and dried in the air before any surface treatments were carried out. In study III, Surtex® titanium (Ti-6Al-4V) alloy posts (Dentatus titanium posts, Stockholm, Sweden) were used to function as implants. All the substrates used were autoclaved using (Tuttnauer Elara11, Breda, Netherlands) for 20 minutes at 121°C before use.

4.2 Surface treatments

Titanium dioxide (TiO_2) coatings were applied to the substrates by using the sol-gel derived MetAlive™ coating (MA) technique or hydrothermal treatment (HT).

4.2.1 Sol-gel derived coating (I, II)

Sol-gel treatment was used to prepare the nanoporous TiO_2 thin film on the titanium substrates to serve as a positive control group (study I & II). The sol was made as initially described by (Peltola et al., 1998). Briefly, tetra isopropyl orthotitanate [$Ti(OCH(CH_3)_2)_4$] was dissolved in absolute ethanol (solution I). Ethylene glycol monoethylether ($CH_3CH_2OCH_2CH_2OH$), deionized water, and fuming hydrochloric acid (HCl 37%) were dissolved in ethanol (solution II). Solutions I and II were mixed rapidly and stirred vigorously for 3 minutes. The sol was kept at 0 °C during the aging and subsequent dip-coating process. The coating procedure started after 24 hours of sol aging, and the resultant solution was used to coat the substrates. The substrates were dipped into the solution and then withdrawn at a speed of 0.3 mm/s. The coated substrates were then sintered at 500 °C for 10 minutes, then cleansed ultrasonically in acetone and ethanol for 5 minutes, and finally dried at the ambient temperature.

4.2.2 Hydrothermal treatment (HT)

Hydrothermal treatment was used to prepare the nanostructure TiO_2 thin film on the titanium substrates. The HT suspension was prepared by dissolving titanium dioxide (TiO_2), purified water, 1:10 diluted tetramethylammonium hydroxide (TMAH) $(N(CH_3)_4^+OH)^-$and mixed for 5 minutes. Titanium substrates were laid at the bottom of Teflon containers, consisting of a Teflon inner vessel and a stainless-steel jacket; thus, the hydrothermal suspension was added. Next, the vessel was kept at 150 ± 10 °C at a constant-temperature oven for 48 hours (Figure 5). After the HT treatment period, the titanium substrates were removed from the vessel and cooled in the air. All the coated substrates were washed with distilled water in an ultrasonic bath for 10 minutes.

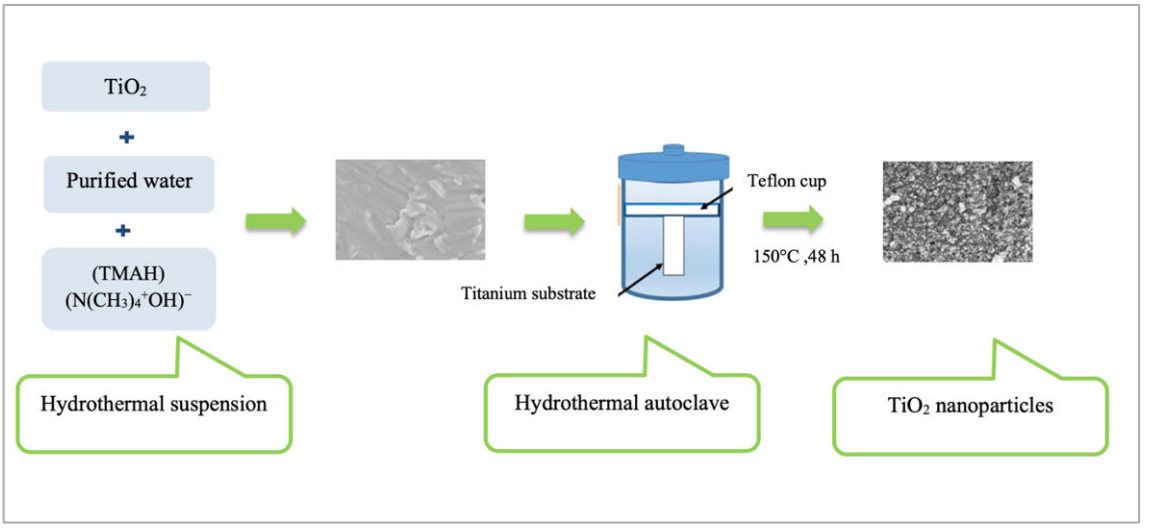

Figure 5. A simplified illustration of the hydrothermal treatment used in this thesis to produce nanostructure TiO_2 thin film on the titanium substrates.

4.2.3 Ultraviolet light treatment (I, II, IV)

TiO_2 coated and non-coated substrates were treated with UV light from 15 to 60 minutes in (I, II, and IV) under ambient conditions using a 36 W puritec HNS germicidal ultraviolet-C lamp (Osram GmbH; Germany), with a dominant wavelength of 254 nm. These UV parameters are shown to have a photocatalytic effect on TiO_2 (Fujishima et al., 2008). The UV treated titanium substrates were used for the experiments immediately following the UV light treatment (fresh surface).

4.3 Surface characterization (I)

The chemical composition of the HT coated substrates was examined by X-ray photoelectron spectroscopy (XPS). HT coated substrates were treated with UV for various times (5, 15, 60 minutes). The substrates were allowed to stay in contact with air for two weeks after the production to compare the substrate material surfaces. Comparative cleaning of samples was performed using deionized water and ethanol in an ultrasonic bath for 5 minutes. HT coated substrates were treated with UV light directly as received from storage, whereas the native surface (before UV) was analyzed as received from storage. The XPS measurements were carried out using a Physical Electronics Quantum 2000 instrument with a monochromatic Al Kα X-ray excitation, operated at 24.4 W. The diameter of the analysis spot was 100 μm.

4.4 Scanning electron microscopy (I, II)

In study (I), the substrates' surface topography was characterized using field-emission scanning electron microscopy (SEM). An approximately 20-nm-thick gold layer was applied on the substrates with a sputter coater, and secondary electron images were recorded with SEM. Furthermore, the platelet morphological characteristics were observed with SEM. In study (II), SEM images of the tested substrates were carried out to observe the adherent fibroblasts and to confirm the proliferation results on the substrates investigated. All the tested substrates were fixed with a 2.5% glutaraldehyde solution, rinsed in PBS, and dehydrated at increasing alcohol concentrations (35%, 50%, 70%, 95%, and 100%) for 30 minutes each. The final 100% ethanol wash was then replaced with hexamethyldisilazane (HMDS) 50% for 30 minutes, followed by 100% HDMS overnight. The samples were stored in the desiccator for 24 hours before used for SEM analysis. An approximately 20-nm-thick gold layer was applied on samples with a sputter coater for examination in an SEM (Phenom ProX-Netherlands).

4.5 Surface wettability (I, II)

4.5.1 Contact angle measurements

The water contact angle measurements were used to determine the surface wettability of a material. Equilibrium contact angles (θ_C) were measured using the sessile drop method, with a contact angle meter (KSVCAM100 KSV, Instrument LTD, Helsinki, Finland). A drop was deposited on the surface of the substrates and images were recorded for 20 seconds by collecting one image per 2 seconds using a video camera. The contact angles were calculated on substrates by the device’s

image analysis system using the Young-Laplace equation, giving values for the contact angles on both sides of the droplet and their mean values. Three liquids were used as a probe for SFE calculations: distilled water, diiodomethane, and formamide. The result was the contact angle mean value of at least 6 drops for each liquid on each tested substrate type.

4.5.2 Surface free energy calculations

The SFE of the substrates was calculated using the Owens-Wendt (OW) approach. In the OW approach, the SFE (γ_s) of solid material is a sum of the short-range polar (hydrogen bonding) (γ^p) and the long-range dispersion (Lifshitz-van der Waals) (γ^d) components. The total (γ^{tot}), dispersive (γ^d), and the polar (γ^p) SFE components were calculated. The following equation was used:

$$1 + \cos\tau = 2\left(\gamma_s^d\right)^{\frac{1}{2}}\left(\frac{\left(\gamma_L^d\right)^{\frac{1}{2}}}{\gamma_L}\right) + 2\left(\gamma_s^P\right)\left(\frac{\left(\gamma_L^P\right)^{\frac{1}{2}}}{\gamma_L}\right)$$

Where θ is the contact angle between the tested surface and standard liquid, γ_s is the SFE of the surface, and γ_L is the SFE of the liquid.

4.6 Thrombogenicity and blood response (I)

4.6.1 Blood clotting

The blood clotting time of the titanium substrates was assessed using a whole blood kinetic clotting time method, as previously described (Huang et al., 2003; Abdulmajeed et al., 2014). Fresh human blood was drawn from a healthy non-smoker adult female volunteer, who had not taken any medications for the past 14 days, by venipuncture into vacutainer tubes. A total of 96 titanium substrates were used. Each of the experimental group (HT; MA; NC) had 32 substrates. Half of the substrates (n=16) were UV treated in each group, while the other half were left without UV treatment. To avoid contamination with tissue thromboplastin caused by needle puncture, the first 3 ml of the drawn blood was discarded. Each substrate (Square-shaped; 10x10x1 mm) was settled in wells of a 12-well plate, and then, 100 µl volume of the blood was immediately added to the surface of the UV and non-UV treated substrates. All substrates were incubated at room temperature for 10, 20, 40, and 60 minutes. Four technical replicates (n=4) per each group were used for each time point, and the experiment was repeated twice. At the end of each time point, the substrates were incubated with 3 ml of ultrapure water for 5 minutes. The addition of ultrapure water lysed the red blood cells that had not been trapped in a

thrombus, thereby releasing their hemoglobin into the water for subsequent measurement. For clotting time measurement, each well was sampled in triplicate (200 µl each) and transferred to a 96-well plate. Free hemoglobin concentration in the water was assessed by measuring the absorbance level of the solution using an ELISA plate reader (Multiskan MS, Labsystems, Helsinki, Finland) at 570 nm. The clot size formed on the surfaces of the substrates is inversely proportional to the absorbance value recorded (Abdulmajeed et al., 2014). In other words, a lower absorbance value recorded means a lower hemoglobin concentration in the whole blood solution, which translates to more extensive thrombus formation on the substrate.

4.6.2 Platelets adhesion and morphology

A platelet adhesion test was conducted to evaluate the morphology and the adhesion behavior of the platelets on the UV and non-UV treated titanium substrates. Fresh human blood was collected from a healthy adult volunteer and treated with an anticoagulant (0.109 M solution of sodium citrate) at a dilution ratio of 9:1 (blood/sodium citrate solution). Platelet-rich plasma (PRP) was obtained by centrifuging the anticoagulated blood at 1500 rpm for 15 minutes at room temperature. A total of 18 titanium substrates were used. Each of the experimental group (HT; MA; NC) had six substrates. In each group, half of the substrates were UV treated, while the other half were not exposed to UV treatment. Three technical replicates per each group were used (n = 3) and the experiment was repeated twice. The PRP (100 µl) was carefully added to the substrates' surface and then they were incubated at 37 °C for 1 hour according to a previous study performed in our laboratory (Abdulmajeed et al., 2014). After the incubation period, the substrates were rinsed thoroughly three times with phosphate buffered saline (PBS) to remove weakly adherent platelets. The adhered platelets were then fixed for 2 hours at room temperature with 2.5% glutaraldehyde solution. Eventually, all substrates were rinsed in PBS and dehydrated at increasing alcohol concentrations (35%, 50%, 70%, 95%, and 100%) for 15 minutes each. The dried substrates were mounted on a metal stub and coated with a carbon sputtering coating of 10–20 nm thick.

The platelet morphologies were assessed through scanning electron microscopy (SEM) based on qualitative analysis. Two images per each substrate at different magnifications were collected at randomly selected fields. The adherent platelet's activated patterns were assessed based on the criteria described by Goodman et al.,1984. Accordingly, the platelets were defined as round or discoid cells; dendritic shape; early pseudopodial spread; and fully spread.

4.6.3 Protein adsorption and analysis

The collection of adsorbed proteins on the substrates' surfaces was made with few modifications to the previously described method (Tanner et al., 2003). Twelve titanium substrates were equally divided into six experimental groups (NC, UVNC, MA, UVMA, HT, and UVHT). Each group had two technical replicates (n = 2) and the experiment was repeated twice. The titanium substrates (Square-shaped; 10x10x1 mm) were rolled for 1 hour at room temperature in tubes containing human plasma diluted with PBS at a ratio of 1:4. The substrates were then removed and washed twice with PBS for 2 minutes.

Microbrushes (Quick-Stick® Dentsolv AB, Saltsjö-Boo, Sweden) were wetted with 4 µl of sodium dodecyl sulphate polyacrylamide gel electrophoresis (SDS-PAGE) buffer (1 mM Na-phosphate buffer, 2% SDS, 0.003% bromophenol blue). Proteins bound to the substrates were desorbed by rubbing the top and bottom surfaces of each substrate with two wet brushes and finally with one dry one. The tips of these microbrushes were then collected in an Eppendorf tube containing 20 µl of the buffer. The tubes containing the microbrushes were then heated in boiling water for 7 minutes. The tubes were then perforated with a needle and placed in larger tubes that collected the sample solutions after centrifugation for 2 minutes (Heareus PICO17, ThermoFisher Scientific, Waltham, USA). Samples of duplicate specimens (from each surface) were collected in the same tube.

The electrophoresis was performed in a non-reducing condition and equal volumes of each sample (10 µl) were loaded in the gel. The protein solutions were analyzed with SDS-PAGE and silver staining using gradient Mini-Protean TGX gels (4–12%; Bio-Rad Laboratories, Berkeley, USA). An imaging system (ChemiDoc MP, Bio-Rad Laboratories, Hercules, USA) was used to take images and examine the resultant gels. The same procedure was repeated by rolling the substrates in a solution of 0.125 mg/ml bovine fibronectin (Sigma-Aldrich, St. Louis, USA), to evaluate the adsorption of fibronectin on the substrates.

4.7 Cell culture experiments (II)

4.7.1 Fibroblast cell cultures

Human gingival fibroblasts were obtained from a gingival biopsy sample of a periodontally healthy young adult female volunteer (Oksanen & Hormia., 2002). Cells were maintained in Dulbecco's modified Eagle's medium (DMEM) supplemented with 10% fetal bovine serum and antibiotics (100 IU/ml penicillin and 100 µg/ml streptomycin) (Gibco BRL, Life Technologies, Paisley, UK) and incubated at 37 °C in a 5% CO_2 environment. Semi-confluent cultures were

trypsinized, and cells were counted and resuspended in a complete culture medium. The culture medium was changed three times a week. Human gingival fibroblasts were collected from passage 8 –10 to evaluate the cell adhesion resistance and cell proliferation on experimental surfaces.

4.7.2 Cell adhesion resistance against enzymatic detachment

Fibroblasts were plated at a density of 20,000 cells/cm^2 (38,000 cells/well) on UV and non-UV treated coated and non-coated titanium substrates. Seventy-two titanium substrates (Square-shaped; 7x7x1 mm) were used on six experimental groups (NC, UVNC, MA, UVMA, HT, and UVHT), n=12. Two 24-well plates were used (one for the non-trypsinized and one for the trypsinized substrates). Six technical replicates were used for each group (trypsinated and non-trypsinated), and the experiment was repeated twice.

Fibroblast cells were allowed to adhere for 6 hours at 37 °C. The resistance against enzymatic detachment was evaluated by trypsinizations with 1:10 diluted enzymes in phosphate-buffered saline (PBS; 0.005% trypsin, 0.05 mM ethylenediaminetetraacetic acid [EDTA]; Gibco, Invitrogen). This method was used with few modifications made to the method previously described by Meretoja et al. (2010). After the incubation period, both non-trypsinized and trypsinized substrates were washed three times with PBS to remove non-adherent cells. Trypsinized plates were placed on clean culture plates with enzyme solution (1.25 ml per substrate) and incubated on a rotary shaker (Max Q 2000; Barnstead International, Iowa), with an orbital speed of 100 rpm at room temperature for 15 minutes. Trypsin was removed and DMEM was placed. The substrates were then washed three times with PBS. The cells on both non-trypsinized and trypsinized substrates were fixed with formalin for 15 minutes and washed three times with PBS. A fluorescence stain (Hoechst 33342) was used, and the substrates were incubated on a rotary shaker (100 rpm at room temperature) for 15 minutes, after which the substrates were washed three times with PBS. A fluorescence microscope was used for cell imaging (Zeiss-stereo-lumar-v12), with an objective lens of NeoLumar 0.8×, for both trypsinized and non-trypsinized samples.

The images were analyzed for cell counting using ImageJ automatic cell counter. The total surface area was imaged for each substrate; six images for each group were analyzed (trypsinized and non-trypsinized), and the percentage of detached cells was calculated. Cell counting was repeated three times by three different investigators. After that, the substrates were rinsed in PBS and dried in increasing ethanol series (35%, 50%, 70%, 95%, and 100%). The 100% ethanol wash was replaced with HMDS 50% for 30 minutes, followed by 100% HDMS overnight. The dried

substrates were mounted on a metal stub and coated with a carbon sputtering coating of 10–20 nm thick. The substrates surfaces were then analyzed by SEM (Phenom ProX-Netherlands). SEM images with different magnifications were collected for trypsinized and non-trypsinized groups.

4.7.3 Cell proliferation

Human gingival fibroblasts were plated at a density of 20,000 cells/cm^2 on the titanium substrates (7x7x1 mm) and cultured for up to 10 days. The proliferation of cultured cells was determined using Alamar Blue assay (BioSource International, Camarillo, California) in colorimetric format. The titanium substrates (n=4) were withdrawn from the culture at predetermined times (Days 1, 3, 7, and 10) and placed into sterile culture plates containing fresh culture medium with 10% assay reagent. After 3 hours of incubation, the absorbance values were read at 570 and 595 nm using an ELISA plate reader (Multiskan MS, Labsystems, Helsinki, Finland). Measured absorbances were used to calculate the reduction of assay reagent, and the cell proliferation rate was normalized in respect to the proliferation rate of the control at the first time point, which was arbitrarily set to 100%. A linear relationship between the cell number and absorbance readings was established on tissue culture polystyrene substrates. The cell proliferation rate was measured at different time points. Then, the substrates were rinsed three times with PBS and fixed with 2.5% glutaraldehyde. All substrates were rinsed with PBS and dried through a series of graded alcohol. SEM images of the investigated substrates were made to confirm the proliferation results on the substrates.

4.8 Tissue culture model (III)

4.8.1 Implant preparation

Surtex® titanium endodontic posts (Dentatus Ltd, Stockholm, Sweden) were used to function as implants. They were inserted in the pig mandible with a length of 10 mm and a diameter of 1.35 mm (n=40). The titanium posts were delivered with two different surface treatments; machined non-coated (NC) titanium implants used as control samples and nanostructured TiO_2 coated surfaces obtained by the (HT) coating method. The implants (posts) were polished using a polishing brush followed by pumice with cotton polishing buff wheels. Then the HT treatment was carried out. The posts were cleansed ultrasonically with acetone and ethanol for 5 minutes each and then dried in air. Before the implantation, all substrates were sterilized in an autoclave (Tuttnauer Elara11, Breda, Netherlands) for 20 minutes at 121 ºC and sealed in blister packages.

4.8.2 Implantation and tissue culture

Five mandibles were obtained directly from freshly slaughtered pigs. The implants were inserted in the mandibles using the self-tapping flapless technique. Then, the tissue/implant specimens were dissected using a 6 mm biopsy punch (Stiefel® Biopsy Punch; Stiefel Laboratorium GmbH, Offenbach am Main, Germany), followed by a 6 mm Trephine bur (Ulrich Storz GmbH, Tuttlingen, Germany) (Figure 6). The tissue/implant specimens were rinsed in PBS supplemented with penicillin, streptomycin, and amphotericin B. They were then individually cultured at the air/liquid interface on a stainless-steel grid, in 6-well plates containing Eagle's minimum essential medium (EMEM M-2279; Sigma-Aldrich, St Louis, MO.), supplemented with 10 % fetal bovine serum (FBS), 100 U/Ig penicillin, streptomycin 100 Ig/ml, and 200 mM L-glutamine (Gibco BRL, Life Technologies, Paisley, UK). The specimens were first covered with the medium for two days. On day three, the culture medium level was reduced, and the specimens were cultured at an air-liquid interface for two weeks (Figure 7). The specimens were incubated at 37 ºC in a 5% CO_2 environment, and the culture medium was changed every 24 hours up to 7 and 14 days (n=10/time point). At the end of each tissue culture time point, the specimens were placed in suitable embedding cassettes and fixed in 10 % buffered formalin for one day at room temperature.

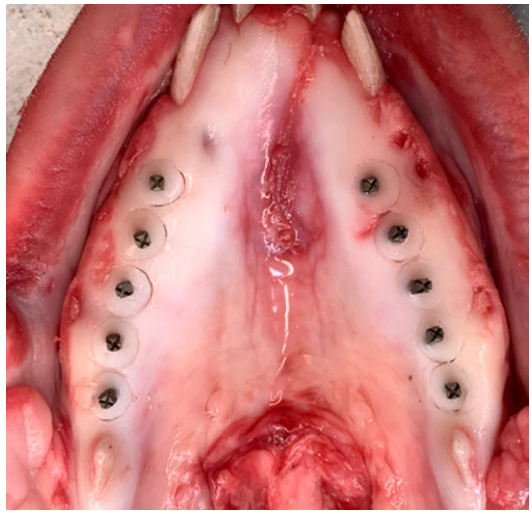

Figure 6. Titanium posts were inserted in freshly slaughtered pig mandible. The tissue/implant specimens were dissected using a 6 mm biopsy punch followed by a 6 mm Trephine bur.

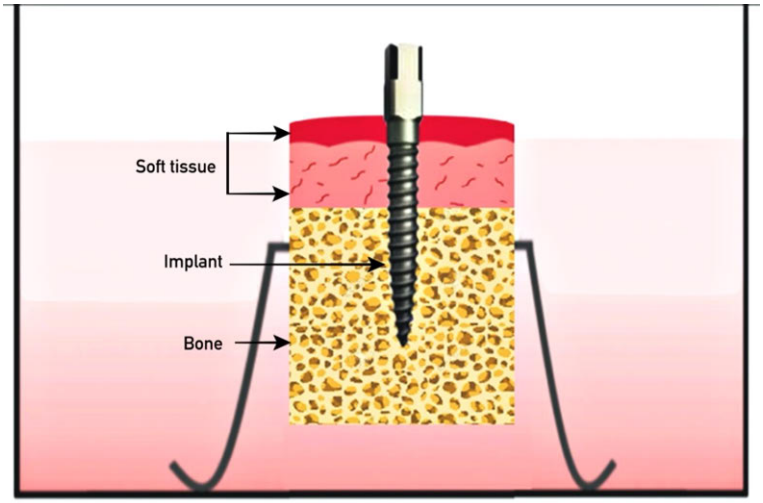

Figure 7. Schematic view of the pig tissue culture model. Tissue/ implant specimens were first soaked in the culture medium for two days; then, the specimens were lifted to the air/liquid interface.

4.8.3 Embedding of tissue culture samples

A modification of an earlier described embedding method using Technovit 9100 New® polymerization system (Kulzer GmbH, Hanau, Germany) was used (Bako, 2015; Willbold, 2010). The polymerization system is a polymethyl methacrylate (PMMA) based technical resin. It polymerizes in the absence of oxygen and at low temperatures (-2 to -20°C), enabling different histological and immunohistochemical stainings for hard tissues. It is suitable for implant-tissue interface studies (Willbold, 2010). This embedding system involves different steps and components that are required to initiate the polymerization reaction, as illustrated in Table 1.

After fixation, the tissue/implant specimens were embedded in PMMA resin (Technovit 9100 New® Kulzer GmbH, Hanau, Germany). This embedding procedure was described previously (Shahramian et al., 2020). In brief, the specimens were washed with running tap water for several hours and then dehydrated in a series of alcohol and xylene at room temperature in the following steps: 70% alcohol, twice 96% alcohol, twice 100% alcohol, twice xylene overnight for each step. After dehydration, the specimens were placed in pre-infiltration solution 1, followed by pre-infiltration solution 2, overnight at room temperature. The specimens were then incubated overnight in pre-infiltration solution 3 and then in the infiltration solution at +4 °C for both steps.

For the tissue polymerization step, 45 ml of stock A solution and 5 ml of stock B solution were mixed. Each tissue specimen was transferred from the embedding cassettes using plastic forceps and placed into the bottom of a precooled Teflon mold

stored at +4 °C. The polymerization solution was then added into the mold. The Teflon molds were placed in a vacuum desiccator cooled down to -4 °C.

The specimens were evacuated carefully for 200–400 mbar for 30 minutes until no gas bubbles on the surface were detected. The pressure was let out of the vacuum desiccator and the molds were closed with the top covers. The desiccator was closed and stored at -4 °C, and the polymerization process was completed after two days. The hardened tissue blocks were pulled out of the molds and kept overnight under a lab fume hood for complete evaporation.

Table 1. A modification of the Technovit 9100 New® embedding system illustrates the different solutions, steps, and incubation times used. PMMA = polymethyl methacrylate; BS = base solution; RT = room temperature.

Embedding steps	Solution	Temperature	Incubation time
Fixation	10% buffered formalin	(RT)	One day
Dehydration	70% alcohol	(RT)	Overnight
	2 x 96% alcohol	(RT)	Overnight
	2 x 100% alcohol	(RT)	Overnight
	2 x xylene	(RT)	4 hours each
Pre-infiltration solution 1	200 ml xylene + 200 ml stabilized BS	(RT)	Overnight
Pre-infiltration solution 2	l g dibenzoylperoxide (hardener 1) + 200 ml stabilized BS	(RT)	Overnight
Pre-infiltration solution 3	l g hardener 1 + 200 ml destabilized BS	+4 °C	Overnight
Infiltration solution	1 g hardener 1 + 200ml destabilized BS + 20 g PMMA powder. (destabilized BS was added until the volume reached 250ml).	+4 °C	Overnight
Polymerization		-4 °C	Two days
Stock solution A	80 g PMMA + 400 ml destabilized BS + 3g hardener1. (more destabilized BS was added until the volume of the mixture reached 500 ml)		
Stock solution B	30 ml destabilized BS + 4 ml hardener 2+2 ml regulator. (more destabilized BS was added until the total volume reached 50 ml).		
	Solutions A and B are mixed in proportion are mixed in the proportion of (9:1).		

4.8.4 Sectioning

Before the tissue blocks sectioning procedure, plastic slides were first glued onto the tissue blocks using a photocuring adhesive (Technovit 7210 VLC Kulzer GmbH, Hanau, Germany). The block's surfaces were then ground using P800, P1200, and P2500 silicon carbide papers (Exakt Technologies, Oklahoma City, OK, USA). A glass slide was roughened using a silicon carbide P800 paper, washed in distilled water, and cleaned with 100% alcohol. Then one drop of RC adhesion primer (Kulzer GmbH, Hanau, Germany) was placed in the middle of the glass slide, and the slide was let to dry. Technovit 7210 VLC precision adhesive (Kulzer GmbH) was used to glue the glass slide onto the tissue block-plastic slide complex using a gluing machine (Exakt Technologies) with UV light for 15 minutes. The tissue block was sandwiched in with two slides. The sandwiched tissue blocks were sectioned at 100 µm thickness using a diamond band saw (Exakt Technologies). The thickness was then further reduced to 20 µm by grinding the sections with silicon carbide papers of P500, P800, P1200, P2500, and polished with K4000 (Exakt Technologies). Ten specimens were used per group (HT and NC) for each time point. Due to the sectioning process's technical difficulty, approximately 1–2 sections were obtained from each specimen.

4.8.5 Histological analysis

Before histological stainings, deplastination of the methyl methacrylate-embedded sections was performed. The sections were incubated twice in xylene, twice in methoxyethyl acetate, twice in acetone, and twice in distilled water. The sections were then stained with Hematoxylin-Eosin, Van Gieson, and Masson Trichrome Goldner stains according to standard protocols. One specimen (per each stain and each time point) from each group were used for the analysis. After stainings, the sections were rinsed in distilled water and dehydrated in a graded series of ethanol and xylene in the following steps: 70% ethanol, 96% ethanol, absolute ethanol, xylene, and then mounted with a rapid drying medium (Pertex, Histolab Products, Gothenburg, Sweden). The histological analysis of the implant-tissue interface was carried out using a light microscope (Leitz Aristoplan, Leica Microsystems, Wetzlar, Germany). The images were captured using a digital camera (Leica DFC 320, Leica Microsystems) and imaging software (Leica Application Suite version 4.1.0, Leica Microsystems).

4.8.6 Immunohistological analysis

For immunohistochemical staining, the methyl methacrylate-embedded sections were first deplastinated, as mentioned earlier. Antigen retrieval on PMMA sections

was performed to detect the cytokeratin (CK) 14 protein (one specimen per each group) at day 14-time point was used. The sections were immersed in citrate buffer (pH 6.0) to perform heat-induced epitope retrieval for 10 minutes, followed by Trisbuffered saline (TBS) wash. The sections were then incubated at room temperature in a bath of 3% hydrogen peroxide for 10 minutes and washed again with TBS.

After that, the samples were incubated for 30 minutes at room temperature with anti-cytokeratin 14 antibody (1:30, BioGenex, Fremont, CA) and washed again in TBS. The sections were then incubated with Labelled polymer-HRP (Detection kit Envision + Dual-link system HRP [DAB+], Dako, Carpinteria, CA, USA) for 30 minutes at room temperature. The TBS wash was repeated, and finally, the samples were incubated with diaminobenzidine (DAB) for 10 minutes at room temperature, followed with aqua wash. The sections were counterstained by placing them in hematoxylin for 3 minutes at room temperature, and aqua wash was repeated. The samples were then blued with tap water, followed with aqua wash, and dehydrated in a graded series of ethanol and xylene in the following steps: 70% ethanol, 96% ethanol, absolute ethanol, xylene, and then mounted with the drying medium (Pertex, Histolab Products). The immunohistochemical stainings were analyzed as histological samples.

4.9 Early biofilm formation *in vivo* experiment (IV)

4.9.1 Experimental design

A total of 40 (Ti-6Al-4V) alloy discs with a diameter of 4 mm and 1 mm height divided into four groups with different surface treatments (NC, UVNC, HT, UVHT) were used. *In vivo* plaque formation was studied in 10 healthy, nonsmoking adult volunteers (6 males, 4 females, mean age 39.7 years, ranging from 25 to 56 years). Each participant (subject) received four discs (one of each group). The study's information and instructions were given to the subjects, and they have been asked to provide their written informed consent.

After the HT coating, all substrates' bottom surfaces were subjected to sandblasting with large grit aluminum oxide particles (250–500 µm) using an air abrasion device (LM Pro power, Pargas, Finland) to enhance their attachment on the teeth surfaces. The sandblasting process was performed using 5 bars of air pressure at a 90° angle for 20 seconds. All the subjects were tested for *Streptococcus mutans* (*S. mutans)* by collecting stimulated whole saliva for bacterial cultivation. The UV treatment for half of the substrates was administered immediately (fresh surface) before attaching the discs to subjects' molars. Titanium discs were attached to the subjects' buccal surfaces of their maxillary molars (Figure 8), and they were

randomly distributed among the maxillary first and second molars. The subjects were advised not to brush their teeth and not use xylitol-containing products or antimicrobial mouth rinses during the plaque accumulation period (24 hours). Each subject was advised to maintain their usual diet during the test period. However, one day before and during the experiment, sucrose-containing cookies, chocolate, or candies were encouraged to be consumed 3–5 times a day, which supposedly promoted the adhesion of *S. mutans* to the materials (Koo et al., 2013). None of the participants used antimicrobial drugs during the study.

The maxillary molars and premolars were cleaned with pumice, an area on the buccal surface of the tooth was etched with 37% orthophosphoric acid for 30 seconds, rinsed, and dried thoroughly. A bonding agent (Scotchbond) was applied (3M Deutschland GmbH, Neuss, Germany) and then light-cured for 10 seconds. A small amount of flowable composite resin was applied (3M Deutschland GmbH), titanium discs were placed on the top of the composite and then cured with light for 20 seconds. Sharp edges were then rounded using rotating polishing instruments and water cooling.

Figure 8. Coated and non-coated titanium discs attached to the buccal surfaces of maxillary molars. Adapted from original publication IV.

4.9.2 Plaque collection

The adherent plaque was collected according to a previously described method (Tanner et al., 2005). In brief, after 24 hours, the outer (top) surface of the attached substrates was gently rinsed with saline. The plaque was collected by rubbing the surface of each substrate with three microbrushes (Quick-Stick® Dentsolv AB, Saltsjö-Boo, Sweden) containing approximately 4 µl of NaCl solution. The tips of the microbrushes were cut off and collected into a tube containing 900 µl of tryptic soy broth (TSB). The samples were stored at -70 °C before cultivation. For the assessment of salivary counts of *S. mutans*, samples of stimulated saliva were collected using a paraffin wax chewing stimulation method. Then, 100 µl of the

saliva was inoculated into 900 µl of (TSB) and stored as frozen. After plaque collection, the substrates were debonded, and the excess composite was removed using rotating polishing instruments. Finally, fluoride varnish was applied on the polished enamel surfaces. All clinical procedures were performed by one investigator (NA). The primary outcome measures were counts of *S. mutans*. The secondary outcome measures were total of streptococci or "non-*mutans streptococci*," which are essential biofilm components in early peri-implant biofilm (Kumar et al., 2012).

4.9.3 Microbiological analysis

The cultivation procedure was initiated by thawing and vortexing the transport tubes of the plaque and saliva samples thoroughly. The bacteria were detached from the collection tips by treating the samples in an ultrasonic bath for 10 seconds. Ten microliter aliquots of serial tenfold dilutions of the plaque samples were plated on agar plates. Mutans streptococci (MS) were cultured on *Mitis salivarius* agar containing bacitracin (MSB, Becton, Le Pont-de-Claix, France). The plates were incubated for two days in a 7% CO_2 atmosphere at 37 ºC, and *S. mutans* were identified based on colony morphology and counted using a stereomicroscope. Low counts of *S. sobrinus* was detected from the samples of only one subject. The counts were combined with *S. mutans* counts. Non- *mutans streptococci* were cultured for two days in air on *Mitis salivarius* agar at 37 °C. All streptococcal-like colonies were counted as non-*mutans streptococci.* Total facultative were cultured for three days anaerobically on blood agar (obtained from Turku University Hospital) at 37 °C. All colonies were counted.

4.10 Statistical Analysis

Statistical analysis was performed using Statistical Package software (SPSS. Inc., Chicago, II, USA) version 23.0.

In study I, the comparison of the absorbance means (optical density) obtained from blood clotting measurement and differences in contact angles between groups were analyzed using one-way analysis of variance (ANOVA) followed by Tukey's post-hoc test.

In study II, the data were analyzed using a one-way analysis of variance (ANOVA). The differences among several means were performed with Tukey's post-hoc test. The independent variable was surface treatment, and the dependent variables were contact angle, cell detachment %, and cell activity.

In study IV, the mean logarithmic CFU counts *of S. mutans,* non-*mutans streptococci,* and total facultative bacteria in the plaque collected from the studied

materials were analyzed with one-way analysis of variance (ANOVA). The differences among several means were evaluated using Tukey's post-hoc test.

Differences were considered significant at 95% confidence level, with p-values below 0.05 (*$p < 0.05$; **$p < 0.01$; ***$p < 0.001$).

5 Results

5.1 Surface characteristics (I, II)

SEM evaluation was carried out to investigate the surface topography of the substrates. The NC titanium substrates showed a smooth surface with some grinding lines spreading over the surfaces. The MA TiO_2 coated surfaces showed a uniform smooth surface with extensive cracking, whereas the HT TiO_2 surfaces were entirely covered with the coating crystals consisting of nearly spherical nanoparticles of 20–50 nm (Figure 9). The surface does not change in appearance as a result of the UV treatment, and all the UV and non-UV substrates have the same surface morphology.

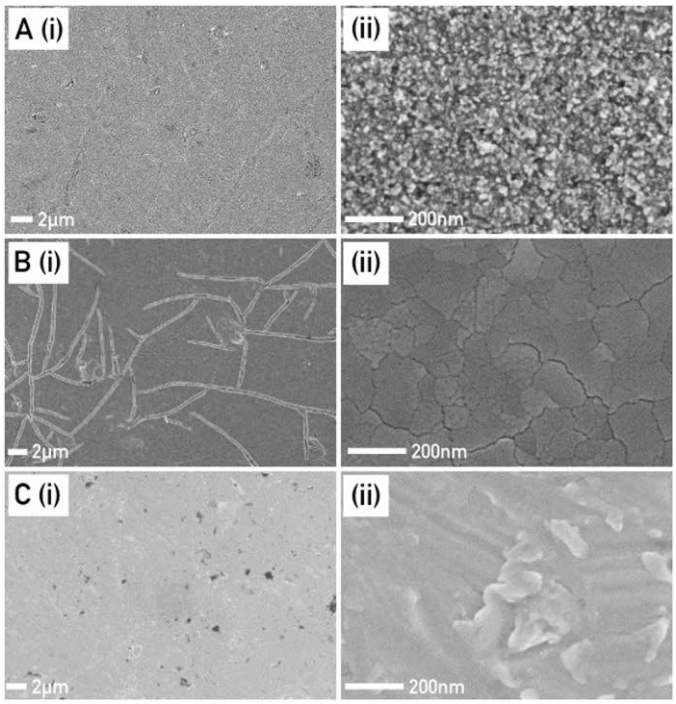

Figure 9. Scanning electron microscope images of the substrates investigated show surfaces topography at (i) low and (ii) high magnifications. (**A**) hydrothermal induced TiO_2 coating, (**B**) sol-gel-derived TiO_2 coating, (**C**) non-coated titanium surface. Modified from original publication I and II.

The X-ray photoelectron spectroscopy (XPS) of the HT substrates revealed signals of titanium, carbon, and oxygen on their surfaces before and after UV treatment. HT substrates treated with UV treatment for 60 minutes showed higher oxygen, titanium, and lower carbon contents on the substrate surfaces (68.3, 17.0, and 8.5 respectively) compared with non-UV treated substrates (57.0, 13.3, and 24.5 respectively). Ultrasonic cleaning in deionized water/ethanol and UV treatment (5 & 15 minutes) removed some carbon from the surfaces (data not shown). UV treatment for 60 minutes removed almost 66% of the surface carbon, indicating less adsorption of CO_2 and other organic impurities from the atmosphere.

5.2 Surface wettability (I, II)

5.2.1 Contact angle

Figure 10 represents the water contact angles obtained by the sessile drop method on different substrates. The HT group had the lowest water contact angle value (40.1°), followed by MA (42.0°), whereas the NC group had the highest contact angle value (56.0°). The UV light treatment significantly enhanced substrates surface wettability. The water contact angles dropped for all substrates after UV treatment, being 15.7°, 11.8°, and 33.8° for HT, MA, and NC, respectively ($^{***}p<0.001$). There was no significant difference between the HT and MA UV treated groups. However, their contact angles were significantly lower than that of the NC UV group ($^{***}p<0.001$).

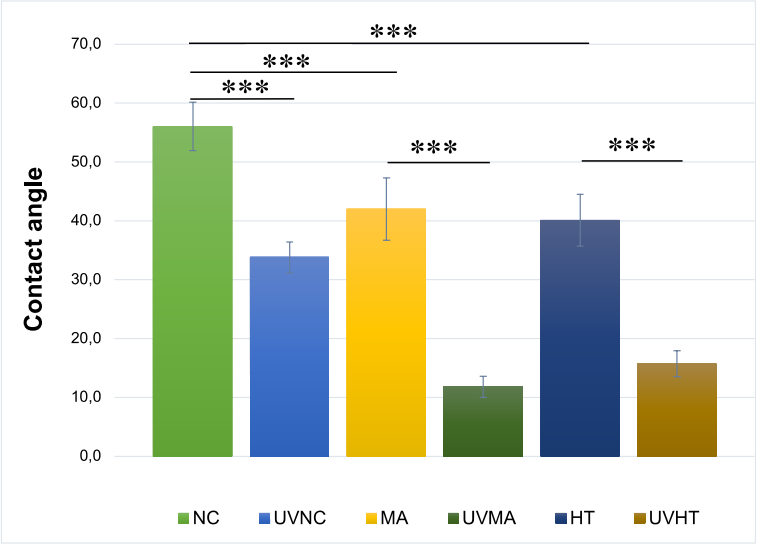

Figure 10. Mean values ± SD of water contact angle measurements for the investigated substrates. Significant differences (***p<0.001) between hydrothermal (HT) and MetAlive (MA) sol-gel-derived TiO_2 coat groups and the non-coated (NC) group and within the same groups before and after UV treatment. Modified from original publication I and II.

The contact angles values for the other two liquids (diiodomethane and formamide) were also significantly lower on the TiO_2 coated surfaces compared to the non-coated surfaces ($^{***}p<0.001$) (Table 2). These values dropped for all substrates after UV treatment.

Table 2. Test liquids and their mean values and standard deviations of contact angle measurements on non-coated and TiO_2 coated substrates. Significant differences (***p<0.001) within the same groups before and after UV treatment. NC: non-coated, MA: MetAlive sol-gel-derived TiO_2 coating, HT: hydrothermal TiO_2 coating.

Contact angles (θC) ± SD		
Groups	Formamide	Diiodomethane
NC	45.0±3.4	40.5±0.8
UVNC	18.5±1.7 ***	28.7±2.6 ***
MA	33.8±5.3	33.6±2.0
UVMA	6.7±2.7 ***	11.6±2.5 ***
HT	27.9±5.6	16.1±2.0
UVHT	4.9±1.8 ***	7.6±1.8 ***

5.2.2 Surface free energy

The different components of SFE are shown in Figure 11. Before UV treatment, the HT and MA groups showed higher polar (γ^p), dispersive (γ^d), and total (γ^{tot}) SFE components compared with the NC group. After UV treatment, the SFE components were higher for all substrates, and there were significant differences between the UV and non-UV treated substrates ($^{***}p<0.001$). Although there was no significant difference between the HT and MA UV treated groups, their SFE components were significantly higher than that of the NC UV group ($^{***}p<0.001$).

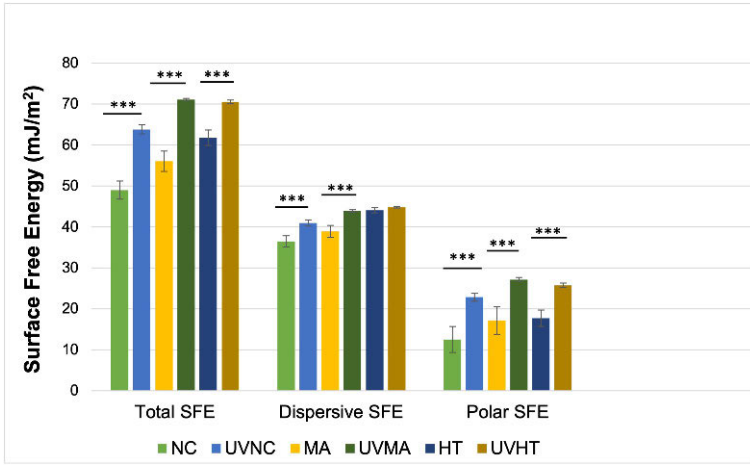

Figure 11. Dispersive (γ^d), polar (γ^p), and total (γ^{tot}) components of surface free energy (SFE) for non-coated and TiO_2 coated substrates before and after (UV) treatment calculated using the Owens-Wendt approach. NC: non-coated, MA: MetAlive sol-gel-derived TiO_2 coating, HT: hydrothermal induced TiO_2 coating. Modified from original publication I.

5.3 Thrombogenicity and blood response (I)

5.3.1 Blood clotting

The blood clotting profiles for UV and non-UV titanium substrates at all time points are represented in Figure 12. The absorbance of the hemolyzed hemoglobin solution varies with time, and the lower the absorbance value, the better the thrombogenic behavior. The absorbance values of UV treated groups were lower than non-UV treated groups at 10, 20, and 40 minute time points, which reflect a higher amount of blood clotting. Blood is considered clotted at an absorbance value of 0.1. The total clotting time for the UV treated HT, MA, and NC titanium substrates were almost 40 minutes compared to 60 minutes for non-UV substrates, indicating faster blood clotting ability of the UV treated groups. Although there were no significant

differences among the UV treated groups, the total clotting time for the HT, MA, and NC UV treated groups were significantly shorter than that of the non-UV NC group ($p = 0.002, 0.004, 0.004$) respectively. UV light treatment significantly enhances coagulation rates.

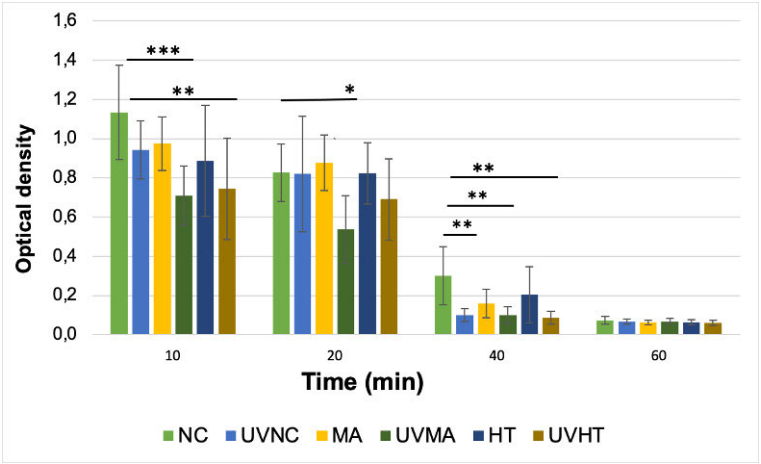

Figure 12. Blood clotting profiles for non-coated and TiO_2 coated substrates with and without (UV) treatment, showing the optical density versus time. Data are presented as mean (±SD). Significant differences (*p<0.05, **p<0.01, and ***p<0.001) between the substrate types are indicated. NC: non-coated, MA: MetAlive sol-gel-derived TiO_2 coating, HT: hydrothermal induced TiO_2 coating. Modified from original publication I.

5.3.2 Platelets adhesion and morphology

Figure 13 displays the platelet morphology after one-hour adhesion period. The platelets' morphologies were observed through SEM images with comparable magnifications of the substrates investigated based on randomly selected fields. Platelets adhered to all UV and non-UV treated surfaces. However, there was variability in platelet morphologies in different areas. The platelets on the NC substrates maintained their round or discoid shapes, indicating a lower activation state. In contrast, the HT and MA TiO_2 substrates showed more platelet transformation to dendritic and early spread state. Also, some platelets with filopodia extending to form a connection with each other, which indicates a higher activation state. UV treatment did not affect platelet adhesion and activation.

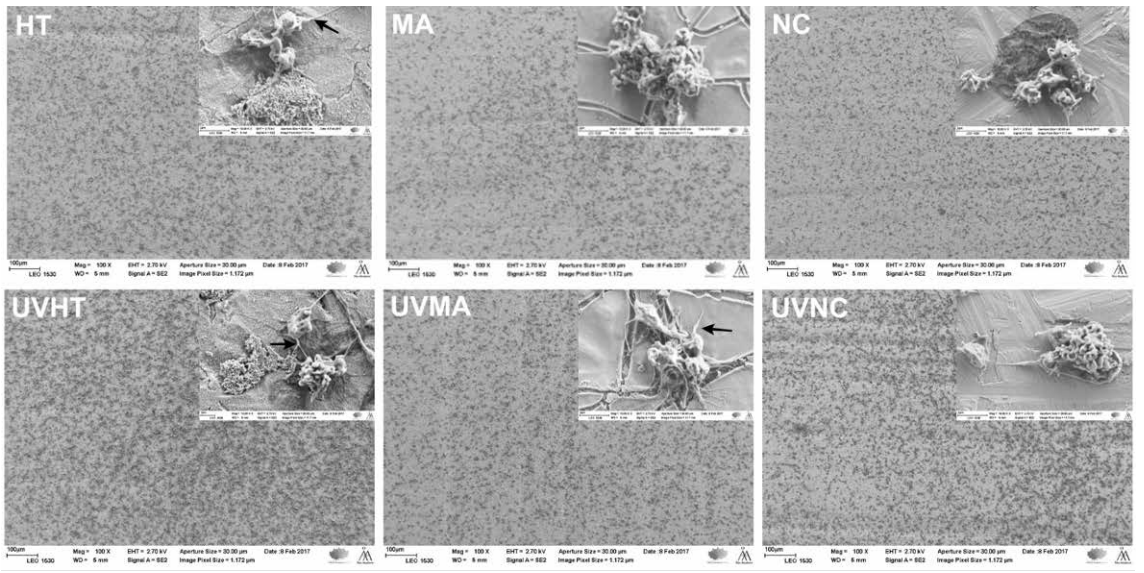

Figure 13. Scanning electron micrographs of platelet morphologies after 1-hour adhesion period on UV and non-UV treated hydrothermal (HT), MetAlive sol-gel derived TiO_2 coating (MA), and non-coated (NC) substrates. Inner images are high magnification of the same titanium substrate. NB. Black arrows show platelets filopodia. Modified from original publication I.

5.3.3 Protein adsorption and analysis

The protein adsorption analysis showed similar protein-binding profiles on all substrates. Based on visual assessment, albumin and fibronectin bands' intensities were similar on the HT, MA, and NC groups (Figure 14). There were no qualitative differences in protein adsorption between the UV and non-UV treated substrates.

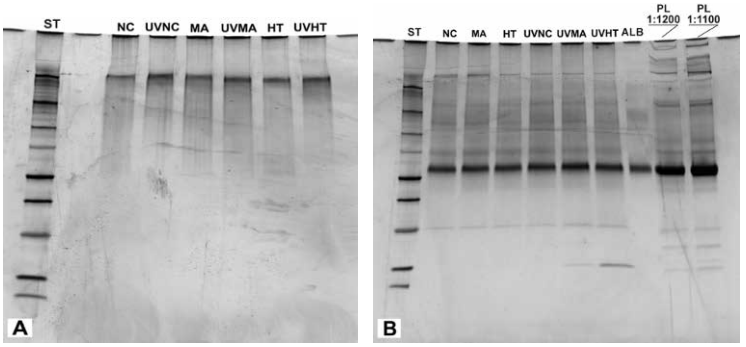

Figure 14. Gel electrophoresis for (**A**) fibronectin and (**B**) plasma proteins adsorbed on different titanium substrates; NC: non-coted, MA: MetAlive^{TM} sol-gel-derived TiO_2 coating, HT: hydrothermal induced TiO_2 coating. UV: ultraviolet treatment. The protein standard contained proteins with the following molecular weights, in kD: 250, 150, 100, 75, 50, 37, 25, 20, 15, 10. PL: plasma; ALB: albumin; ST: standard protein. Modified from original publication I.

5.4 Cell culture experiments (II)

5.4.1 Cell adhesion resistance against enzymatic detachment

Human gingival fibroblasts were incubated for 6 hours on titanium substrates. After the incubation time, similar amounts of cells adhered to all substrate types (data not shown). The strength of cell adhesion against enzymatic detachment was studied after 6 hours of adhesion using gentle trypsinization for 15 minutes at room temperature. Human gingival fibroblasts were more resistant to enzymatic detachments on sol-gel derived and HT coated substrates than on the NC group ($p = .039$, $.049$), with detachment percentages of 35.8%, 36.4%, and 70.7%, respectively (Figure 15). However, no significant difference in cell detachment rate was observed between the UV- treated and non-UV treated groups.

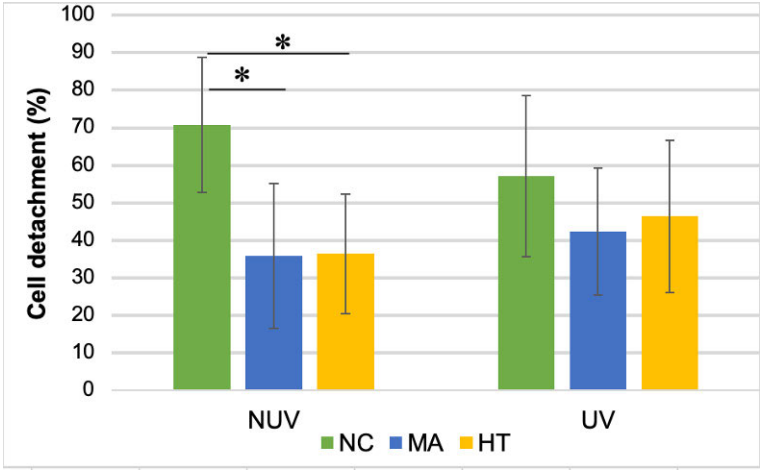

Figure 15. The cumulative amounts of fibroblast detached from titanium substrates. Data are presented as mean± standard deviation. Statistically significant differences between the coated and non-coated groups (*p<0.05). NC = non-coated, MA = sol-gel derived MetAlive™ coating, HT = hydrothermal TiO_2 coating, NUV = Non-UV treated, UV = UV treated. Modified from original publication II.

Figure 16 displays SEM images of adherent fibroblasts on the substrate surfaces after 6 hours of adhesion followed by 15 minutes of trypsinization. Cells were able to adhere to all substrate surfaces at the time point tested. Based on the SEM images, it was evident that more cells with an elongated shape were observed on HT and MA coated surfaces compared to fewer cells with a rounded shape on the NC surfaces. Most of the cells on the HT and MA coated surfaces showed multipolar and bipolar spindle shapes with apparent lamellar cytoplasm surrounding the nucleus, which

demonstrated well-spread morphology. The cells on MA appear to have a larger surface area than the cells on HT, with extracellular fibrils extending out from the cell body towards the treated surface, which might also indicate more advance spreading. However, no differences in the mode of cell adhesion between the HT and MA groups were noticed. These findings were consistent among the different parallel images.

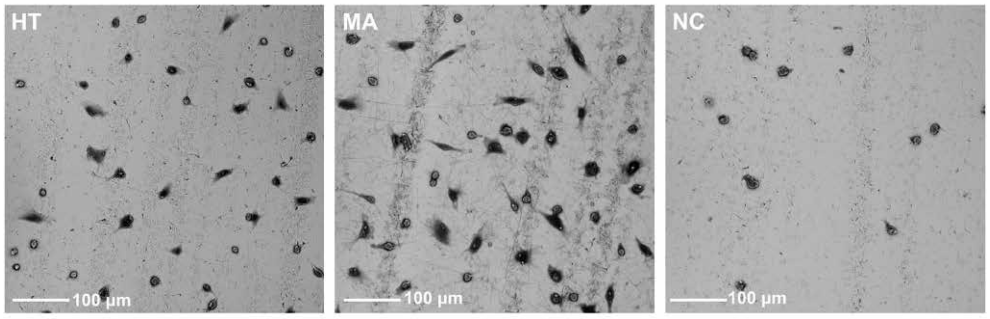

Figure 16. Scanning electron micrographs of adherent fibroblasts on the HT, MA, and NC titanium surfaces. After 6 hours of adhesion followed by 15 minutes of trypsinization. HT: hydrothermal induced TiO_2 coating, MA: MetAlive^{TM} sol-gel-derived TiO_2 coating, NC: non-coated. NB. Representative results obtained from six images per each group and two independent experiments are shown. Modified from original publication II.

5.4.2 Cell proliferation

Human gingival fibroblasts were cultured for 10 days on the titanium substrates. Fibroblasts proliferation on all substrate types increased consistently with the increasing culture time (Figure17). There was a significant difference in cell proliferation rate among the non-UV-treated substrates at all times (*$p<0.05$); at day 1 and 3, cell proliferation was higher on the MA (sol-gel) group, whereas at day 7 and 10, the NC group showed higher cell proliferation rate. However, the HT group showed a lower proliferation rate. After UV light treatment, all the substrate types showed an increase in proliferation rate throughout the observation period. Proliferation results for UV-treated substrates were confirmed with SEM images showing a thick and uniform cell mass at day 10 (Figure 18).

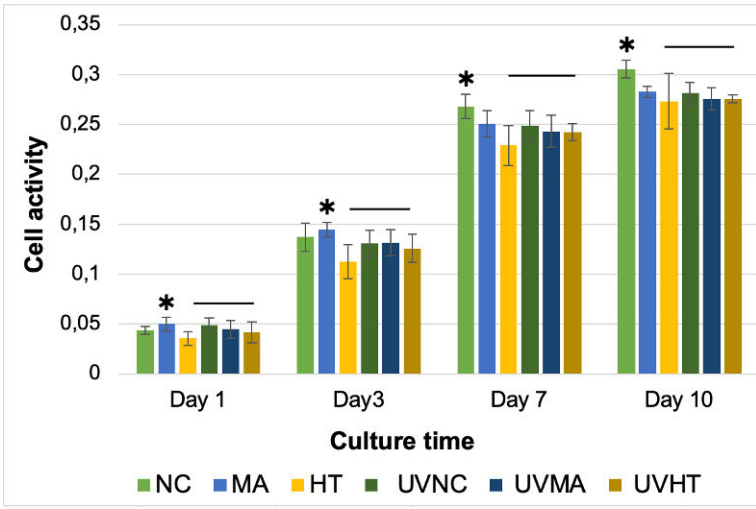

Figure 17. The proliferation rate of human gingival fibroblasts on different substrates. Significant difference between the groups at the marked time points (*p<0.05). After UV light treatment, all the substrate types showed an increase in proliferation rate throughout the observation period. HT: hydrothermal; MA: MetAlive™; NC: non-coated. Modified from original publication II.

Figure 18. Proliferation results for UV treated substrates were confirmed with scanning electron micrographs showing a thick and uniform cell mass at day 10. Modified from original publication II.

5.5 Tissue culture model (III)

5.5.1 Histological and immunohistological analysis

Under light-microscopic examination, the overall structure of the pig tissue explants was intact and maintained throughout the culture period. The epithelial, connective tissue, and bone tissue were attached to both implant surfaces (Figure 19 A through 19 C). The epithelial cells of the pig tissue explants migrated to cover the biopsy sample's margins at day 14 of culture (Figure 19 D), suggesting that the epithelial cells were viable throughout the culture period and appeared to be in close contact with the coated implant surface (Figure 19 B and 19 E). The superficial layers of the epithelium that

start to slough off from the more basal layers during *in vitro* tissue culture were firmly attached to the HT coated implant surface (Figure 19 B through 19 F).

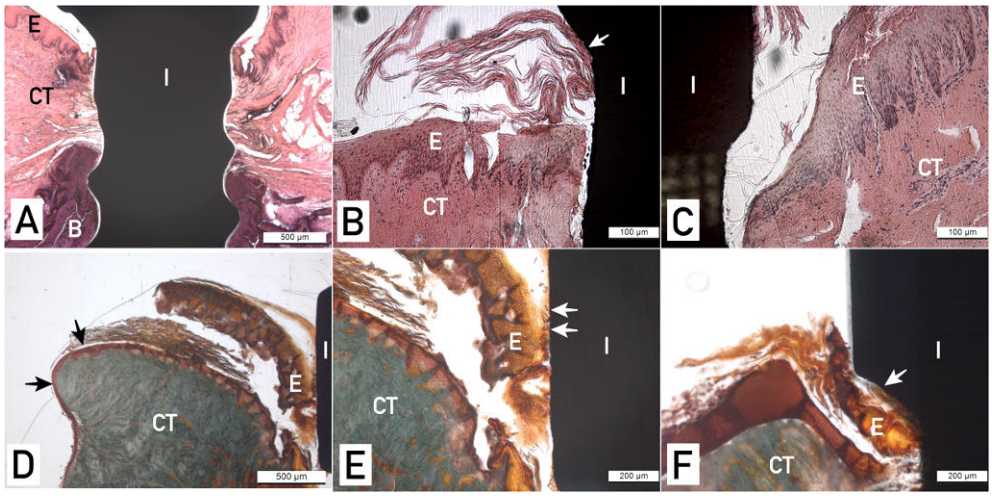

Figure 19. Light microscopy images of pig tissue/implant complexes cultured *in vitro*. Hematoxylin-Eosin-stained sections of pig tissue explants attached to: (**A**) and (**B**) hydrothermal (HT) coated and (**C**) non-coated implants at day 7 of culture. Despite the sloughing of the uppermost epithelial cell layers (a phenomenon that happened in the epithelium of all tissue explants), the upper part of the epithelium was still tightly attached to the coated implant surface (white arrow). Masson´s Trichrome stained sections of pig tissue explants attached to (**D**) and (**E**) HT TiO_2 coated. (**F**) non-coated implants at day 14 of culture. Epithelial migration is visible on the side edges of the biopsy sample (black arrows). White arrows indicate the epithelial attachment to the coated and non-coated implant surfaces. I: implant, E: epithelium, CT: connective tissue, B: bone.

Immunohistochemical staining showed CK14 positivity in the basal layers of the stratified gingival epithelium (Figure 20 A and 20 B). The staining of basal layers ended a few hundred micrometers away from the implant surface. There was also some faint positivity in the innermost cells facing the coated implant surface (Figure 20 B).

Sections from day 7 of culture revealed a firm attachment of connective tissue to both implant surfaces (Figure 21 A and 21 B), with more fibroblasts, were detected along the coated implant surface. It seemed that after two weeks of culture, the collagen fiber organization had started. There were apparently some new dense and thick collagen bundles running parallel or slightly oblique to the coated implant surface (Figure 21 C). In the sections harvested at day 14 of culture, both non-coated and coated implant surfaces were histologically in direct contact with the surrounding bone tissue (Figure 21 D and 21 E). Moreover, some tissue debris and coagulated blood from the original bone were detected between the implant and the bone (Figure 21 E). New bone formation was seen within small pieces of bone at the side edges of the tissue biopsy sample with the coated implant and in near contact with the epithelial cells derived from the gingival epithelium (Figure 21 F).

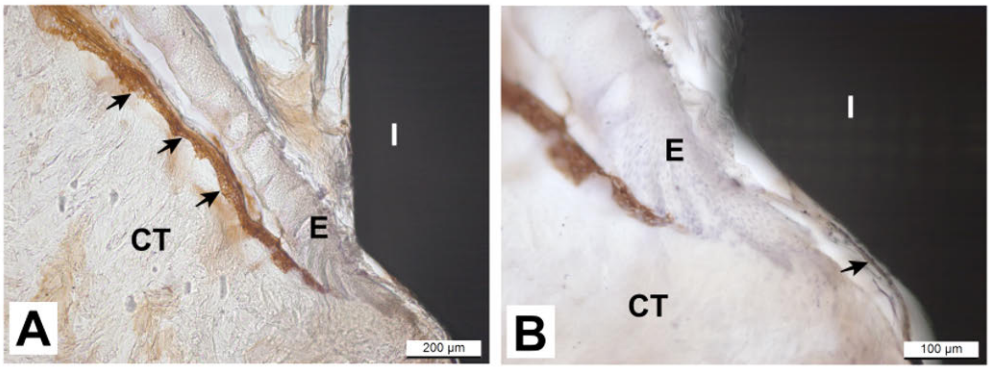

Figure 20. Immunohistochemical analysis of pig tissue/implant complexes at day 14 of culture using antibody directed against cytokeratin (CK)14. (**A**) A non-coated implant/tissue complex. Black arrows show CK14 positive staining. (**B**) HT TiO_2 Coated implant/tissue complex. CK14 positive staining of basal layers of gingival epithelium ends approximately 200 µm apart from the implant surface. The black arrow shows faint positivity in the innermost cells facing the coated implant surface. There is a small gap between the epithelium and the implant because of the tissue cutting process.

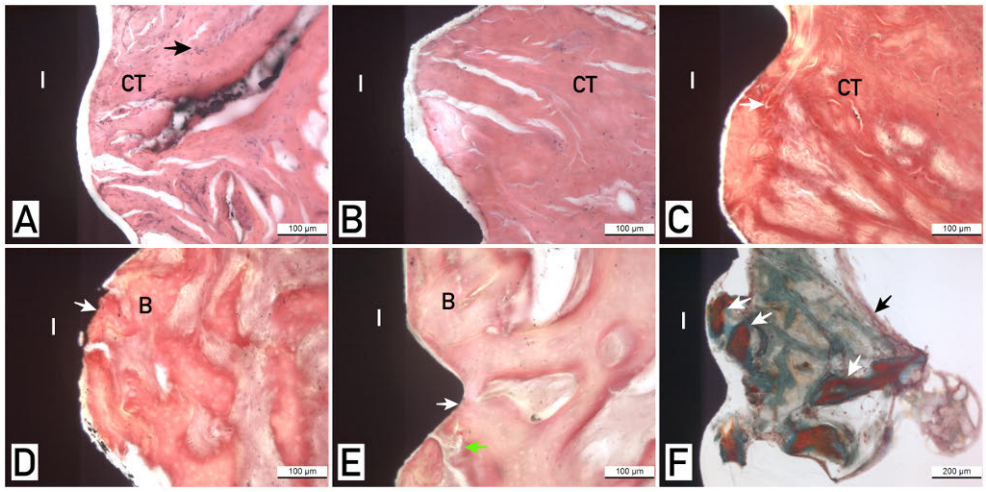

Figure 21. Van Gieson -stained sections of pig tissue explants attached to (**A**) HT TiO_2 coated and (**B**) non-coated titanium implant at day 7 of culture. The black arrow indicates fibroblasts. (**C**) coated implant/tissue complex at day 14 of culture. White arrow indicates thick collagen fibers (intense pink color). Both (**D**) coated and (**E**) non-coated implant surfaces are in direct contact with the surrounding vital bone tissue at day 14 of culture (white arrows). The green arrow shows tissue debris and coagulated blood. (**F**) Masson´s Trichrome-stained section of coated implant/tissue complex. White arrows indicate new bone formation in close contact to the coated implant surface (orange staining on bone shows new bone formation). The black arrow shows migrated epithelial cells. NB. The gap between the tissues and the implant was an artifact because of tissue processing.

5.6 Early biofilm formation *in vivo* experiment (IV)

5.6.1 Plaque collection

Figure 22 illustrates the distribution of subjects according to *S. mutans* counts found on the studied materials. NC substrates showed over two times more *S. mutans* in the early biofilm than the HT induced nanoporous TiO_2 surface. The numbers of colonized surfaces on NC and HT surfaces were equal to 7 and 3, respectively. *S. mutans* was detected in the saliva in 7 out of 10 subjects. Three subjects showed no salivary *S. mutans* counts (0 colony-forming units [CFU]/ml), two showed low counts ($<10^5$ CFU/ml), and five showed high counts ($>10^5$ CFU/ml). Low counts of *S. sobrinus* was detected from the samples of only one subject. The counts were combined with *S. mutans* counts. All subjects with salivary *S. mutans* present showed some adherence of it to the studied materials. The mean logarithmic CFU counts (±SD) were 0.35 ± 0.4 for NC, 0.07 ± 0.2 for HT, 0.25 ± 0.4 for UVNC, and 0.16 ± 0.3 for UVHT (not statistically significant differences). After cultivation, the plaque samples of non-coated groups (NC and UVNC) showed more often *S. mutans* in the biofilms than the coated hydrothermal groups (HT and UVHT) with the number of colonized surfaces equal to 7 and 3, respectively.

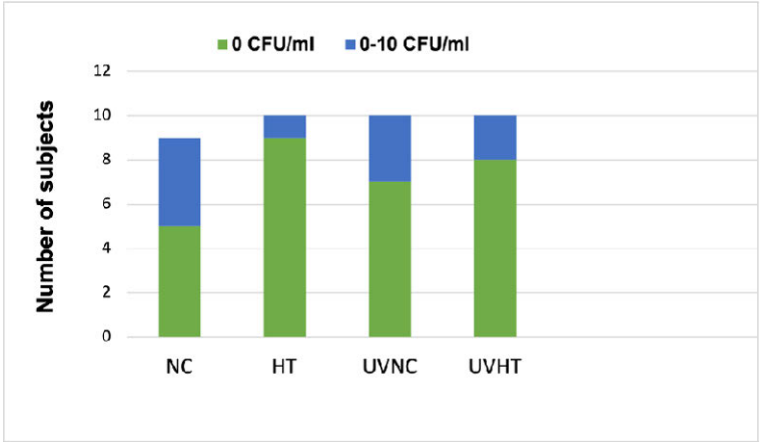

Figure 22. The number of subjects having no (0 CFU/ml) or low (< 10 CFU/ml) *S. mutans* counts in the plaque collected from the titanium substrates investigated. NC: non-coated, HT: hydrothermal induced TiO_2 coating, UV: ultraviolet. Modified from original publication IV.

5.6.2 Microbiological analysis

The microbiological examinations of non-*mutans streptococci* and total facultative bacteria found from the samples of the studied materials are shown in Figures 23 and

24. No statistically significant differences were found between the groups. UVHT showed the lowest means for both non-*mutans streptococci* and total facultative bacteria counts, and NC showed the highest mean counts (5.97 ± 0.5 and 6.09 ± 0.4) and (6.16 ± 0.5 and 6.26 ± 0.5), respectively. This trend was, however, not significant.

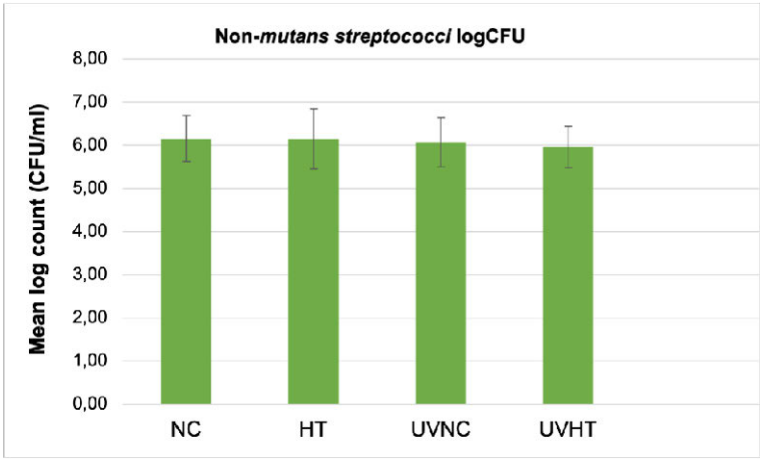

Figure 23. Mean logarithmic CFU counts (±SD) of non-*mutans streptococci* in the plaque collected from the titanium substrates investigated. NC: non-coated, HT: hydrothermal induced TiO_2 coating, UV: ultraviolet. Modified from original publication IV.

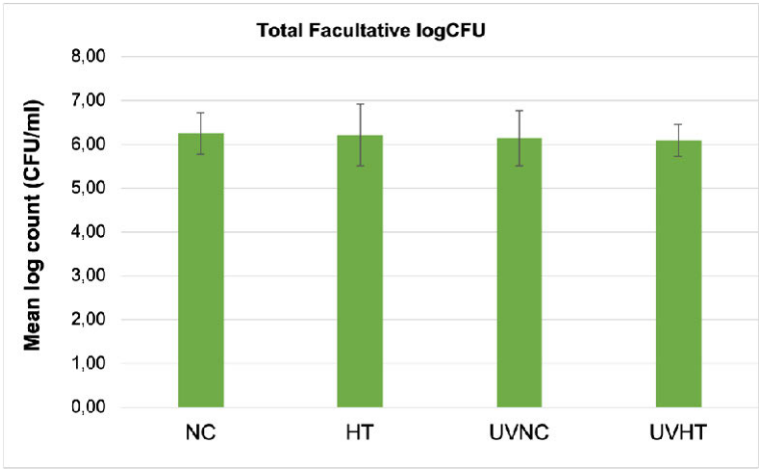

Figure 24. Mean logarithmic CFU counts (±SD) of total facultative bacteria in the plaque collected from the titanium substrates investigated. NC: non-coated, HT: hydrothermal induced TiO_2 coating, UV: ultraviolet. Modified from original publication IV.

6 Discussion

6.1 General discussion

The purpose of this series of *in vitro* and *in vivo* studies was to evaluate hydrothermally induced nanostructured TiO_2 coated surfaces aimed to be used as oral implant and abutment coatings. The final goal was to develop a titanium surface treatment method that promotes implant wound healing and enhances soft tissue attachment on titanium surfaces. The studies presented in this thesis were designed to explore the biological and physicochemical properties of HT derived nanostructured TiO_2 coating. Furthermore, the aim was to study the effect of UV light treatment on the coating's surface reactivity in terms of surface wettability, cytocompatibility, thrombogenicity, and bactericidal properties. In the studies (I & II), the sol-gel group was used as a positive control to the HT (experimental group) in relation to wettability, cell adhesion, proliferation, and blood response. However, in study III, a new culture model was used, and the purpose was to determine first if this model will maintain tissue viability and allow for further analysis. Therefore, only the HT and the non-coated groups were included since the hydrothermal treatment has recently attracted attention due to its relative simplicity and feasibility to produce anatase crystalline TiO_2 coating (Nakagawa et al., 2005; Shi et al., 2015; Zuldesmi et al., 2015). However, data on the effect of HT induced nanostructured TiO_2 coatings on peri-implant soft tissues was not known. Therefore, study IV was designed to compare the HT induced TiO_2 coated group with the non-coated group in an *in vivo* condition. Only the implants that truly integrate with peri-implant soft tissues can prevent microbial penetration into the peri-implant area and possibly prevent many peri-implantitis cases, which would significantly improve the success rate of oral implants.

During implantation, the first tissue that comes into contact with the implant surface is blood (Park & Davies 2000). This initial interaction may influence clot formation around the implant by platelet aggregation and activation of clotting factors. The blood clot represents the connection site between the implant surfaces and the surrounding tissues and initiates the peri-implant wound healing process (Davies, 2003; Di Iorio et al., 2005; Hong et al., 1999; Park & Davies 2000; Thor et al., 2007). Therefore, the first study of this thesis was conducted to evaluate the initial

blood and platelet responses to nanostructured TiO_2 coatings *in vitro*. Furthermore, the effect of UV light treatment on blood clotting ability, platelet activation, and protein adsorption was also examined. This study showed that the coagulation rate was faster (short clotting time) on nanostructured TiO_2 surfaces, which also had higher platelet response than non-coated surface. UV treatment improved blood coagulation rate, both on coated and non-coated titanium surfaces. The observed enhanced blood responses have good potential to improve wound healing and tissue integration.

As already indicated in the introduction section, the surface wettability of an implant material is a predictive indicator of cytocompatibility (Kasemo, 1983). The SFE of the material surface determines its wettability and influences the host reactions at the tissue-implant interface (Gittens et al., 2014; Kohavi et al., 2013). Therefore, all coated and non-coated titanium substrate surfaces were characterized in terms of wettability and SFE calculation. A further step was taken to explore the effect of UV light treatment on the biological and physicochemical properties of these surfaces. This study revealed that TiO_2 coatings turn titanium surfaces hydrophilic, which is further enhanced by UV light treatment.

Human gingival fibroblasts have been used extensively in implant materials research to evaluate the biological properties of biomaterials. Hence, the effect of nanostructured TiO_2 coatings on human gingival fibroblast function in terms of adhesion and proliferation rate was evaluated under cell culture conditions (study II). It was found that nanostructured TiO_2 coatings enhance the human gingival fibroblast adhesion and proliferation when compared with non-coated surfaces. However, the cell culture models used are primarily based on two-dimensional monolayer cell culture systems that fail to replicate complex three-dimensional oral mucosal tissue completely.

Therefore, a further step was taken to get these findings closer to *in vivo* environment by using a novel three-dimensional tissue culture model of pig mandibular blocks. The mandibular blocks that include alveolar bone and gingival tissues were used to evaluate the tissue attachment to titanium alloy implants provided with HT induced TiO_2 coatings (study III). This tissue culture model maintains the viability of pig tissue and allows to histologically and immunohistochemically evaluate the tissue-implant interface. This study indicated that HT induced nanostructured TiO_2 coating could encourage the formation of soft and hard tissue attachment to the titanium implant surface. However, further *in vivo* studies are still necessary before any definitive conclusions can be drawn.

The bacterial biofilm formation on implant surfaces and their restorative components is considered an essential step in the initiation of peri-implant disease (Berglundh et al., 2011; Mombelli & Lang, 1998). Therefore, bacterial adhesion and early plaque formation on nanoporous TiO_2 coatings were evaluated under *in vivo*

conditions (study IV). The purpose of this study was to examine whether nanoporous TiO_2 surface modifies salivary microbial adhesion and biofilm formation and if the bacterial attachment and subsequent biofilm formation can be decreased with UV light activation. This study showed that TiO_2 coated surface inhibits salivary microbial (mostly *S. mutans*) adhesion and initial biofilm formation compared with non-coated surfaces. UV light treatment provided titanium surfaces with antibacterial properties and showed a trend towards less biofilm formation than non-UV treated titanium surfaces.

6.2 Surface characteristics (I, II)

The interaction of the implanted material with blood, tissues, or interstitial fluids is guided mostly by its surface characteristics. Surface topography, surface roughness, surface chemistry, and surface wettability have been recognized as crucial factors that affect the initial cell response at cell-material interface and ultimately affecting soft tissue health and stability (Abrahamsson et al., 2002; Guida et al., 2013; Hamdan et al., 2006; Kohavi et al., 2013).

The surface topography was characterized using SEM examination in studies I & II. The differences in surface topographies and crystalline structures of the coatings were evaluated from the SEM images. The sol-gel (MA) surface showed a uniform smooth surface with extensive cracking, resulting from the substrate preparation and the coating process. In contrast, the HT surfaces were entirely covered with the coating crystals consisting of nearly spherical nanoparticles. Moreover, the surfaces did not change in appearance due to the UV treatment, which can be explained by the fact that UV light treatment alters the surface physicochemical properties without altering its topographical or morphological features (Fujishima et al., 2008). However, the XPS measurement showed apparent differences in the chemical composition of UV and non-UV HT treated surfaces. Higher carbon contents were observed on non-UV surfaces compared to UV treated surfaces, and carbon content reduced with increasing UV exposure time. This result was in accordance with previous studies, which have shown that UV treatment cleans the hydrocarbons that accumulate on titanium surfaces (Aita et al., 2009a, b). In this study, the UV treatment was performed in air and the HT coated substrates were moved directly into the XPS vacuum chamber so that the influence of further contamination was minimized. However, it cannot be ruled out that some carbon was immediately adsorbed onto the surfaces.

The wettability behavior of the substrates was evaluated in studies I & II by measuring the contact angles and the surface free energies, which are considered critical parameters that influence cell adhesion and proliferation on different implant surfaces (Kasemo, 1983; Schwarz et al., 2007). Previous studies have demonstrated

that hydrophilic surfaces with high SFE enhance fibroblast attachment, spreading, and proliferation compared with hydrophobic surfaces (Altankov et al., 1996; Ruardy et al., 1995; Webb et al., 1998). Shi et al. (2015) observed that HT treated titanium nitride coating with a contact angle of around 40° improves fibroblast adhesion and proliferation.

In study I, the SFE of the substrates was calculated using the Owens-Wendt (OW) approach based on the contact angle data obtained. The TiO_2 coated surfaces showed better wettability (low contact angle) and higher SFE than non-coated surfaces. The differences in SFE among the groups we observed were related to their surface topographies and crystalline structures. After UV light treatment, all surfaces became remarkably more hydrophilic. These findings agreed with Wang et al. (1997), who showed that UV irradiation of crystalline TiO_2 surfaces increased surface hydrophilicity and enhanced wettability. The TiO_2 coated surfaces were further improved by UV treatment since UV treatment converts already hydrophilic TiO_2 coated surfaces to superhydrophilic and cleans the contaminants of hydrocarbons that accumulate on titanium surfaces (Aita et al., 2009a, b). Hydrocarbon contaminations on implant surfaces are shown to reduce the surface energy and compromise the initial stages of tissue-healing (Baier et al., 1984; Rupp et al., 2018). These findings mean, in other words, that the hydrophilicity of the TiO_2 coated surfaces was stronger than that of non-coated surfaces, which explains the good results of fibroblast cell adhesion, blood coagulation, and platelet response.

6.3 Thrombogenicity and blood response (I)

Blood clot serves as the connection site between the surrounding living tissues and the implant surface; therefore, bonds wound together with the implant or abutment surfaces (Park et al., 2001). Furthermore, it induces an inflammatory process that results in tissue remodeling and serves as a pathway for the migration of cells to the implant surface (Di Iorio et al., 2005; Park & Davies, 2000; Sculean et al., 2014; Tomasi et al., 2016). This early event of wound healing around the implant and abutment surfaces protects the implant surfaces from the external environment and acts as a barrier against possible infection. The blood clotting ability of the implant surface has been considered an essential factor in hemostasis. Therefore, in this project, study I evaluated the blood and platelet responses to nanostructured TiO_2 coatings. The effect of UV light treatment on blood clotting ability, platelet activation, and protein adhesion was also investigated. Fresh whole blood was deposited on the substrates under static and air-contacting conditions to mimic the clinical situation where implant abutments interact with blood. One biological donor model was used according to the previously published method (Abdulmajeed et al.,

2014). This approach was used to avoid the effect of individual physiological differences in blood reactivity while exploring the reactivity of several surfaces.

The optical density (OD) of the hemolyzed hemoglobin solution decreases with time. A lower OD value relates to lower hemoglobin concentration in blood solution, which translates to a faster thrombus formation on the substrate surfaces (Abdulmajeed et al., 2014). In this study, the optical density values of the nanostructured TiO_2 surfaces were lower than non-coated surfaces. The TiO_2 coated surfaces had a faster coagulation rate than non-coated surfaces, which was enhanced after UV treatment. This is probably related to the wettability behavior of the substrates, which showed that the TiO_2 coated surfaces possess higher SFE and better wettability than non-coated surfaces. UV light treatment improved the wettability of all examined Ti-6Al-4V surfaces, which explains the reason for enhanced blood clotting ability even on non-coated surfaces.

Platelet adhesion and morphology on all UV and non-UV treated substrates were evaluated after a one-hour adhesion period using SEM images. Different platelet activation patterns are ranging from low activated to high activated states, which can be categorized into (a) round or discoid; (b) dendritic; (c) early pseudopodial, spread dendritic; (d) intermediate pseudopodial, spreading; and (e) fully spread (Goodman et al., 1984). In study I, the adherent platelets on the non-coated substrates were at a lower activated state (discoid). In contrast, the platelets on TiO_2 coated substrates were in a higher activated state (early pseudopodial), indicating platelet activation compared with the non-coated substrates. However, after UV treatment, no differences in platelet adhesion and activation were noticed, which indicates that enhanced wettability alone cannot explain the differences in platelet response. This is merely related to the differences in morphological features of the surface nanostructure.

The adsorption of plasma proteins and fibronectin on coated and non-coated substrates was evaluated. The protein adsorption analysis showed similar protein-binding profiles on all substrates. The intensities of albumin and fibronectin bands were similar on the coated and non-coated groups. There were no qualitative differences in protein adsorption between the UV and non-UV treated substrates. Chen et al. (2015) showed that a prolonged UV treatment time for several hours could enhance fibrinogen adsorption and platelet adhesion. This might be related to the decomposition of adsorbed hydrocarbons and an increase of the positive charge which may promote the electrostatic attraction of negatively charged fibrinogen and platelets (Gittens et al., 2014; Sharma, 1984). However, in this study, no additional effect of UV treatment on protein adsorption and platelet adhesion was found, probably due to the relatively short UV exposure time (1 hour). The differences in surface chemistry of used titanium, UV treatment time, and the wavelength utilized may produce different biological effects.

The exposure of TiO_2 to UV light results in the excitation of an electron from the valence band to the conduction band. The excited electron, and the created positive hole on a superficial layer of TiO_2, catalyze the chemical reaction (Wang et al., 1997). Recent studies have found that UV treatment-induced super hydrophilicity and the electropositive charge on titanium surfaces have a regulatory role in determining their bioactivity, which attracts negatively charged proteins, such as fibrinogen and albumin, as well as blood cells on titanium surfaces without the aid of bridging ions (Hori et al., 2010b; Iwasa et al., 2010; Wu et al., 2015). Study I showed that nanostructured TiO_2 coatings increase the coagulation rate and enhanced platelet response, which can be further improved by UV light treatment. Enhanced blood response has good potential to improve wound healing and tissue integration around the implant and abutment surfaces.

6.4 Cell response (II)

Cell adhesion and proliferation process represent the first steps in tissue-biomaterial integration. The human gingival fibroblasts are the most abundant cells in the gingiva and are responsible for wound healing and repair (Bartold et al., 2000). Moreover, the gingival fibroblasts are involved in the biomaterials-soft tissue response and play a key role in maintaining peri-implant tissue integrity (Areva et al., 2007; Meretoja et al., 2010). Therefore, it is important to evaluate their biological behavior on implant materials. Thus, study II was designed to evaluate the effect of nanostructured TiO_2 coatings on human gingival fibroblast functions in terms of adhesion and proliferation rate.

The strength of human gingival fibroblast adhesion against enzymatic detachment was evaluated after 6 hours of adhesion using gentle trypsinization. TiO_2 coated substrates showed better adhesion strength than non-coated substrates. This is probably related to the higher surface wettability characteristics of the TiO_2 coated substrates, which strongly influence fibroblast attachment and spreading (Webb et al., 1998). However, after the UV light treatment, the number of detached cells did not differ significantly among the MA, HT, or NC surfaces. The UV treatment time used in study II (15 minutes) seemed to be sufficient to enhance surface wettability but may not be optimal to improve cell attachment. Different UV treatment times may be required for optimizing the conditions for varied biological responses.

The SEM image analysis of the attached fibroblasts on the substrate surfaces showed fewer cells with a rounded shape on the non-coated substrate surfaces, whereas the coated surfaces showed more cells with an elongated shape. Most of the cells on the coated surfaces showed multipolar and bipolar spindle shapes with extracellular fibrils extending towards the treated surface, indicating surface-related differences in cell maturation and state of attachment. The enzymatic detachment method used in this study provides only indirect evidence about a single cell's

adhesion strength on the solid surface. Real mechanical adhesion strength evaluation would require using a method that facilitates single cell mechanical loading in several directions.

Human gingival fibroblasts were cultured for 10 days on the coated and non-coated substrates. All the substrate surfaces showed an increase in proliferation rate throughout the observation period. Non-UV-treated substrates showed significant differences in cell activities among the materials at all time points. Proliferation rates were higher on non-coated than on hydrothermal coated surfaces at days 7 and 10. These findings might be explained by the fact that cells simply attach better on the HT and MA surfaces, which may slow down the proliferation rate. After UV light treatment, all the substrate types showed an increase in proliferation rate throughout the observation period.

The results of this study indicate that nanostructured TiO_2 coatings enhance the surface wettability and encourage human gingival fibroblast adhesion and proliferation, which may consequently promote the early stages of implant wound healing. However, this *in vitro* cell culture model cannot fully replicate the complex human oral mucosal tissue. Therefore, further studies in real tissue environments are needed before any definitive conclusion can be drawn.

6.5 Tissue response (III)

Dental implant research focused on evaluating the soft tissue attachment to dental implant surfaces has relied mostly on animal models (Berglundh et al., 2007; Paldan et al., 2008; Rossi et al., 2008; Welander et al., 2008). The European Directive 2010/63/EU introduced the concept of the three R's, Replace, Reduce, and Refine, limiting the use of animals for scientific purposes to the minimum (Roffel et al., 2019). However, two-dimensional monolayer cell culture models fail to replicate the three-dimensional human oral mucosal tissue completely. Therefore, study III aimed to describe a novel tissue culture model and create a real *in vivo* like atmosphere using mandibular blocks of freshly slaughtered pigs. Furthermore, the aim was to evaluate the formation of peri-implant tissue attachment on TiO_2 coated and non-coated implants.

The pig model was used in study III because of its similarity to human periodontal tissue in terms of molecular composition and histological characteristics (Wang et al., 2007; Wong et al., 2009). In this *in vitro* study, the pig tissue model's overall structure was maintained throughout the culture period (14 days). The viability of tissues was also confirmed by the fact that the epithelial cells had migrated to cover the side edges of the biopsy sample. This was further supported by histological observations that showed a close contact of epithelial, connective, and bone tissues to both implant surfaces, indicating their good biocompatibility.

The soft tissue seal around the dental implant is formed as a result of the wound healing process. This process starts immediately after the implant/abutment surgery when the blood proteins adsorb on the implant or abutment surfaces. This initial interaction may influence clot formation at the peri-implant wound site, which induces an inflammatory process and leads to tissue formation (Berglundh et al., 2007; Salvi et al., 2015; Sculean et al., 2014; Tomasi et al., 2016). The potentials of HT induced TiO_2 coating to promote blood coagulation and consequently accelerate the wound healing process were reported in study I.

The findings of study III agree with a previous *in vivo* animal study describing the mucosal attachment to titanium implants (Berglundh et al., 2007), which showed that the first signs of epithelial proliferation in histological specimens occurs after 1–2 weeks of healing. The first few weeks after implantation are highly important for the formulation of the epithelial seal. Although the epithelium's uppermost layers started to slough off from the more basal layers during the tissue culture, the epithelial cells were still tightly attached to the HT coated implant surface. This finding provides evidence about the benefit of nanoporous TiO_2 coating on PIE attachment.

In this study, an advanced embedding technique (Technovit 9100 New®) was used to describe the immunolocalization of the CK 14 protein. CK 14 is typically expressed by basal cells of stratified epithelium. In the *in vitro* model described here, CK 14 was detected in the basal layers of pig gingival epithelium but not in the epithelium close to the implant surface, mimicking the PIE. It was also detected in the down growing epithelium at the side edges of the tissue sample. These results are in line with a recent study by Roffel et al. (2019) evaluating the implant-soft tissue interface on a reconstructed human gingiva model. They reported that the down-growing epithelium adjacent to the titanium abutment surface adapted its phenotype into a more basal cell-like and showed a specific immunoprofile resembling PIE. Cytokeratin 19, basement membrane proteins collagen IV, and laminin-332 were expressed between the epithelium and the hydrogel used in their model. Furthermore, a recent review investigating epithelium attachment to abutment surface by Gibbs et al. (2019) showed that in the presence of the implant abutment, the epithelium starts to resemble a gingival margin, sulcular, and junctional epithelium and express the associated physiological epithelial proteins, external and internal basement membrane proteins during the early days of the healing process. The results of this study using the advanced embedding method allow further evaluation of the precise immunoprofile of the developing peri-implant epithelium.

Additionally, a firm attachment of connective tissue was seen on both implant surfaces, with more fibroblasts being detected along the coated implant surface. At two weeks of culture, the connective tissue collagen fibers along the implant-

connective tissue attachment seemed more pronounced, with some thick collagen bundles running parallel or slightly oblique to the coated implant surface.

The incorporation of bone tissue in the model gives support and basis for the soft tissue reactions and enables to investigate the association between the different cell types and tissues. It also creates a real *in vivo* like atmosphere for the study of the primary formation of soft and hard tissue attachment to the implant surface. Almela et al. (2018) developed an *in vitro* tissue engineering model consisting of hard and soft tissues. The model was based on primary cells isolated from oral tissues to mimic the natural structure of alveolar bone with an overlying oral mucosa. They showed that this model could mimic the native oral tissues and act as an alternative to *in vivo* animal models.

Light-microscopic examination showed that both implant surfaces were in direct contact with the surrounding bone tissue. In the sections harvested at 14 days of culture, the osteoid formation was observed within small pieces at the side edges of the tissue biopsy on the coated implant. This finding is in agreement with earlier *in vivo* studies of Abrahamsson et al. (2004) and Berglundh et al. (2003) that described the early events of bone formation on the titanium implant surface. Newly formed woven bone was detected on titanium implant surfaces at 1-2 weeks of healing, and it was considered to represent the first phase of osseointegration.

While the pig tissue model used in study III includes all essential elements needed for *in vitro* studies of cellular and molecular interaction with dental implant/abutment. There are some limitations in the current *in vitro* model that need to be assessed. Keeping the pig tissue explant intact and alive for prolonged culture time can be challenging. Soft tissue dehydration was seen in some histological images with longer culture time. Soaking the tissues in the culture medium for several days before lifting the cultures to the air-liquid interface may improve the tissue culture environment and prevent tissue dehydration. Owing to the lack of blood supply, this model does not truly represent the events of wound healing biological processes. However, it allows for the evaluation of the first events of peri-implant tissue attachment. Furthermore, due to the sectioning process's technical difficulty, a small number of samples were obtained.

The findings of study III seem to support the previous *in vitro* studies of this thesis and suggested that HT induced nanostructured TiO_2 coating may promote the formation of soft and bone tissue attachment to the titanium implant surface. However, a larger sample number is needed for a thorough evaluation. Moreover, further studies using quantitative parameters are required to evaluate the tissue attachment and analyze the presence of adhesion molecules in the implant-tissue interface.

6.6 Early biofilm formation *in vivo* (IV)

The initiation of peri-implant disease is associated with plaque accumulation and the formation of bacterial biofilms on the implant/abutment surfaces (Berglundh et al., 2011; Mombelli & Lang, 1998). Therefore, study IV of this thesis was conducted to evaluate bacterial adhesion (*S. mutans*) and early plaque formation on nanoporous TiO_2 coatings under *in vivo* conditions.

Adherence of oral bacteria to implant or abutment surfaces is initiated by the adhesion of the early Gram-positive bacterial colonizers such as streptococci, which can further facilitate the binding of secondary bacterial colonizers leading to the formation of an anaerobic Gram-negative microbial environment and the maturation of the biofilm (Kolenbrander et al., 2006). *Streptococcus* spp. and *Actinomyces naeslundii* have been considered as early colonizers on tooth/implant material surfaces (Al-Ahmad et al., 2010; Li et al., 2004). Studies have shown that healthy peri-implant sulcus is mainly colonized by oral streptococci, which constitutes 45% to 86% of supra-and subgingival peri-implant microbiota (Quirynen et al., 2005; Elter et al., 2008). These bacteria play a crucial role in providing the basis for the subsequent colonization of facultative and obligate anaerobes. Likewise, in study IV, streptococci were the most predominant species in a 24-hour plaque formed on the studied substrates.

Although *S. mutans* is usually associated with caries occurrence, however, it is also found in peri-implant biofilms owing to its ability to produce an insoluble polymer matrix, survive at low pH values, and able to form high-affinity biofilm to implant materials (Koo et al., 2013; Tamura et al., 2009). Also, more S. *mutans* have been found around infected implants compared to healthy implant sites (Kumar et al., 2012). Therefore, *S mutans* as an initial colonizer is assumed to facilitate the process that can lead to the development of peri-implantitis and may eventually lead to implant failure (Nakazato et al., 1989).

Proper adherence of mucosal tissue to implant or abutment surfaces might prevent biofilm formation in peri-implant environments, which subsequently improve soft tissue attachment and preserve the alveolar ridge. A microbial biofilm can be affected by many factors, including local factors of implant and abutment surface topography and oral environment factors of saliva and protein (Katsikogianni & Missirlis, 2004). The surface roughness has been recognized as the predominant factor for biofilm formation on implant surfaces, as more biofilm is formed on rough surfaces compared with smooth surfaces (Burgers et al., 2010; Elter et al., 2008; Teughels et al., 2006). Therefore, study IV was planned to explore *in vivo* early *S. mutans* biofilm formation on HT induced nanoporous TiO_2 surfaces and to examine the effect of UV light activation on the biofilm development.

In this study, the amount of plaque accumulation based on the counts of non-*mutans streptococci* and total facultative bacteria showed no difference between the

HT coated and non-coated substrates, which may be explained by surface roughness values of the investigated substrates, which ranged from 0.15 to 0.2 µm. These findings agree with a previous study suggesting that a roughness (Ra) value of 0.2 µm is a threshold limit below which surface roughness has no significant effect on the biofilm formation or colonization (Bollen et al., 1996). Furthermore, implants' surface characteristics, such as surface free energy (SFE), and wettability have been shown to play essential roles in bacterial adhesion and biofilm formation. High SFE has been shown to attract more microorganisms than low SFE materials (Quirynen & Bollen, 1995). On the contrary, the opposite result has also been reported (Villard et al., 2015). A previous *in vivo* study by Tanner et al. (2005) showed that polyethylene FRC with low SFE promotes plaque accumulation and adhesion of *S. mutans* more than dental ceramic and restorative composites with high SFE. The results of study IV are in agreement with these findings.

Studies I & II have shown that while HT nanostructured TiO_2 coating improves surface wettability, which was demonstrated by lower water contact angles and higher SFE than the NC surface, it promotes blood coagulation and human gingival fibroblast attachment. This *in vivo* study found that the HT induced TiO_2 surface does not enhance salivary microbial (*mostly S. mutans*) adhesion and initial biofilm formation compared with non-coated surfaces. These results seem to agree with Rochford et al. (2014), who showed that SFE could be improved on implant surfaces for better cell response without more bacteria adhesion. Previous studies have shown that nanoscale modification of the implant surface can alter the surface chemistry and topography, which influences the initial cell response at the cell-material interface and improves bioactivity and bactericidal properties (Frojd et al., 2011; Unosson et al., 2013). In study IV, the HT samples showed almost no *S. mutans* in the biofilms, whereas *S. mutans* was found on nearly half of the non-coated samples after cultivation. The plaque samples of non-coated groups (NC, UVNC) harbored more frequently *S. mutans* in the biofilm than the coated hydrothermal groups (HT, UVHT), with the number of colonized surfaces being equal to 7 and 3, respectively.

The results of the UV-treated TiO_2 surfaces have demonstrated superhydrophilicity and bactericidal properties (Aita et al., 2009a; Suketa et al., 2005). Furthermore, UV light treatment on various titanium surfaces has been shown to reduce the biofilm formation of wound pathogens (Yamada et al., 2014). This is probably because UV treatment converts already hydrophilic nanostructured surfaces to superhydrophilic and removes the hydrocarbon contaminants on titanium surfaces. In this study, plaque recovered from the UVHT samples showed the lowest counts for both non-*mutans streptococci* and total facultative bacteria counts, whereas NC samples showed the highest counts. However, the differences were not significant, and the real antimicrobial effect of UV treatment could not be confirmed in an oral environment.

The findings of this experimental *in vivo* study support the given hypothesis that HT induced TiO_2 surfaces does not enhance biofilm formation when compared with non-coated surfaces. UV light treatment provided the surfaces with antibacterial properties and showed a trend towards less biofilm formation compared with non-UV treated titanium surfaces. The possibility of adding an *in situ* self-cleaning and antibacterial feature to HT induced TiO_2 surfaces with UV light treatment could minimize implant infection-related complications.

6.7 Future prospective

The studies presented in this thesis were designed to investigate the biological and physicochemical properties of HT induced TiO_2 coating in terms of surface wettability, cytocompatibility thrombogenicity, and bactericidal properties. However, more research is needed to understand the properties of the HT coating. UV light treatment enhanced the wettability and improved the thrombogenicity on all coated and non-coated titanium surfaces. However, no additional effect of UV treatment on protein adsorption and platelet adhesion was found. Therefore, further studies with different UV treatment time may be required for optimizing the conditions for diverse biological responses.

The tissue culture *in vitro* model described in this thesis allowed evaluating the tissue-implant interface histologically and immunohistochemically. Moreover, it is applicable for further studies with quantitative parameters to evaluate the adhesion molecules present in the implant-tissue interface.

In vivo clinical trials with long-term follow-up are necessary to evaluate the behavior of HT induced TiO_2 coating before final conclusions about coating benefits for peri-implant tissue integration and maintenance can be drawn.

7 Conclusions

Based on the results of the studies included in this thesis, the conclusions can be summarized as follows:

1. Hydrothermal induced TiO_2 coatings promote blood coagulation and enhance platelet adhesion and activation.
2. The UV light treatment enhances the wettability and improves thrombogenicity of Ti-6Al-4V surfaces, indicating that UV light treatment has good potential to improve wound healing and tissue integration of various titanium alloy implants.
3. Nanostructured TiO_2 coatings enhance the surface wettability and encourage human gingival fibroblast adhesion and proliferation *in vitro*.
4. Hydrothermal-induced TiO_2 coating may have the potential to induce the formation of soft and hard tissue attachment to the titanium implant surface.

   Furthermore, the organotypic *in vitro* tissue culture model includes alveolar bone and gingival tissue elements, using pig mandibular blocks, maintains the viability of pig tissue, and allows to histologically and immunohistochemically evaluate the tissue-implant interface.
5. Hydrothermal induced TiO_2 coating does not enhance salivary microbial (mostly *S. mutans*) adhesion and initial biofilm formation *in vivo*. UV light treatment provided Ti-6Al-4V surfaces with antibacterial properties and showed a trend towards less biofilm formation than non-UV treated titanium surfaces.

From the above, it can be concluded that hydrothermally treated TiO_2 coatings have a good potential to improve wound healing and enhance soft tissue attachment on titanium dental implant abutments and, at the same time, does not enhance bacterial adhesion and initial biofilm formation.

Acknowledgments

First and foremost, praises are due to God "**Allah**" Al-Wahab, the greatest of all, for giving me the opportunity, determination, and strength to accomplish my goals. His continuous grace and mercy were with me throughout my life and ever more during the tenure of my research.

I would like to faithfully express my sincerest gratitude and heartfelt thanks to my supervisor Professor ***Timo Närhi***. Your guidance, support, and encouragement have been invaluable throughout my PhD journey. I am incredibly grateful for what you have offered me. Your exceptional support, motivation, and immense knowledge helped me all the time of my doctoral journey. It was a great privilege and honor to work and study under your guidance. I could not have imagined a better supervisor.

This thesis was carried out at the Department of Prosthetic Dentistry and Stomatognathic physiology, Institute of Dentistry, and Turku Clinical Biomaterial Centre (TCBC), University of Turku, Finland. I would like to express my great appreciation to the Libyan Ministry of Education's scholarship support and research funding from ITI. In addition to the financial support, I have received from the Finnish Doctoral Program in Oral Sciences (FINDOS-Turku), and Faculty of Medicine, University of Turku. Without their support, this work would not have been possible. Thank you so much.

I would like to extend my sincere respect and thanks to Professor ***Pekka Vallittu***, the dean of the Institute of Dentistry, University of Turku, as well as Dr. ***Lippo Lassila***, the head of TCBC, for their constant effort to create a supportive environment for researchers and research.

I am grateful to Professor ***Nicola Zitzmann*** for accepting the invitation to be my dissertation opponent. Also, I wish to express my appreciation to the official pre-examiners, Docent ***Taina Tervahartiala*** and Professor ***Lari Häkkinen***, for their valuable time in revising my PhD work. Your constructive criticism and comments have greatly improved the academic value of my thesis book. It is a great honor for me to have your contribution to my doctoral dissertation. Thank you.

Undertaking this PhD has been a truly life-changing experience for me, and it would not have been possible to do without the support and guidance that I received

from many people. Therefore, I am thankful for all co-authors who contributed to my articles: ***Ari Peltola***, Dr. ***Ahmed Ballo***, and Dr. ***Johanna Tanner***. Special warm thanks to Prof. ***Eva Söderling*** and Dr***. Jaana Willberg*** for all the scientific help and valuable advice you offered to me.

I would like to extend my sincere appreciation to Dr. ***Ilkka Kangasniemi*** and ID creations Oy for their help and support throughout this PhD project.

I wish to give a very special thanks to the skillful, cheerful, and helpful laboratory technicians: ***Katja Sampalahti***, ***Oona Hällfors***, and ***Mariia Valkama*** for their technical assistance, their friendship, and the warmth they extended to me during my time in the lab and for making me always feels so welcome. I would also like to thank ***Katri Kuismanen*** for her help and assistance during the clinical study involved in this PhD work. I am also grateful to all of the staff and doctoral candidates who voluntarily participated in the biofilm experiment as subjects. Thank you so much.

To my colleagues at the Institute of Dentistry (Dentalia); ***Ikram Salim***, ***Heba Abdelrazik***, ***Anas Salim***, ***Thiago Stape***, ***Kaveh Nikjamal***, and at TCBC; ***Mona Gibreel***, ***Sofyan Garoushi***, and ***Tarek Omran*** for their kind support. Special warm thanks to the always welcoming, helpful, and kind colleague; ***Khalil Shahramian***, for his constant help and support whenever needed. I really appreciate your help, thank you.

I also wish to thank my friend ***Aya Bouazza***. Despite the distances that separate us apart, your warm daily messages bring me comfort and positive energy to complete this journey. I wish you all the best in your life.

Many thanks to my Libyan friends in Turku; ***Enas***, ***Eman***, ***Naziha***, and ***Fatma***, as well as their families. Our friendship has been a source of positive energy and support that encouraging me throughout my study. I would like to extend my sincere thanks to ***Dareen Fteita*** for her help and advice during the thesis submission process. I enjoyed having a great time with you all. Thanks for giving me such a wonderful time.

A special thanks to the distinguished teacher ***Khadija Isteita***. I am very proud of our friendship, and it is an honor to have known you. I ask God to offer you a long life full of health and happiness.

To my second family here in Turku, my closest friend ***Samira*** (Samar), her husband, my brother Dr. ***Ahmed Al-gahawi*** and their two lovely kids, ***Yakoot*** and ***Lulu***. The beginning was from our beloved country Libya when we decided to come to Turku and start this challenging journey together, helping and supporting each other through thick and thin. Thank you, Samar, for the laughs, for the cries, and everything in between. Thank you for staying constant in a world full of change. Thank you for your companionship and selfless support. You have always been there for me, and I can't thank you enough.

I would also like to extend my deepest gratitude to my second family in Libya, ***my parents-in-low***, for their unfailing emotional support. May God bless you with good health and lots of happiness. My respectful "***brothers and sisters-in-law***" and their lovely families.

A very special word of thanks goes to my family in Libya, my dearest two people in the world, ***mom and dad***, who set me off on the road to this PhD a long time ago. You are my inspiration to achieve greatness. Without you, I would not be where I am today. Thank you for giving me the strength to reach for the stars and chase my dreams. Thank you both for your endless love, heartfelt prayers, and encouragement throughout my life. May God bless you with long life, happiness, and good health, "Ameen".

To my beloved ***sisters***, my dear ***brothers***, and their amazing families. Thank you all for supporting and encouraging me spiritually throughout my life. I miss you so much, and I hope we will meet soon.

To my lovely children: ***Rahaf***, ***Roua***, ***Ahmed***, and ***Mohamed***, the most incredible pride and joy of my life. Your unconditional trust, love, and endless patience raised me up every time I fell down. You have made me stronger, better, and more fulfilled than I could have ever imagined. I love you more than anything, and I appreciate all your encouragement and support during this journey. Thank you now and always.

Last, but definitely most important, to my soulmate, my dearest husband, and my best friend, ***Faleh***. I find it difficult to express my appreciation because it is so boundless. You are my most enthusiastic cheerleader. Without your sunny optimism, love, and support, this dissertation would have taken even longer to complete. I am so grateful to you not just because of your endless help and encouragement, but because we have shared a wonderful life, and we were always together in every step we take, side by side, helping and supporting each other with constant love, understanding and caring. Thank you for being in my life.

Turku, February 17th 2021
Nagat Areid

References

Abdulmajeed, A., Walboomers, XF., Massera, J., Kokkari, AK., Vallittu, PK., Närhi, T. (2014). Blood and fibroblast responses to thermoset BisGMA-TEGDMA/glass fiber-reinforced composite implants in vitro. *Clinical Oral Implants Research*, 25(7), 843–851.

Abrahamsson, I., Berglundh, T., & Lindhe, J. (1998). Soft tissue response to plaque formation at different implant systems. A comparative study in the dog. *Clinical Oral Implants Research*, 9(2), 73–79.

Abrahamsson, I., Berglundh, T., Wennstrom, J., & Lindhe, J. (1996). The peri-implant hard and soft tissues at different implant systems. A comparative study in the dog. *Clinical Oral Implants Research*, 7(3), 212–219.

Abrahamsson, I., & Cardaropoli, G. (2007). Peri-implant hard and soft tissue integration to dental implants made of titanium and gold. *Clinical Oral Implants Research*, 18(3), 269–274.

Abrahamsson, I., Zitzmann, N. U., Berglundh, T., Linder, E., Wennerberg, A., & Lindhe, J. (2002). The mucosal attachment to titanium implants with different surface characteristics: an experimental study in dogs. *Journal of Clinical Periodontology*, 29(5), 448–455.

Abrahamsson, I., Berglundh, T., Linder, E., Lang, N. P., & Lindhe, J. (2004). Early bone formation adjacent to rough and turned endosseous implant surfaces. An experimental study in the dog. *Clinical Oral Implants Research,* 15(4), 381–392.

Adell, R., Lekholm, U., Rockler, B., Branemark, P. I., Lindhe, J., Eriksson, B., & Sbordone, L. (1986). Marginal tissue reactions at osseointegrated titanium fixtures (I). A 3-year longitudinal prospective study. *International Journal of Oral and Maxillofacial Surgery*, 15(1), 39–52.

Aita, H., Hori, N., Takeuchi, M., Suzuki, T., Yamada, M., Anpo, M., & Ogawa, T. (2009a). The effect of ultraviolet functionalization of titanium on integration with bone. *Biomaterials*, 30(6), 1015–1025.

Aita, H., Att, W., Ueno, T., Yamada, M., Hori, N., Iwasa, F., Tsukimura, N., & Ogawa, T. (2009b). Ultraviolet light-mediated photofunctionalization of titanium to promote human mesenchymal stem cell migration, attachment, proliferation and differentiation. *Acta Biomaterialia*, 5(8), 3247–3257.

Al-Ahmad, A., Wiedmann-Al-Ahmad, M., Faust, J., Bächle, M., Follo, M., Wolkewitz, M., Hannig, C., Hellwig, E., Carvalho, C., Kohal, R. (2010). Biofilm formation and composition on different implant materials in vivo. *Journal of Biomedical Materials Research Part B:* Applied Biomaterials, 95(1),101–109.

Albayrak, O., El-Atwani, O., & Altintas, S. (2008). Hydroxyapatite coating on titanium substrate by electrophoretic deposition method: Effects of titanium dioxide inner layer on adhesion strength and hydroxyapatite decomposition. *In Surface and Coatings Technology*, 202(11), 2482–2487.

Albrektsson, T., & Isidor, F. (1994). Consensus report of session IV. In N.P. Lang & T. Karring (Eds.), *Proceeding of the 1st European workshop on periodontology* (pp. 365–369). Quintessence Publishing Co.

Albrektsson, T., Wennerberg, A. (2004). Oral implant surfaces: Part 1-review focusing on topographic and chemical properties of different surfaces and in vivo responses to them. *The International Journal of Prosthodontics,*17(5)*, 536–543.*

Almela, T., Al-Sahaf, S., Bolt, R., Brook, I. M., & Moharamzadeh, K. (2018). Characterization of Multilayered Tissue-Engineered Human Alveolar Bone and Gingival Mucosa. *Tissue Engineering - Part C: Methods,* 24(2), 99–107

Altankov, G., Grinnell, F., & Groth, T. (1996). Studies on the biocompatibility of materials: fibroblast reorganization of substratum-bound fibronectin on surfaces varying in wettability. *Journal of Biomedical Materials Research*, 30(3), 385–391.

Andersson, B., Taylor, A., Lang, B. R., Scheller, H., Scharer, P., Sorensen, J. A., & Tarnow, D. (2001). Alumina ceramic implant abutments used for single-tooth replacement: a prospective 1- to 3-year multicenter study. *The International Journal of Prosthodontics*, 14(5), 432–438.

Andrukhov, O., Huber, R., Shi, B., Berner, S., Rausch-Fan, X., Moritz, A., Spencer, N. D., & Schedle, A. (2016). Proliferation, behavior, and differentiation of osteoblasts on surfaces of different microroughness. *Dental Materials*, 32(11), 1374–1384.

Areva, S., Aaritalo, V., Tuusa, S., Jokinen, M., Linden, M., Peltola, T., & Areva, S. (2007). Sol-Gel-derived TiO_2-SiO2 implant coatings for direct tissue attachment. Part II: Evaluation of cell response. *Journal of Materials Science: Materials in Medicine,* 18(8), 1633–1642.

Åstrand, P., Anzén, B., Karlsson, U., Sahlholm, S., Svärdström, P., & Hellem, S. (2000). Nonsubmerged implants in the treatment of the edentulous upper jaw: A prospective clinical and radiographic study of ITI implants--results after 1 year. *Clinical Implant Dentistry and Related Research*, 2(3), 166–174.

Astrand, P., Engquist, B., Dahlgren, S., Engquist, E., Feldmann, H., & Grondahl, K. (1999). Astra Tech and Branemark System implants: a prospective 5-year comparative study. Results after one year. *Clinical Implant Dentistry and Related Research,* 1(1), 17–26.

Atsuta, I., Yamaza, T., Yoshinari, M., Goto, T., Kido, M. A., Kagiya, T., Mino, S., Shimono, M., & Tanaka, T. (2005). Ultrastructural localization of laminin-5 (gamma2 chain) in the rat peri-implant oral mucosa around a titanium-dental implant by immuno-electron microscopy. *Biomaterials*, 26(32), 6280–6287.

Ayukawa Y., Oshiro W., Atsuta I., Furuhashi, A., Kondo, R., Jinno, Y., Koyano, K. (2019). Long Term Retention of Gingival Sealing around Titanium Implants with CaCl Hydrothermal Treatment: A Rodent Study. *Journal of Clinical Medicine,* 8:1560.

Baharloo, B., Textor, M., & Brunette, D. M. (2005). Substratum roughness alters the growth, area, and focal adhesions of epithelial cells, and their proximity to titanium surfaces. *Journal of Biomedical Materials Research.*Part A, 74(1), 12–22.

Baier, R. E., Meyer, A. E., Natiella, J. R., Natiella, R. R., & Carter, J. M. (1984). Surface properties determine bioadhesive outcomes: methods and results. *Journal of Biomedical Materials Research*, 18(4), 337–355.

Baier, R. E., Shafrin, E. G., & Zisman, W. A. (1968). Adhesion: mechanisms that assist or impede it. *Science,* 162, 1360–1368.

Bako, P. (2015). Methyl methacrylate embedding to study the morphology and immunohistochemistry of adult guinea pig and mouse cochleae. *Journal of Neuroscience Methods,* 254, 86–93.

Bartold, P. M., Walsh, L. J., & Narayanan, A. S. (2000). Molecular and cell biology of the gingiva. *Periodontology 2000*, 24, 28–55.

Becker, W., Becker, B. E., Ricci, A., Bahat, O., Rosenberg, E., Rose, L. F., Handelsman, M., & Israelson, H. (2000). A Prospective Multicenter Clinical Trial Comparing One- and Two-Stage Titanium Screw-Shaped Fixtures with One-Stage Plasma-Sprayed Solid-Screw Fixtures. *Clinical Implant Dentistry and Related Research,* 2(3), 159–165.

Berglundh, T., Abrahamsson, I., Welander, M., Lang, N. P., & Lindhe, J. (2007). Morphogenesis of the peri-implant mucosa: an experimental study in dogs. *Clinical Oral Implants Research*, 18(1), 1–8.

Berglundh T, Armitage G, et al. (2018). Peri-implant diseases and conditions: Consensus report of workgroup 4 of the 2017 World Workshop on the Classification of Periodontal and Peri-Implant Diseases and Conditions. *Journal of Periodontology,* 89, 313–318.

Berglundh, T, & Lindhe, J. (1996). Dimension of the periimplant mucosa. Biological width revisited. *Journal of Clinical Periodontology,* 23(10), 971–973.

Berglundh, T, Lindhe, J., Ericsson, I., Marinello, C. P., Liljenberg, B., & Thomsen, P. (1991). The soft tissue barrier at implants and teeth. *Clinical Oral Implants Research*, 2(2), 81–90.

Berglundh, T, Zitzmann, N. U., & Donati, M. (2011). Are peri-implantitis lesions different from periodontitis lesions? *Journal of Clinical Periodontology*, 38, 188–202.

Berglundh, Tord, Abrahamsson, I., Lang, N. P., & Lindhe, J. (2003). De novo alveolar bone formation adjacent to endosseous implants. *Clinical Oral Implants Research*, 14(3), 251–262.

Block, M. S., Kent, J. N., & Kay, J. F. (1987). Evaluation of hydroxylapatite-coated titanium dental implants in dogs. *Journal of Oral and Maxillofacial Surgery*, 45(7), 601–607.

Bollen, C. M., Papaioanno, W., Eldere, J. van, Schepers, E., Quirynen, M., & van Steenberghe, D. (1996). The influence of abutment surface roughness on plaque accumulation and peri-implant mucositis. *Clinical Oral Implants Research,* 7(3), 201–211.

Bosshardt, D. D., & Lang, N. P. (2005). The junctional epithelium: from health to disease. *Journal of Dental Research,* 84(1), 9–20.

Botos, S., Yousef, H., Zweig, B., Flinton, R., & Weiner, S. (2011). The effects of laser microtexturing of the dental implant collar on crestal bone levels and peri-implant health. *The International Journal of Oral & Maxillofacial Implants,* 26(3), 492–498.

Browne, M., & Gregson, P. J. (2000). Effect of mechanical surface pre-treatment on metal ion release. *Biomaterials,* 21(4), 385–392.

Burgers, R., Gerlach, T., Hahnel, S., Schwarz, F., Handel, G., & Gosau, M. (2010). In vivo and in vitro biofilm formation on two different titanium implant surfaces. *Clinical Oral Implants Research*, 21(2), 156–164.

Buser, D., Nydegger, T., Hirt, H. P., Cochran, D. L., & Nolte, L. P. (1998). Removal torque values of titanium implants in the maxilla of miniature pigs. *The International Journal of Oral & Maxillofacial Implants*, 13(5), 611–619.

Buser, D., Schenk, R. K., Steinemann, S., Fiorellini, J. P., Fox, C. H., & Stich, H. (1991). Influence of surface characteristics on bone integration of titanium implants. A histomorphometric study in miniature pigs. *Journal of Biomedical Materials Research*, 25(7), 889–902.

Buser, D., Weber, H. P., Donath, K., Fiorellini, J. P., Paquette, D. W., & Williams, R. C. (1992). Soft tissue reactions to non-submerged unloaded titanium implants in beagle dogs. *Journal of Periodontology*, 63(3), 225–235.

Byrappa, K., & Adschiri, T. (2007). Hydrothermal technology for nanotechnology. *In Progress in Crystal Growth and Characterization of Materials*, 53(2), 117–166.

Canullo, L., Tallarico, M., Penarrocha-Oltra, D., Monje, A., Wang, H. L., & Penarrocha-Diago, M. (2016). Implant Abutment Cleaning by Plasma of Argon: 5-Year Follow-Up of a Randomized Controlled Trial. *Journal of Periodontology*, 87(4), 434–442.

Carcuac, O., Abrahamsson, I., Albouy, J. P., Linder, E., Larsson, L., & Berglundh, T. (2013). Experimental periodontitis and peri-implantitis in dogs. *Clinical Oral Implants Research,* 24(4), 363–371.

Carcuac, O., & Berglundh, T. (2014). Composition of human peri-implantitis and periodontitis lesions. *Journal of Dental Research*, 93(11), 1083–1088.

Cate, T., & Nanci, A. (2017). *Ten Cate's Oral Histology: development,structure,and function.* (Antonio Nanci, Ed.) (9th ed.). St Louis, Missouri: Elsevier Mosby.

Chai, W. L., Moharamzadeh, K., Brook, I. M., Emanuelsson, L., Palmquist, A., & van Noort, R. (2010). Development of a novel model for the investigation of implant-soft tissue interface. *Journal of Periodontology*, 81(8), 1187–1195.

Chen, J., Yang, P., Liao, Y., Wang, J., Chen, H., Sun, H., & Huang, N. (2015). Effect of the duration of UV irradiation on the anticoagulant properties of titanium dioxide films. *ACS Applied Materials & Interfaces*, 7(7), 4423–4432.

Cheng, F. T., Shi, P., & Man, H. C. (2004). A preliminary study of TiO_2 deposition on NiTi by a hydrothermal method. *Surface and Coatings Technology*, 187(1), 26–32.

Choi, S. H., Jeong, W. S., Cha, J. Y., Lee, J. H., Yu, H. S., Choi, E. H., Kim, K. M., & Hwang, C. J. (2016). Time-dependent effects of ultraviolet and nonthermal atmospheric pressure plasma on the biological activity of titanium. *Scientific Reports*, 6(1), 33421.

Cochran, D. L., Hermann, J. S., Schenk, R. K., Higginbottom, F. L., & Buser, D. (1997). Biologic width around titanium implants. A histometric analysis of the implanto-gingival junction around unloaded and loaded nonsubmerged implants in the canine mandible. *Journal of Periodontology*, 68(2), 186–198.

Cochran, D., Simpson, J., Weber, H. P., & Buser, D. (1994). Attachment and Growth of Periodontal Cells on Smooth and Rough Titanium. *The International Journal of Oral & Maxillofacial Implants*, 9(3), 289–297.

Coelho, P. G., Granjeiro, J. M., Romanos, G. E., Suzuki, M., Silva, N. R., Cardaropoli, G., Thompson, V. P., & Lemons, J. E. (2009). Basic research methods and current trends of dental implant surfaces. *Journal of Biomedical Materials Research.Part B, Applied Biomaterials*, 88(2), 579–596.

Collings, E. W. (1984) *The physical metallurgy of Titanium alloys*. In: Gegel HL (ed) ASM Series in Metal Processing. Edward Arnold Publications, Cleveland, Metals Park, OH

Cooper, L., Zhou, Y., Takebe, J., Guo, J., Abron, A., Holmén, A., & Ellingsen, J. (2006). Fluoride modification effects on osteoblast behavior and bone formation at TiO 2 grit-blasted c.p. titanium endosseous implants. *Biomaterials*, 27(6), 926–936.

Costa, F. O., Takenaka-Martinez, S., Cota, L. O., Ferreira, S. D., Silva, G. L., & Costa, J. E. (2012). Peri-implant disease in subjects with and without preventive maintenance: a 5-year follow-up. *Journal of Clinical Periodontology*, 39(2), 173–181.

Darvell, B.W. (2018). More Metals. *In Materials Science for Dentistry*. (10th ed.), 719–744. Woodhead Publishing, Elsevier.

Davies, J. E. (2003). Understanding peri-implant endosseous healing. *Journal of Dental Education,* 67(8), 932-949.

de Avila, E. D., Lima, B. P., Sekiya, T., Torii, Y., Ogawa, T., Shi, W., & Lux, R. (2015). Effect of UV-photofunctionalization on oral bacterial attachment and biofilm formation to titanium implant material. *Biomaterials*, 67, 84–92.

Derks, J., & Tomasi, C. (2015). Peri-implant health and disease. A systematic review of current epidemiology. *Journal of Clinical Periodontology*, 42, 158-171.

Di Iorio, D., Traini, T., Degidi, M., Caputi, S., Neugebauer, J., & Piattelli, A. (2005). Quantitative evaluation of the fibrin clot extension on diffferent implant surfaces: An in vitro study. *Journal of Biomedical Materials Research - Part B Applied Biomaterials*, 74 (1), 636–642.

Doundoulakis, J. H. (1987). Surface analysis of titanium after sterilization: role in implant-tissue interface and bioadhesion. *The Journal of Prosthetic Dentistry*, 58(4), 471–478.

Drnovšek, N., Daneu, N., Rečnik, A., Mazaj, M., Kovač, J., & Novak, S. (2009). Hydrothermal synthesis of a nanocrystalline anatase layer on Ti6A4V implants. *Surface and Coatings Technology*, 203(10), 1462–1468.

Ellingsen, J. E. (1991). A study on the mechanism of protein adsorption to TiO_2. *Biomaterials*, 12(6), 593–596.

Ellingsen, J. E. (1995). Pre-treatment of titanium implants with fluoride improves their retention in bone. *Journal of Materials Science: Materials in Medicine*, 6(12), 749–753.

Ellingsen, J. E., Johansson, C. B., Wennerberg, A., & Holmén, A. (2004). Improved retention and bone-to-implant contact with fluoride-modified titanium implants. *The International Journal of Oral & Maxillofacial Implants,* 19(5), 659–666.

Elter, C., Heuer, W., Demling, A., Hannig, M., Heidenblut, T., Bach, F. W., & Stiesch-Scholz, M. (2008). Supra- and subgingival biofilm formation on implant abutments with different surface characteristics. *The International Journal of Oral & Maxillofacial Implants,* 23(2), 327–334.

Emecen-Huja, P., Eubank, T., Shapiro, V., Yildiz, V., Tatakis, D., & Leblebicioglu, B. (2013). Peri-implant versus periodontal wound healing. *Journal of Clinical Periodontology*, 40(8), 816–824.

Esposito, M., Hirsch, J. M., Lekholm, U., & Thomsen, P. (1998). Biological factors contributing to failures of osseointegrated oral implants. (I). Success criteria and epidemiology. *European Journal of Oral Sciences, 106(1), 527–551.*

Foster, H. A., Ditta, I. B., Varghese, S., & Steele, A. (2011). Photocatalytic disinfection using titanium dioxide: spectrum and mechanism of antimicrobial activity. *Applied Microbiology and Biotechnology*, 90(6), 1847–1868.

Frojd, V., Linderback, P., Wennerberg, A., de Paz, L. C., Svensater, G., & Davies, J. R. (2011). Effect of nanoporous TiO_2 coating and anodized Ca2+ modification of titanium surfaces on early microbial biofilm formation. *BMC Oral Health*, 11(8), 6831.

Fujishima, A., Zhang, X., & Tryk, D. A. (2008). TiO_2 photocatalysis and related surface phenomena. *Surface Science Reports,* 63(12), 515–582.

Gargiulo AW., Wentz FM., Orban B. (1961). Dimensions and relations of the dentogingival junction in humans. *Journal of Periodontology*,32, 261-267.

Gibbs, S., Roffe, S., Meyer, M., & Gasser, A. (2019). Biology of soft tissue repair: Gingival epithelium in wound healing and attachment to the tooth and abutment surface. *European Cells and Materials*, *38*, 63–78.

Gittens, R. A., Scheideler, L., Rupp, F., Hyzy, S. L., Geis-Gerstorfer, J., Schwartz, Z., & Boyan, B. D. (2014). A review on the wettability of dental implant surfaces II: Biological and clinical aspects. *Acta Biomaterialia*, 10(7), 2907–2918.

Goodman, S. L., Lelah, M. D., Lambrecht, L. K., Cooper, S. L., & Albrecht, R. M. (1984). In vitro vs. ex vivo platelet deposition on polymer surfaces. *Scanning Electron Microscopy*, 1, 279–290.

Grassi, S., Piattelli, A., de Figueiredo, L. C., Feres, M., de Melo, L., Iezzi, G., Jr., R. C. A., & Shibli, J. A. (2006). Histologic Evaluation of Early Human Bone Response to Different Implant Surfaces. *Journal of Periodontology,* 77(10), 1736–1743.

Guida, L., Oliva, A., Basile, M. A., Giordano, M., Nastri, L., & Annunziata, M. (2013). Human gingival fibroblast functions are stimulated by oxidized nano-structured titanium surfaces. *Journal of Dentistry*, 41(10), 900–907.

Hamad, K., Kon, M., Hanawa, T., Yokoyama, K., Miyamoto, Y., & Asaoka, K. (2002). Hydrothermal modification of titanium surface in calcium solutions. *Biomaterials,* 23(10), 2265–2272.

Hamdan, M., Blanco, L., Khraisat, A., & Tresguerres, I. F. (2006). Influence of titanium surface charge on fibroblast adhesion. *Clinical Implant Dentistry and Related Research*, 8(1), 32–38.

Häkkinen, L., Koivisto, L., Heino, J., & Larjava, H. (2015). Chapter 50 - Cell and Molecular Biology of Wound Healing. *In Stem Cell Biology and Tissue Engineering in Dental Sciences*, 669–690.

Heitz-Mayfield, L. J. A., & Salvi, G. E. (2018). Peri-implant mucositis. *Journal of Periodontology*, 89, 257–266.

Hong, J., Andersson, J., Ekdahl, K. N., Elgue, G., Axen, N., Larsson, R., & Nilsson, B. (1999). Titanium is a highly thrombogenic biomaterial: possible implications for osteogenesis. *Thrombosis and Haemostasis*, 82(1), 58–64.

Hori, N., Ueno, T., Suzuki, T., Yamada, M., Att, W., Okada, S., Ohno, A., Aita, H., Kimoto, K., & Ogawa, T. (2010a). Ultraviolet light treatment for the restoration of age-related degradation of titanium bioactivity. *The International Journal of Oral & Maxillofacial Implants,* 25(1), 49–62.

Hori, N., Ueno, T., Minamikawa, H., Iwasa, F., Yoshino, F., Kimoto, K., Lee, M. C., & Ogawa, T. (2010b). Electrostatic control of protein adsorption on UV-photofunctionalized titanium. *Acta Biomaterialia*, 6(10), 4175–4180.

Hoshi, N., Negishi, H., Okada, S., Nonami, T., & Kimoto, K. (2010). Response of human fibroblasts to implant surface coated with titanium dioxide photocatalytic films. J*ournal of Prosthodontic Research*, 54(4), 185–191.

Huang, N., Yang, P., Leng, YX., Chen, J.Y ; Sun, H., Wang, J., Wang, G.J., Ding, P.D., Xi, T.F., Leng, Y. (2003). Hemocompatibility of titanium oxide films. *Biomaterials*, 24, 2177–87.

Hulshoff, J., Dijk, K., Waerden, J., Wolke, J., Kalk, W., & Jansen, J. (1996). Evaluation of plasma-spray and magnetron-sputter Ca-P-coated implants: An in vivo experiment using rabbits. *Journal of Biomedical Materials Research*, 31(3), 329–337

Hung, K., Lai, H., & Feng, H. (2017). Characteristics of RF-Sputtered Thin Films of Calcium Phosphate on Titanium Dental Implants. Coa*tings (Basel)*, 7(8), 126.

Ikeda, H., Shiraiwa, M., Yamaza, T., Yoshinari, M., Kido, M. A., Ayukawa, Y., Inoue, T., Koyano, K., & Tanaka, T. (2002). Difference in penetration of horseradish peroxidase tracer as a foreign substance into the peri-implant or junctional epithelium of rat gingivae. *Clinical Oral Implants Research*, 13(3), 243–251.

Ingber, J. S., Rose, L. F., & Coslet, J. G. (1977). The "biologic width" a concept in periodontics and restorative dentistry. *The Alpha Omegan*, 70(3), 62–65.

Ivanoff, C. J., Widmark, G., Johansson, C., & Wennerberg, A. (2003). Histologic evaluation of bone response to oxidized and turned titanium micro-implants in human jawbone. *The International Journal of Oral & Maxillofacial Implants,* 18(3), 341–348.

Ivanovski, S., & Lee, R. (2018). Comparison of peri-implant and periodontal marginal soft tissues in health and disease. *Periodontology* 2000, 76(1), 116–130.

Iwasa, F., Hori, N., Ueno, T., Minamikawa, H., Yamada, M., & Ogawa, T. (2010). Enhancement of osteoblast adhesion to UV-photofunctionalized titanium via an electrostatic mechanism. *Biomaterials*, 31(10), 2717–2727.

Jakobi, M. L., Stumpp, S. N., Stiesch, M., Eberhard, J., & Heuer, W. (2015). The Peri-Implant and Periodontal Microbiota in Patients with and without Clinical Signs of Inflammation. *Dentistry Journal*, 3(2), 24–42.

Jepsen, S., Berglundh, T., Genco, R., Aass, A. M., Demirel, K., Derks, J., Figuero, E., Giovannoli, J. L., Goldstein, M., Lambert, F., Ortiz-Vigon, A., Polyzois, I., Salvi, G. E., Schwarz, F., Serino, G., Tomasi, C., & Zitzmann, N. U. (2015). Primary prevention of peri-implantitis: managing peri-implant mucositis. *Journal of Clinical Periodontology*, 42, 152–157.

Jimbo, R., Sawase, T., Baba, K., Kurogi, T., Shibata, Y., & Atsuta, M. (2008). Enhanced initial cell responses to chemically modified anodized titanium. *Clinical Implant Dentistry and Related* Research, 10(1), 55–61.

Karbach, J., Callaway, A., Kwon, Y. D., d'Hoedt, B., & Al-Nawas, B. (2009). Comparison of five parameters as risk factors for peri-mucositis. *The International Journal of Oral & Maxillofacial Implants*, 24(3), 491–496.

Kasemo, B. (1983). Biocompatibility of titanium implants: surface science aspects. *The Journal of Prosthetic Dentistry,* 49(6), 832–837.

Kasemo, B., & Lausmaa, J. (1988). Biomaterial and implant surfaces: on the role of cleanliness, contamination, and preparation procedures. *Journal of Biomedical Materials Research*, 22, 145–158.

Katsikogianni, M., & Missirlis, Y. F. (2004). Concise review of mechanisms of bacterial adhesion to biomaterials and of techniques used in estimating bacteria-material interactions. *European Cells & Materials,* 8, 37–57.

Kim, H., Koh, Y., Li, L. H., Lee, S., & Kim, H. (2004). Hydroxyapatite coating on titanium substrate with titania buffer layer processed by sol-gel method. *Biomaterials*, 25(13), 2533–2538.

Kim, H. M., Miyaji, F., Kokubo, T., & Nakamura, T. (1996). Preparation of bioactive Ti and its alloys via simple chemical surface treatment. *Journal of Biomedical Materials Research*, 32(3), 409–417.

Kim, Y. S., Shin, S. Y., Moon, S. K., & Yang, S. M. (2015). Surface properties correlated with the human gingival fibroblasts attachment on various materials for implant abutments: a multiple regression analysis. *Acta Odontologica Scandinavica,* 73(1), 38–47.

Klinger, A., Steinberg, D., Kohavi, D., & Sela, M. N. (1997). Mechanism of adsorption of human albumin to titanium in vitro. *Journal of Biomedical Materials Research*, 36(3), 387–392.

Kohavi, D., Hauslich, L. B., Rosen, G., Steinberg, D., & Sela, M. N. (2013). Wettability versus electrostatic forces in fibronectin and albumin adsorption to titanium surfaces. *Clinical Oral Implants Research*, 24(9), 1002–1008.

Kokubo, T., Kim, H.-M., & Kawashita, M. (2003). Novel bioactive materials with different mechanical properties. *Biomaterials, 2*4(13), 2161–2175.

Kolenbrander, P. E., Jr, R. J. P., Rickard, A. H., Jakubovics, N. S., Chalmers, N. I., & Diaz, P. I. (2006). Bacterial interactions and successions during plaque development. *Periodontology 2000,* 42(1), 47–79.

Koo, F., Falsetta, M.L., & Klein, M.I. (2013). The Exopolysaccharide Matrix: A Virulence Determinant of Cariogenic Biofilm. *Journal of Dental Research*, 92(12), 1065–1073

Kubo, K., Tsukimura, N., Iwasa, F., Ueno, T., Saruwatari, L., Aita, H., Chiou, W. A., & Ogawa, T. (2009). Cellular behavior on TiO_2 nanonodular structures in a micro-to-nanoscale hierarchy model. *Biomaterials*, 30(29), 5319–5329.

Kumar, P. S., Mason, M. R, Brooker, M. R., O'Brien, K. (2012). Pyrosequencing reveals unique microbial signatures associated with healthy and failing dental implants. *Journal of Clinical Periodontology*, 39, 425–433.

Larjava, H., Koivisto, L., Hakkinen, L., & Heino, J. (2011). Epithelial integrins with special reference to oral epithelia. *Journal of Dental Research*, 90(12), 1367–1376.

Lee, B. H., Kim, J. K., Kim, Y. D., Choi, K., & Lee, K. H. (2004). In vivo behavior and mechanical stability of surface-modified titanium implants by plasma spray coating and chemical treatments. *Journal of Biomedical Materials Research.Part A*, 69(2), 279–285.

Lee, C. T., Huang, Y. W., Zhu, L., & Weltman, R. (2017). Prevalences of peri-implantitis and peri-implant mucositis: systematic review and meta-analysis. *Journal of Dentistry,* 62, 1–12.

Le Guéhennec, L., Soueidan, A., Layrolle, P., & Amouriq, Y. (2007). Surface treatments of titanium dental implants for rapid osseointegration. *Dental Materials,* 23(7), 844-854.

Lekholm, U., Grondahl, K., & Jemt, T. (2006). Outcome of oral implant treatment in partially edentulous jaws followed 20 years in clinical function. *Clinical Implant Dentistry and Related Research,* 8(4), 178–186.

Li, J, Helmerhorst, E.J., Leone, C.W., Troxler, R.F., Yaskell, T., Haffajee, A.D., Socransky, S.S., Oppenheim, F.G. (2004). Identification of Early Microbial Colonizers In Human Dental Biofilm. *Journal of applied microbiology*, 97(6), 1311-1318.

Lindhe, J., & Meyle, J. (2008). Peri-implant diseases: Consensus Report of the Sixth European Workshop on Periodontology. *Journal of Clinical Periodontology*, 35(8), 282–285.

Linkevicius, T., & Apse, P. (2008). Influence of abutment material on stability of peri-implant tissues: a systematic review. *The International Journal of Oral & Maxillofacial Implants*, 23(3), 449–456.

Linkevicius, T., & Vaitelis, J. (2015). The effect of zirconia or titanium as abutment material on soft peri-implant tissues: a systematic review and meta-analysis. *Clinical Oral Implants Research*, 26(1), 139–147.

Listgarten, M. A., Lang, N. P., Schroeder, H. E., & Schroeder, A. (1991). Periodontal tissues and their counterparts around endosseous implants. *Clinical Oral Implants Research*, 2(3), 1–19.

Listgarten, M. O. (1975). Electronmicroscopic study of the odonto-gingival junction. *Mondo Odontostomatologico,* 17(5), 10–24.

Liu, X., Chen, S., Tsoi, J. K. H., & Matinlinna, J. P. (2017). Binary titanium alloys as dental implant materials-a review. *Regenerative Biomaterials*, 4(5), 315–323.

Liu, X., Chu, P. K., & Ding, C. (2004). Surface modification of titanium, titanium alloys, and related materials for biomedical applications. *Materials Science and Engineering R: Reports*, 47(3–4), 49–121.

Lops, D., Bressan, E., Chiapasco, M., Rossi, A., & Romeo, E. (2013). Zirconia and titanium implant abutments for single-tooth implant prostheses after 5 years of function in posterior regions. The *International Journal of Oral & Maxillofacial Implants*, 28(1), 281–287.

Maness, P. C., Smolinski, S., Blake, D. M., Huang, Z., Wolfrum, E. J., & Jacoby, W. A. (1999). Bactericidal activity of photocatalytic TiO(2) reaction: toward an understanding of its killing mechanism. *Applied and Environmental Microbiology*, 65(9), 4094–4098.

Massaro, C., Rotolo, P., Riccardis, F. de., Milella, E., Napoli, A., Wieland, M., Textor, M., Spencer, N. D., & Brunette, D. M. (2002). Comparative investigation of the surface properties of commercial titanium dental implants. Part I: chemical composition. *Journal of Materials Science.Materials in Medicine*, 13(6), 535–548.

Meirelles, L., Currie, F., Jacobsson, M., Albrektsson, T., & Wennerberg, A. (2008). The effect of chemical and nanotopographical modifications on the early stages of osseointegration. *The International Journal of Oral & Maxillofacial Implants,* 23(4), 641–647.

Mendonca, G., Mendonca, D. B., Aragao, F. J., & Cooper, L. F. (2008). Advancing dental implant surface technology--from micron- to nanotopography. *Biomaterials*, 29(28), 3822–3835.

Meretoja, V. v, Rossi, S., Peltola, T., Pelliniemi, L. J., & Narhi, T. O. (2010). Adhesion and proliferation of human fibroblasts on sol-gel coated titania. *Journal of Biomedical Materials Research.Part A*, 95(1), 269–275.

Meyer, S., Giannopoulou, C., Courvoisier, D., Schimmel, M., Muller, F., & Mombelli, A. (2017). Experimental mucositis and experimental gingivitis in persons aged 70 or over. Clinical and biological responses. *Clinical Oral Implants Research,* 28(8), 1005–1012.

Mombelli, A, & Lang, N. P. (1998). The diagnosis and treatment of peri-implantitis. *Periodontology 2000*, 17, 63–76.

Morra, M., Cassinelli, C., Bruzzone, G., Carpi, A., Santi, G. di, Giardino, R., & Fini, M. (2003). Surface chemistry effects of topographic modification of titanium dental implant surfaces: 1. Surface analysis. *The International Journal of Oral & Maxillofacial Implants,* 18(1), 40–45.

Müeller, W.-D., Gross, U., Fritz, T., Voigt, C., Fischer, P., Berger, G., Rogaschewski, S., & Lange, K.-P. (2003). Evaluation of the interface between bone and titanium surfaces being blasted by aluminium oxide or bioceramic particles. *Clinical Oral Implants Research*, *14*(3), 349–356.

Nakagawa, M., Zhang, L., Udoh, K., Matsuya, S., & Ishikawa, K. (2005). Effects of hydrothermal treatment with $CaCl_2$ solution on surface property and cell response of titanium implants. *Journal of Materials Science.Materials in Medicine*, *16*(11), 985–991.

Nakazato, G., Tsuchiya, H., Sato, M., Yamauchi, M. (1989). In vivo plaque formation on implant materials. *International Journal of Oral & Maxillofacial Implants,* 4, 321– 326.

Nevins, M., Camelo, M., Nevins, M. L., Schupbach, P., & Kim, D. M. (2012). Connective tissue attachment to laser-microgrooved abutments: a human histologic case report. *The International Journal of Periodontics & Restorative Dentistry,* 32(4), 385–392.

Nevins, M., Kim, D. M., Jun, S. H., Guze, K., Schupbach, P., & Nevins, M. L. (2010). Histologic evidence of a connective tissue attachment to laser microgrooved abutments: a canine study. *The International Journal of Periodontics & Restorative Dentistry,* 30(3), 245–255.

Niinomi, M. (2008). Mechanical biocompatibilities of titanium alloys for biomedical applications. *Journal of the Mechanical Behavior of Biomedical Materials,* 1(1), 30–42.

Novaes, A. B., Souza, S. L., de Oliveira, P. T., & Souza, A. M. (2002). Histomorphometric analysis of the bone-implant contact obtained with 4 different implant surface treatments placed side by side in the dog mandible. *The International Journal of Oral & Maxillofacial Implants,* 17(3), 377–383.

Oksanen, J., & Hormia, M. (2002). An organotypic In vitro model that mimics the dento-epithelial junction. *Journal of Periodontology*, 73, 86–93.

Ong, J. L., Carnes, D. L., & Bessho, K. (2004). Evaluation of titanium plasma-sprayed and plasma-sprayed hydroxyapatite implants in vivo. *Biomaterials*, 25(19), 4601–4606.

Oshiro, W., Ayukawa, Y., Atsuta, I., Furuhashi, A., Yamazoe, J., Kondo, R., Sakaguchi, M., Matsuura, Y., Tsukiyama, Y., & Koyano, K. (2015). Effects of CaCl2 hydrothermal treatment of titanium implant surfaces on early epithelial sealing. *Colloids and Surfaces.B, Biointerfaces,* 131, 141–147.

Paldan, H., Areva, S., Tirri, T., Peltola, T., Lindholm, T. C., Lassila, L., Pelliniemi, L. J., Happonen, R. P., & Narhi, T. O. (2008). Soft tissue attachment on sol-gel-treated titanium implants i*n vivo. Journal of Materials Science.Materials in Medicine,* 19(3), 1283–1290.

Park, J. Y., & Davies, J. E. (2000). Red blood cell and platelet interactions with titanium implant surfaces. *Clinical Oral Implants Research*, 11(6), 530–539.

Park, J. Y., Gemmell, C. H., & Davies, J. E. (2001). Platelet interactions with titanium: modulation of platelet activity by surface topography. *Biomaterials*, 22(19), 2671–2682.

Park, K. H., Heo, S. J., Koak, J. Y., Kim, S. K., Lee, J. B., Kim, S. H., & Lim, Y. J. (2007). Osseointegration of anodized titanium implants under different current voltages: A rabbit study. *Journal of Oral Rehabilitation,* 34(7), 517–527.

Peltola, T., Patsi, M., Rahiala, H., Kangasniemi, I., & Yli-Urpo, A. (1998). Calcium phosphate induction by sol-gel-derived titania coatings on titanium substrates in vitro. *Journal of Biomedical Materials Research,* 41(3), 504–510.

Polmear I.J. (1981). *Titanium alloys*. In: Light alloys, chapter 6. Edward Arnold Publications, London

Pontoriero, R., Tonelli, M. P., Carnevale, G., Mombelli, A., Nyman, S. R., & Lang, N. P. (1994). Experimentally induced peri-implant mucositis. A clinical study in humans. *Clinical Oral Implants Research,* 5(4), 254–259.

Quirynen, M., & Bollen, C. M. (1995). The influence of surface roughness and surface-free energy on supra- and subgingival plaque formation in man. A review of the literature. *Journal of Clinical Periodontology,* 22(1), 1–14.

Quirynen, M., Soete, M. de, & van Steenberghe, D. (2002). Infectious risks for oral implants: a review of the literature. *Clinical Oral Implants Research*, 13(1), 1–19.

Quiynen, M., Vogels, R., Pauwels, M., Haffajee, A.D., Socransky, S.S., Uzel, N.G., van Steenberghe, D. (2005). Initial subgingival colonization of 'pristine' pockets. *Journal of dental research*, 84(4), 340-344.

Riley, D. J., Bavastrello, V., Covani, U., Barone, A., & Nicolini, C. (2005). An in-vitro study of the sterilization of titanium dental implants using low intensity UV-radiation. *Dental Materials*, 21(8), 756–760.

Roccuzzo, M., Bonino, F., Aglietta, M., & Dalmasso, P. (2012). Ten-year results of a three arms prospective cohort study on implants in periodontally compromised patients. Part 2: clinical results. *Clinical Oral Implants Research,* 23(4), 389–395.

Rochford, E. T., Subbiahdoss, G., Moriarty, T. F., Poulsson, A. H., van der Mei, H. C., Busscher, H. J., & Richards, R. G. (2014). An in vitro investigation of bacteria-osteoblast competition on oxygen plasma-modified PEEK. *Journal of Biomedical Materials Research.Part A*, 102(12), 4427–4434.

Rodrigo, D., Martin, C., & Sanz, M. (2012). Biological complications and peri-implant clinical and radiographic changes at immediately placed dental implants. A prospective 5-year cohort study. *Clinical Oral Implants Research*, 23(10), 1224–1231.

Roffel, S., Wu, G., Nedeljkovic, I., Meyer, M., Razafiarison, T., & Gibbs, S. (2019). Evaluation of a novel oral mucosa in vitro implantation model for analysis of molecular interactions with dental abutment surfaces. *Clinical Implant Dentistry and Related Research,* 21(S1), 25–33.

Rompen, E., Domken, O., Degidi, M., Pontes, A. E., & Piattelli, A. (2006). The effect of material characteristics, of surface topography and of implant components and connections on soft tissue integration: a literature review. *Clinical Oral Implants Research,* 17(2), 55–67.

Roos-Jansaker, A. M., Lindahl, C., Renvert, H., & Renvert, S. (2006a). Nine- to fourteen-year follow-up of implant treatment. Part II: presence of peri-implant lesions. *Journal of Clinical Periodontology*, 33(4), 290–295.

Roos-Jansaker, A. M., Renvert, H., Lindahl, C., & Renvert, S. (2006b). Nine- to fourteen-year follow-up of implant treatment. Part III: factors associated with peri-implant lesions. *Journal of Clinical Periodontology,* 33(4), 296–301.

Rossi, S., Tirri, T., Paldan, H., Kuntsi-Vaattovaara, H., Tulamo, R., & Närhi, T. (2008). Peri-implant tissue response to O surface modified implants. *Clinical Oral Implants Research,* 19(4), 348–355.

Ruardy, T. G., Schakenraad, J. M., van der Mei, H. C., & Busscher, H. J. (1995). Adhesion and spreading of human skin fibroblasts on physicochemically characterized gradient surfaces. *Journal of Biomedical Materials Research,* 29(11), 1415–1423.

Rupp, F., Gittens, R. A., Scheideler, L., Marmur, A., Boyan, B. D., Schwartz, Z., & Geis-Gerstorfer, J. (2014). A review on the wettability of dental implant surfaces I: theoretical and experimental aspects. *Acta Biomaterialia*, 10(7), 2894–2906.

Rupp, F., Haupt, M., Klostermann, H., Kim, H. S., Eichler, M., Peetsch, A., Scheideler, L., Doering, C., Oehr, C., Wendel, H. P., Sinn, S., Decker, E., von Ohle, C., & Geis-Gerstorfer, J. (2010). Multifunctional nature of UV-irradiated nanocrystalline anatase thin films for biomedical applications. *Acta Biomaterialia,* 6(12), 4566–4577.

Rupp, F., Liang, L., Geis-Gerstorfer, J., Scheideler, L., & Huttig, F. (2018). Surface characteristics of dental implants: A review. *Dental Materials*, 34(1), 40–57.

Salvi, G E, Aglietta, M., Eick, S., Sculean, A., Lang, N. P., & Ramseier, C. A. (2012). Reversibility of experimental peri-implant mucositis compared with experimental gingivitis in humans. *Clinical Oral Implants Research,* 23(2), 182–190.

Salvi, Giovanni E, Bosshardt, D. D., Lang, N. P., Abrahamsson, I., Berglundh, T., Lindhe, J., Ivanovski, S., & Donos, N. (2015). Temporal sequence of hard and soft tissue healing around titanium dental implants. *Periodontology 2000*, 68(1), 135–152.

Schroeder, H. E., & Listgarten, M. A. (1977). *Fine structure of the developing epithelial attachment of human teeth* (2. rev. ed.). Monographs in Developmental Biology, Vol. 2, Basel, Switzerland, S. Karger.

Schroeder, H. E., & Listgarten, M. A. (1997). The gingival tissues: the architecture of periodontal protection. *Periodontology 2000*, 13(1), 91-120.

Schupbach, P., & Glauser, R. (2007). The defense architecture of the human periimplant mucosa: A histological study. *Journal of Prosthetic Dentistry*, 97(6), 15–25.

Schwarz, F., Mihatovic, I., Becker, J., Bormann, K. H., Keeve, P. L., & Friedmann, A. (2013). Histological evaluation of different abutments in the posterior maxilla and mandible: an experimental study in humans. *Journal of Clinical Periodontology*, 40(8), 807–815.

Schwarz, F., Derks, J., Monje, A., & Wang, H.-L. (2018). Peri-implantitis. *Journal of Clinical Periodontology,* 45, 246–266.

Schwarz, F., Ferrari, D., Herten, M., Mihatovic, I., Wieland, M., Sager, M., & Becker, J. (2007). Effects of Surface Hydrophilicity and Microtopography on Early Stages of Soft and Hard Tissue Integration at Non-Submerged Titanium Implants: An Immunohistochemical Study in Dogs. *Journal of Periodontology*, 78(11), 2171–2184.

Sculean, A., Gruber, R., & Bosshardt, D. D. (2014). Soft tissue wound healing around teeth and dental implants. *Journal of Clinical Periodontology*, 41(15), 6–22.

Shahramian, K., Gasik, M., Kangasniemi, I., Walboomers, X. F., Willberg, J., Abdulmajeed, A., & Närhi, T. (2020). Zirconia implants with improved attachment to the gingival tissue. *Journal of Periodontology,*1-12.

Sharma, C. P. (1984). LTI carbons: blood compatibility. *Journal of colloid and interface science*,97,585–586.

Shi, X., Xu, L., Munar, M. L., & Ishikawa, K. (2015). Hydrothermal treatment for TiN as abrasion resistant dental implant coating and its fibroblast response. *Materials Science & Engineering, C*, 49, 1–6.

Shibli, J. A., Grassi, S., de Figueiredo, L. C., Feres, M., Marcantonio, E., Iezzi, G., & Piattelli, A. (2007). Influence of implant surface topography on early osseointegration: a histological study in human jaws. *Journal of Biomedical Materials Research.Part B, Applied Biomaterials,* 80(2), 377–385.

Steinberg, D., Klinger, A., Kohavi, D., & Sela, M. N. (1995). Adsorption of human salivary proteins to titanium powder. I. Adsorption of human salivary albumin. *Biomaterials,* 16(17), 1339–1343.

Stern, I. B. (1981). Current concepts of the dentogingival junction: the epithelial and connective tissue attachments to the tooth. *Journal of Periodontology*, 52(9), 465–476.

Suketa, N., Sawase, T., Kitaura, H., Naito, M., Baba, K., Nakayama, K., Wennerberg, A., & Atsuta, M. (2005). An antibacterial surface on dental implants, based on the photocatalytic bactericidal effect. *Clinical Implant Dentistry and Related Research,* 7(2), 105–111.

Sul, Y.-T., Jeong, Y., Johansson, C., & Albrektsson, T. (2006). Oxidized, bioactive implants are rapidly and strongly integrated in bone. Part 1 – experimental implants. *Clinical Oral Implants Research*, 17(5), 521–526.

Sul, Y.-T., Johansson, C., Wennerberg, A., Cho, L.-R., Chang, B.-S., & Albrektsson, T. (2005). Optimum surface properties of oxidized implants for reinforcement of osseointegration: surface chemistry, oxide thickness, porosity, roughness, and crystal structure. *The International Journal of Oral & Maxillofacial Implants,* 20(3), 349–359.

Surmenev, R., Surmeneva, M., Grubova, I., Chernozem, R., Krause, B., Baumbach, T., Loza, K., & Epple, M. (2017). RF magnetron sputtering of a hydroxyapatite target: A comparison study on polytetrafluorethylene and titanium substrates. *Applied Surface Science,* 414, 335–344.

Takebe, J., Ito, S., Miura, S., Miyata, K., & Ishibashi, K. (2012). Physicochemical state of the nanotopographic surface of commercially pure titanium following anodization-hydrothermal treatment reveals significantly improved hydrophilicity and surface energy profiles. *Materials Science and Engineering C,* 32(1), 55–60.

Tamura, S., Yonezawa, H., Motegi, M., Nakao, R., Yoneda, S., Watanabe, H., Yamazaki, T., Senpuku, H. (2009). Inhibiting effects of Streptococcus salivarius on competence-stimulating peptide-dependent biofilm formation by Streptococcus mutans. *Oral microbiology and immunology*, 24(2), 152-161.

Tanner, J., Carlen, A., Soderling, E., & Vallittu, P. K. (2003). Adsorption of parotid saliva proteins and adhesion of Streptococcus mutans ATCC 21752 to dental fiber-reinforced composites. *Journal of Biomedical Materials Research.Part B, Applied Biomaterials*, 66(1), 391–398.

Tanner, J., Robinson, C., Soderling, E., & Vallittu, P. (2005). Early plaque formation on fibre-reinforced composites in vivo. *Clinical Oral Investigations*, 9(3), 154–160.

Teughels, W., Assche, N. van, Sliepen, I., & Quirynen, M. (2006). Effect of material characteristics and/or surface topography on biofilm development. *Clinical Oral Implants Research*, 17(2), 68–81.

Thor, A., Rasmusson, L., Wennerberg, A., Thomsen, P., Hirsch, J. M., Nilsson, B., & Hong, J. (2007). The role of whole blood in thrombin generation in contact with various titanium surfaces. *Biomaterials*, *28*(6), 966–974.

Tomasi, C., Tessarolo, F., Caola, I., Piccoli, F., Wennstrom, J. L., Nollo, G., & Berglundh, T. (2016). Early healing of peri-implant mucosa in man. *Journal of Clinical Periodontology,* 43(10), 816–824.

Tomsia, A. P., Lee, J. S., Wegst, U. G., & Saiz, E. (2013). Nanotechnology for dental implants. *The International Journal of Oral & Maxillofacial Implants,* 28(6), 535–546.

Ueda, M., Uchibayashi, Y., Otsuka-Yao-Matsuo, S., & Okura, T. (2008). Hydrothermal synthesis of anatase-type TiO_2 films on Ti and Ti–Nb substrates. *Journal of Alloys and Compounds*, 459(1-2), 369–376.

Unosson, E., Persson, C., Welch, K., & Engqvist, H. (2012). Photocatalytic activity of low temperature oxidized Ti-6Al-4V. *Journal of Materials Science.Materials in Medicine*, 23(5), 1173–1180.

Unosson, E., Tsekoura, E. K., Engqvist, H., & Welch, K. (2013). Synergetic inactivation of Staphylococcus epidermidis and Streptococcus mutansin a TiO_2/H_2O_2/UV system. *Biomatter*, 3(4),1-6.

van Brakel, R., Cune, M. S., van Winkelhoff, A. J., de Putter, C., Verhoeven, J. W., & van der Reijden, W. (2011). Early bacterial colonization and soft tissue health around zirconia and titanium abutments: an in vivo study in man. *Clinical Oral Implants Research*, 22(6), 571–577.

van Steenberghe, D., Mars, G. de, Quirynen, M., Jacobs, R., & Naert, I. (2000). A prospective split-mouth comparative study of two screw-shaped self-tapping pure titanium implant systems. *Clinical Oral Implants Research,* 11(3), 202–209.

Vigolo, P., Givani, A., Majzoub, Z., & Cordioli, G. (2006). A 4-year prospective study to assess peri-implant hard and soft tissues adjacent to titanium versus gold-alloy abutments in cemented single implant crowns. *Journal of Prosthodontics,* 15(4), 250–256.

Villard, N., Seneviratne, C., Tsoi, J. K., Heinonen, M., & Matinlinna, J. (2015). Candida albicans aspects of novel silane system-coated titanium and zirconia implant surfaces. *Clinical Oral Implants Research*, 26(3), 332–341.

Wang, R., Hashimoto, K., Fujishima, A., Chikuni, M., Kojima, E., Kitamura, A., Shimohigoshi, M., & Watanabe, T. (1997). *Light-induced amphiphilic surfaces. Nature*, 388(6641), 431–432.

Wang, S., Liu, Y., Fang, D., & Shi, S. (2007). The miniature pig: a useful large animal model for dental and orofacial research. *Oral Diseases*, 13(6), 530–537.

Wang, X., Hayakawa, S., Tsuru, K., & Osaka, A. (2002). Bioactive titania gel layers formed by chemical treatment of Ti substrate with a H2O2/HCl solution. *Biomaterials*, 23(5), 1353–1357.

Webb, K., Hlady, V., & Tresco, P. A. (1998). Relative importance of surface wettability and charged functional groups on NIH 3T3 fibroblast attachment, spreading, and cytoskeletal organization. Journal of Biomedical Materials Research, 41(3), 422–430.

Webster, T. (2004). Increased osteoblast adhesion on nanophase metals: Ti, Ti6Al4V, and CoCrMo. *Biomaterials*, 25(19), 4731–4739.

Welander, M., Abrahamsson, I., & Berglundh, T. (2008). The mucosal barrier at implant abutments of different materials. *Clinical Oral Implants Research*, 19(7), 635–641.

Wennerberg, A., & Albrektsson, T. (2009). Effects of titanium surface topography on bone integration: a systematic review. *Clinical Oral Implants Research*, 20(4), 172–184.

Wennerberg, A., Jimbo, R., Stübinger, S., Obrecht, M., Dard, M., Berner, S. (2014). Nanostructures and hydrophilicity influence osseointegration: a biomechanical study in the rabbit tibia. *Clinical Oral Implants Research,* 25(9), 1041–1050.

Werner, S., Huck, O., Frisch, B., Vautier, D., Elkaim, R., Voegel, J. C., Brunel, G., & Tenenbaum, H. (2009). The effect of microstructured surfaces and laminin-derived peptide coatings on soft tissue interactions with titanium dental implants. *Biomaterials,* 30(12), 2291–2301.

Willbold, E. (2010). Histology and research at the hard tissue–implant interface using Technovit 9100 New embedding technique. *Acta Biomaterialia*, 6(11), 4447–4455.

Williams, D. F. (2008). On the mechanisms of biocompatibility. *Biomaterials*, 29(20), 2941–2953.

Wilson, C. J., Clegg, R. E., Leavesley, D. I., & Pearcy, M. J. (2005). Mediation of biomaterial-cell interactions by adsorbed proteins: a review. *Tissue Engineering,* 11(1–2), 1–18.

Wong, J. W., Gallant-Behm, C., Wiebe, C., Mak, K., Hart, D. A., Larjava, H., & Häkkinen, L. (2009). Wound healing in oral mucosa results in reduced scar formation as compared with skin: Evidence from the red Duroc pig model and humans. *Wound Repair and Regeneration*, 17(5), 717–729.

Wong, M., Eulenberger, J., Schenk, R., & Hunziker, E. (1995). Effect of surface topology on the osseointegration of implant materials in trabecular bone. *Journal of Biomedical Materials Research*, 29(12), 1567–1575.

Wong, M. H., Cheng, F. T., & Man, H. C. (2007). In situ hydrothermal synthesis of oxide film on NiTi for improving corrosion resistance in Hanks' solution. *Scripta Materialia*, 56(3), 205–208.

Wu, J., Zhou, L., Ding, X., Gao, Y., & Liu, X. (2015). Biological Effect of Ultraviolet Photocatalysis on Nanoscale Titanium with a Focus on Physicochemical Mechanism. *Langmuir,* 31(36), 10037–10046.

Yamada, Y., Yamada, M., Ueda, T., & Sakurai, K. (2014). Reduction of biofilm formation on titanium surface with ultraviolet-C pre-irradiation. *Journal of Biomaterials Applications,* 29(2), 161–171.

Yang, B., Uchida, M., Kim, H. M., Zhang, X., & Kokubo, T. (2004). Preparation of bioactive titanium metal via anodic oxidation treatment. *Biomaterials*, *25*(6), 1003–1010.

Zembic, A., Kim, S., Zwahlen, M., & Kelly, J. R. (2014). Systematic review of the survival rate and incidence of biologic, technical, and esthetic complications of single implant abutments supporting fixed prostheses. *The International Journal of Oral & Maxillofacial Implants, 29* Suppl, 99–116.

Zitzmann, N. U., & Berglundh, T. (2008). Definition and prevalence of peri-implant diseases. *Journal of Clinical Periodontology,* 35(8), 286–291.

Zitzmann, N. U., Berglundh, T., Marinello, C. P., & Lindhe, J. (2001). Experimental peri-implant mucositis in man. *Journal of Clinical Periodontology*, 28(6), 517–523.

Zuldesmi, M., Waki, A., Kuroda, K., & Okido, M. (2015). Hydrothermal treatment of titanium alloys for the enhancement of osteoconductivity. *Materials Science and Engineering: C*, 49, 430–435.

UNIVERSITY OF TURKU

Painosalama Oy, Turku, Finland 2021

ISBN 978-951-29-8388-9 (PRINT)
ISBN 978-951-29-8389-6 (PDF)
ISSN 0355-9483 (Print)
ISSN 2343-3213 (Online)